2014

Role of Poly-N-Acetyl-Glucosamine Nanofibers in Cutaneous Wound Healing

Amanda Haley Buff-Lindner
Medical University of South Carolina

The Role of Poly N Acetyl Glucosamine Nanofibers in Cutaneous Wound Healing

by

Amanda Haley Buff-Lindner

A dissertation submitted to the faculty of the Medical University of South Carolina in partial fulfillment of the requirement for the degree of Doctor of Philosophy in the College of Graduate Studies.

Department of Cell Biology and Regenerative Medicine

2014

Approved by:

Chairman, Advisory Committee _____

. _____

_____

_____

_____

ACKNOWLEDGEMENTS

I would like to express gratitude for those who supported me throughout this process. I am thankful for the guidance, constructive criticism, and advice throughout my project.

I would like to thank Dr. Robin Muise-Helmericks for her unwavering support and mentorship through the years. I would also like to acknowledge and thank my committee members Dr. Amy Bradshaw, Dr. Michael Kern, Dr. Rick Visconti, and Dr. John Vournakis for their guidance during my dissertation research project.

Additionally, I would like to express a heartfelt thank you to Juanita Eldridge and Dr. Daniel Corum for their assistance and friendship in the lab.

Thank you,

Haley Buff-Lindner

TABLE OF CONTENTS

LIST OF FIGURES

LIST OF ABBREVIATIONS

α-SMA - alpha smooth muscle actin

ECM- extracellular matrix

EMT- epithelial to mesenchymal transition

EPSTI1- Epithelial stromal interaction protein 1

EC- endothelial cells

FGF- fibroblast growth factor

MMP- matrix metalloproteinase

pGlcNAc- poly-N-acetyl glucosamine nanofibers

PDGF- platelet derived growth factor

PIP2/3- phosphatidylinositol 4,5-bisphosphate

PTEN- Phosphatase and tensin homolog

SCR- scramble (control)

TIMP- Tissue inhibitor of metalloproteinase

TGF-β- transforming growth factor

TNF- tumor necrosis factor

VEGF- vascular endothelial growth actor

ABSTRACT

Treatment of cutaneous wounds with poly-N-acetyl-glucosamine nanofibers (pGlcNAc), a novel polysaccharide material derived from a marine diatom, results in increases in wound closure, antibacterial activities and innate immune responses. Treatment with nanofibers results in increased defensin, small antimicrobial peptides, expression both *in vitro* and *in vivo*. Induction of defensing expression results in bacterial clearance in a cutaneous wound model. We have also shown that Akt1 plays a central role in the regulation of these activities. We show that pGlcNAc treatment of cutaneous wounds in mice results in decreased

scar sizes. Additionally, treatment of cutaneous wounds with pGlcNAc results in increased elasticity and a rescue of tensile strength. Masson Trichrome staining suggests that pGlcNAc treated wounds exhibit decreased collagen content as well as increased collagen alignment with collagen fibers oriented similarly to unwounded tissue. Utilizing a fibrin gel assay to analyze the effect of pGlcNAc nanofiber treatment on fibroblast alignment *in vitro*, pGlcNAc stimulation of embedded fibroblasts results in fibroblasts alignment as compared to untreated controls, by a process that is Akt1 dependent. Our data shows that in Akt1 null animals pGlcNAc treatment does not increase tensile strength or elasticity. Taken together, our findings suggest that pGlcNAc nanofibers stimulate an Akt1 dependent pathway that results in wound closure, the proper alignment of fibroblasts, decreased scarring, and increased tensile strength during cutaneous wound healing.

Chapter 1

Wound Healing

The primary function of human skin is as a barrier against the environment. Once this protective barrier is lost, the process of wound healing quickly begin in an attempt to prevent further injury or illness. In the United States over 1 million people suffer from burns [1] and another 6.5 million suffer from chronic skin wounds annually. Recent advances in cell and molecular biology have allowed for a better understanding of proper wound healing but also requirements for tissue regeneration. The primary goals of wound treatment are rapid closure and a functional and esthetic scar [2]. Wound healing is an intricate process that requires collaborative efforts of different tissues and involves complex interactions between different cell types, cytokines, and growth factors. The classic model of wound healing can be divided into four sequential, yet overlapping phases: hemostasis, inflammation, proliferation, and remodeling and maturation. **Figure 1.1** depicts the phases of cutaneous wound healing.

Hemostasis

Immediately following injury coagulation and hemostasis take place within the wound [3, 4]. The injured vasculature constricts followed by activation of the coagulation cascade by the endothelium and the platelets. As blood enters the wound site, platelets quickly come into contact with exposed collagen and other extracellular matrix components triggering clot formation. The formation of the clot, which consists of collagen, platelets, fibronectin, and thrombin, funcitons as a protective shield but also a provisional matrix through which cells can migrate to facilitate repair [3, 5]. Importantly, the clot also serves as a reservoir of concentrated cytokines and growth factors that are necessary for the initiation of the wound healing process [5]. These growth factors and cytokines include, but are not limited to, Platelet Derived Growth Factor (PDGF), Vascular Endothelial Growth Factor (VEGF), Transforming Growth Factor Beta (TGFβ), Fibroblast Growth Factor (FGF), and Interleukin 1 (IL-1) (**Table 1**). Conditions that involve inadequate clot formation illustrate the importance of the hemostatic process to wound healing. For example, a deficiency of Factor XIII, which is necessary for stabilizing fibrin, is associated with impaired wound healing [6, 7]

Inflammatory Phase

Following clot formation, cellular signals are generated that result in recruitment of inflammatory cells to the wound site. Neutrophils and monocytes are the predominant cells at the site of injury during the early stages while macrophages arrive during the later phase of inflammation [8]. Both neutrophils and monocytes are recruited to the site from circulation following changes in the endothelial cell

Growth Factor	Source	Function
EGF	Platelets	Keratinocyte mitogen
FGF	Macrophage, Endothelial cells	Angiogenic, Fibroblasts mitogen
VEGF	Keratinocytes, Macrophages	Angiogenesis
TGFβ1/TGFβ2	Platelets, Macrophages	Keratinocytes migration, fibroblasts matrix synthesis and remodeling
TGFβ3	Macrophages	Antiscarring
TGF-α	Macrophages, Keratinocytes	Keratinocyte mitogen
KGF (FGF 7)	Dermal fibroblasts	Keratinocyte mitogen
PDGF	Platelets, macrophages	Chemotactic for various cell types, fibroblast mitogen
TNF-α	Neutrophils	
IL-1α and IL-1β	Neutrophils	Activators of growth factor expression

TABLE 1. Table illustrating Growth Factors and Cytokines and their related function in wound healing .

Table adapted from “Wound Healing--Aiming for Perfect Skin Regeneration.” Science 4 April 1997: vol. 276 no. 5309 75-81 [5].

lining of the vasculature at the wound site [9]. Neutrophils arrive to the wound site within minutes of injury and serve to cleanse the wound of foreign particles and the initial influx of bacteria. More recent studies show that neutrophils are also an important source of pro-inflammatory cytokines that may function as some of the earliest signals to activate keratinocytes and fibroblasts [10]. Neutrophil infiltration typically subsides after approximately 48 hours and macrophages become the predominant inflammatory cells. Macrophages continue the clearance of debris and pathogenic organisms. Additionally, once macrophages are activated, they release a myriad growth factors and cytokines at the wound site including TGFβ, TNFα, VEGF, PDGF, and FGF [5]. Since activated macrophage are responsible for clearing debris and releasing these important factors with known roles in granulation tissue formation, angiogenesis, and fibroblasts proliferation and recruitment, one could argue their importance as regulators of the transition between inflammation and repair. The necessity of macrophages to wound repair is even more evident after recent work utilizing animal models genetically engineered for inducible macrophage depletion. Mice depleted of macrophage pre-injury show defects in re-epithelialization, granulation tissue formation, angiogenesis, and myofibroblast associated wound contraction [11, 12]. More recent data indicates functional phenotypes of macrophage exist. Macrophages exhibiting a classical phenotype have been designated “M1” while other macrophages are designated alternative or “M2.” M1 macrophages are considered to be proinflammatory while M2 cells are

considered anti-inflammatory and may play a critical role in tissue repair and remodeling [13]

Proliferative Phase

The proliferative phase is characterized by the formation of new blood vessels, granulation tissue, and collagen deposition by fibroblasts, keratinocyte proliferation and migration, and wound contraction. An important component of the proliferative phase is epithelialization. In response to cytokines and growth factors, wound margin epithelial cells proliferate and migrate over the wound bed to reestablish the protective barrier. Macrophage produce TGFα which stimulates epithelial proliferation [14] while fibroblasts synthesize and secrete keratinocyte growth factor (KGF) and IL-6 which stimulates keratinocytes to migrate into the wounded area and differentiate into the epidermis [15].

The new connective tissue filled with numerous capillaries during the healing process is termed granulation tissue. During this time, macrophages provide growth factors that stimulate vascularization and fibroblasts produce the new extracellular matrix that is necessary for healing [2]. Angiogenesis, an essential step during the proliferative phase, is an intricate complex that is required to sustain the new tissue. While recent data shows that many molecules may be responsible for the induction of angiogenesis, the most common stimuli are FGF and VEGF production by macrophage and endothelial cells [2]. It has also been shown epidermal keratinocytes can secrete large amounts of VEGF during wound healing [16]. Structural proteins such as fibrin, fibronectin, and hyaluronic

acid help to form this provisional matrix, which serves as a scaffold for cell migration [17].

Maturation and Remodeling

The remodeling and maturation phase of wound healing occurs for weeks up to a year after injury. Once abundant amounts of collagen have been deposited into the wound, the fibroblasts stop producing collagen and the granulation tissue is replaced with a scar. Collagen remodeling is dependent on both the low rate of deposition and its catabolism [2]. Matrix metalloproteinases (MMPs), secreted by macrophages, epidermal cells, fibroblasts, and endothelial cells, are responsible for degradation of collagen in the wound [18] while a balance of MMPs and tissue inhibitors of metalloproteinases (TIMP) are required for repair. Excessive collagen deposition can lead to hypertrophic scarring while more effective deposition will lead to a scar with decreased tensile strength of the healed wound [3].

The collagen in uninjured skin is approximately 90% type I and 10% Type III. During the stages of granulation tissue and early matrix formation of a healing wound, collagen type III makes up approximately 30%, but the ratio decreases back to normal levels in the mature scar [19]. Collagen synthesis and maturation continues for several weeks after wounding resulting in increased amounts of collagen and also the deposition of thicker, more organized collagen fibers. The final result of healing is the formation of a scar, as the collagen does not become as organized as the collagen found in uninjured skin [3]. Resultant wound

strength doesn’t return to normal level with tensile strength and reaches approximately 80% of the original strength one year post injury [20, 21].

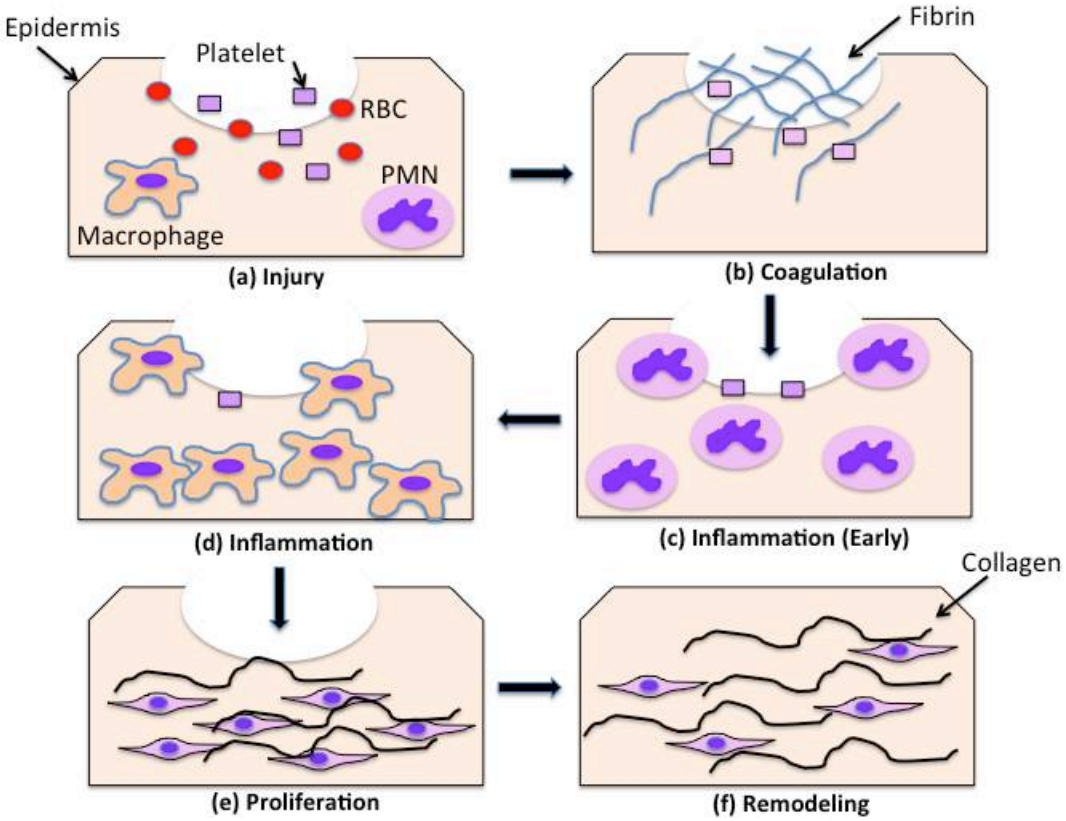

Figure 1.1. Illustration depicting the phases of cutaneous wound healing. (a) Immediately following injury, blood elements are present and neutrophils, platelets and plasma proteins infiltrate. (b) Platelets aggregate with fibrin causing coagulation. (c) Platelets release several which attract PMNs to the wound. (d) Macrophages replace PMNs as the principal inflammatory cell. (e) The proliferation phase begins with fibroblasts being recruited to the site and begin to synthesize collagen. (f) Remodeling of collagen occurs for weeks to months after injury.

Image adapted from *Expert Reviews in Molecular Medicine: Vol. 5; 21 March* 2003

Wound Contraction

Closure of cutaneous wounds involves epithelialization and matrix deposition, but also contraction to bring wound margins together. Contraction of these underlying granulation tissue and extracellular matrix typically results in scar formation. Most studies surrounding wound contraction focus on wound fibroblasts, which are normally quiescent, but become activated shortly after cutaneous wound healing [22]. As early as the 1950's, investigators began to question which component of the healing wound was responsible for the tensile forces and contraction. In 1972, Giabanni *et al.* demonstrated that isolated granulation tissue could undergo smooth muscle-like contraction *in vitro* and that specialized cells within this tissue shared features of smooth muscle cells such as actin filament bundles [22, 23]. The cells, now termed "myo-fibroblasts" were proposed to be responsible for force generation involved in wound contraction [22] and their presence in contractile tissues is fairly well known today.

Myofibroblasts

Myofibroblasts in cutaneous wounds arise from the differentiation of tissue fibroblasts and circulating fibrocyte progenitors [24], both of which migrate into the center of the wound site. Once the wound granulation tissue is populated with myofibroblasts expressing α-smooth muscle actin (α-SMA) contraction begins [25]. While the role of TGF-β in wound healing and scar formation is widely studied, data also indicates that TGF-β along with other growth factors and

cytokines play an important role in myofibroblast activation and therefore contraction. The addition of TGF-β *in vitro* greatly enhances the ability of fibroblasts to contract collagen gels [26]. TGF-β1 is now considered the most important growth factor in development and differentiation of myofibroblasts by inducing the expression of α-SMA [27] as well as a number of cytoskeletal proteins important for the contractile apparatus [28].

In addition to activation by growth factors, myofibroblast activation is also controlled by the mechanical microenvironment. Fibroblasts in normal unwounded tissue are stress-shielded by the crosslinked ECM, the protective structure is lost in injured tissue that is undergoing healing and remodeling [24]. Studies using collagen gels to simulate *in vivo* environments help to elucidate the role of tension in myofibroblasts differentiation. Fibroblasts cultured in “floating gels” with a lack of tension show a lack of actin stress fiber formation. Fibroblasts cultured in attached gels, and therefore provided with of under tension, demonstrate the rapid appearance of actin stress fibers is seen, consistent with myofibroblast morphology [29].

Stress Fibers

Previous studies have shown that wound healing is associated with the appearance of these myofibroblasts, which contain prominent microfilament bundles (stress fibers) that exhibit contractile ability [30]. These stress fibers have been proposed to function as contractile organelles of the cell [31]. Stress fibers contain bundles of 10-30 actin filaments and are held together by actin crosslinking protein α-actinin [32]. More specifically, the contractile apparatus

formed by myofibroblast is composed, at least in part, of F-actin microfilament bundles, α-actinic and non muscle myosin[33]. While some functions of myofibroblasts in wound healing remain unclear, evidence suggests a role for both contraction and mediation of extracellular matrix and remodeling [34]. Interesting, studies in corneal myofibroblasts have demonstrated that these cells establish an interconnected meshwork in which other cells and cellular processes temporally orient parallel to the wound margins during contraction [35]. Petroll *et al.* reports, at least in rabbit corneal healing, the stress fibers develop a unique pattern of alignment parallel to the long axis of the wound [33]. Comparison of fibrobalsts expressing various levels of α-SMA suggests increased α-SMA expression enhances fibroblast contractile activity [36]. The signaling required for formation and maintenance of the actin stress fiber apparatus is mediated by Rho GTPases [37]. While further studies are required to clarify the many funcitons of the myofibroblasts, it is clear that the actin cytoskeleton is critical to the role in wound healing.

Tensile Strength

The skin has important protective functions against mechanical trauma such as friction, impact, pressure, cutting, and shear [38]. Initially after tissue injury, tensile strength of healing skin is fairly weak due the disorganization of the newly formed collagen and extracellular matrix. While collagen and ECM is remodeled to better resist mechanical force, the final tensile strength of the healed wound never reached the strength of uninjured tissue. Over time, the matrix in the healing wound changes. The thinner collagen fibers that are deposited after

injury organize along the stress of the wound which results in increased tensile strength [39]. Collagen fibers and the ECM continue to go through remodeling for up to 1 year, but after three months of healing wound tensile strength does not exceed 80% of unwounded tissue [40].

Insights from Fetal Wound Healing

The primary goal of wound healing treatment is to induce rapid closure but also produce a functional and esthetic scar. In contrast to adult wound healing, early gestation fetal wounds remarkably heal without scar. Scarless fetal wound healing has been confirmed in both animal models and humans [41]. Scarless healing is age dependent, with human embryos exhibiting normal scarring after 24 weeks of gestation and mice begin scarring on embryonic day 18.5 [41, 42] Initially, scarless fetal healing was thought to be a result of the environment *in utero*. Investigators hypothesized that the lack of bacteria and inflammatory mediators in the amniotic fluid resulted in scarless repair. Supporting data shows fetuses that are challenged with bacteria or artificially stimulated to produce an inflammatory response heal with normal scarring [43, 44]. Conversely, other groups showed adult skin that is placed in the fetal environment heals with normal scar formation [45]. Additionally, marsupials, which develop outside of the uterus heal without scar [46] indicating that the uterine environment alone cannot account for the phenomenon of scar-free healing. Much of the current wound healing research is geared toward understanding the differences between adult and fetal wound healing in an effort to better understand the mechanisms underlying tissue regeneration and scar formation. While the exact mechanistic

differences between fetal and adult wound healing remain unknown, significant differences exist among the inflammatory responses, extracellular matrix, cellular mediators, and gene expression profiles of fetal and postnatal wounds [41]. Many of the critical proteins necessary for normal adult wound healing differ in expression or their expression patterns in fetal wound healing.

In contrast to adult epidermal cells that crawl across the wound bed, embryonic epidermal cells are pulled across the wound by actin fiber contraction [47] which causes a rapid reepithelialization. This actin cable assembles almost immediately after injury and requires Rho, a GTPase, for re-epithelialization [48]. Additionally, many growth factors and cytokines show differential expression during fetal wound healing. The differential expression of TGFβ appears to be critical to the lack of scarring seen in fetal wounds. Embryonic wounds show a rapid induction of TGFβ1, a pro-scarring cytokine, shortly after wounding, but a rapid clearance and return to background levels [49]. This is in comparison to adult wounds which express high levels of TGFβ1 through out the duration of the healing process [5]. Neutralization of TGFβ1 and TGFβ2 during wound healing results in reduced scarring [50] while application of exogenous TGFβ3 has a similar effect [51]. These studies indicate that the balance of TGFβ isoforms may play a critical role in scarless repair. **TABLE 1.3** illustrates that a number of differences when comparing adult to fetal healing.

The variances between adult and fetal extracellular matrix may also play a critical role in scarless repair. In fetal wounds, type III collagen is deposited in a fine,

reticular pattern that is indistinguishable from normal skin [52] while postnatal wounds show a higher proportion of collagen type I [53]. Additionally, there are

Adult Wound Healing	Fetal Wound Healing
Slower healing with scar formation	Rapid Healing Response, Scarless
Collagen III : Collagen I ratio lower	Collagen III: Collagen I ratio higher
Increased levels of TGF-β1	Low levels of TGF-β1
Delayed expression of TGF-β3	Increased levels and quicker expression of TGF-β3
Collagen thick and disorganized	Collagen fine and reticular
Lower VEGF levels	Increased VEGF levels
Increased MMP levels	Decreased MMP levels
Myofibroblasts absent/ decreased	Myofibroblasts present

Table 1.3. Fetal vs. Adult Wound Healing. Table is adapted from Namazi et al., 2010 [54] and highlights differences seen when comparing fetal wound healing to normally scarring adult healing

differences in extracellular matrix modulators such as decorin and fibromodulin. Levels of decorin, a proteoglycan that is known to regulate fibrillogenesis of collagen, is up-regulated in adult wounds [55] and decreased expression is associated with pathological scarring in adult models of healing [56]. Fibromodulin, also a modulator of collagen fibrillogenesis is decreased in adult wounds. Interestingly, these extracellular matrix modulators are known to interact with and affect TGFβ expression, which plays an important role in cutaneous scarring [57, 58]. Granulation tissue and myofibroblast expression also plays an important role in the contraction of adult wounds. The presence of myofibroblasts, which are differentiated fibroblasts that express α-smooth muscle actin, is controversial in fetal wound healing. Both mouse and sheep fetal models have been shown to lack α-smooth muscle positive fibroblasts [59] but other groups have shown presence of myofibroblasts in fetal wounds at earlier time points [60]. Fetal wounds also exhibit increased expression of matrix metalloproteinases (MMPs) while expression of their inhibitors (TIMPs) are decreased [61]

Defensins

General Characteristics

Defensins are small (3-4 kDa), cysteine-rich cationic antimicrobial peptides found in mammals, insects, and plants that contribute to host defense against infections. These peptides are classified into subfamilies (α, β, and θ) based on their pattern of disulfide bonding. Antimicrobial peptides carry an average of 40-

50% hydrophobic residues arranged so that the folded peptide is an amphipathic structure [62]. Alpha defensins (α-defensins) are 29-35 amino acids in length maintain the specific cysteine arrangement of C1-C6, C2-C4, and C3-C5 domains, and Beta defensins (β-defensins) are 38-42 amino acids in length and have a C1-C5, C2-C4, C3-C6 cysteine connectivity. HNP1-3 are nearly identical while sequence conservation is mainly limited to the 6 cysteines for the remaining defensins [63]. To date there have been six human α-defensins and four human β-defensins peptides well characterized, though there are many more that have been identified in the human genome. Human α-defensins 1-4, also referred to as human neutrophil peptides (HNP1-4), are typically stored in the primary azurophilic granules of neutrophils, constituting 30-50% of the total protein of these organelles [64] while α-defensins 5 and 6 are typically found in paneth cells of the small intestine. Research has shown that rabbit alveolar macrophages possess α-defensins in levels comparable to rabbit neutrophils [65] indicating defensins are not strictly limited to neutrophil granules. HNPs are released by degranulation of granules in response to proinflammatory stimuli or bacterial stimuli [66].

β-defensins represent the largest family of vertebrate defensins and are constitutively expressed by epithelial cells of the tracheobronchial lining, skin, and kidney where they can be up-regulated in response to infectious or inflammatory stimuli [67]. θ-defensins comprise the most recently identified subfamily of defensins. θ-defensins were discovered in the rhesus monkey and are expressed only in Old World monkeys, lesser apes, and orangutans [63].

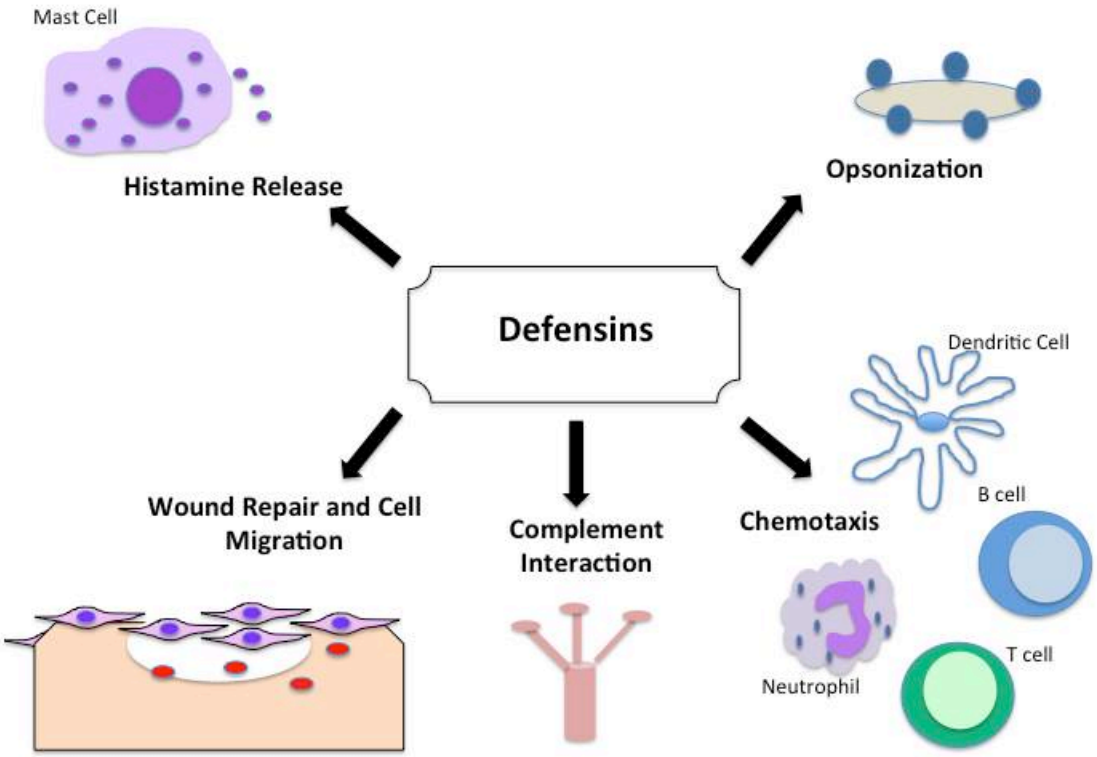

Figure 1.2. Function of Defensins. An Illustration depicting the known various roles of human defensins.

Interestingly, the genes that encode θ-defensins are mutated α-defensins which contain a premature stop codon, resulting in a stop in translation after only 12 residues. While the mechanism is unknown, two of these truncated peptides are spliced together to form a cyclical θ-defensins [63].

Discovery

Approximately fifty years ago, researchers began to focus on the antimicrobial properties of leukocyte extracts. Leukin and phagocytin, acidic extracts from rabbit PMNs, were discovered to be antimicrobial against bacteria [63]. In 1985, these antimicrobial peptides were renamed defensins and recognized as natural peptide antibiotics [63]. In 1991, the first β-defensins were discovered and isolated from bovine trachea al epithelium [68]. Today, β-defensins are much more numerous than their counterpart and interestingly exist in reptiles, suggesting their existence prior to α-defensins [63].

Defensin synthesis and processing

Neutrophil defensins are synthesized in the bone marrow in neutrophil precursor cells [69] as precursor peptides, encoded as a prepropeptide that contains an amino (N)-terminal signal sequence, a propiece, and a (C)-terminal mature cationic defensin [70]. Ganz et al showed that processing of human neutrophil defensins involves sequential cleavage of the preprodefensin to a prodefensin form and then eventually to a mature defensin [70]. While the processing of Paneth Cell defensins (α-defensins 5-6) are similar to that of human neutrophil defensins, the activity of these defensins requires proteolytic activation by matrix metalloproteinase-7 [71]. The β-defensin precursor structure is simpler than that

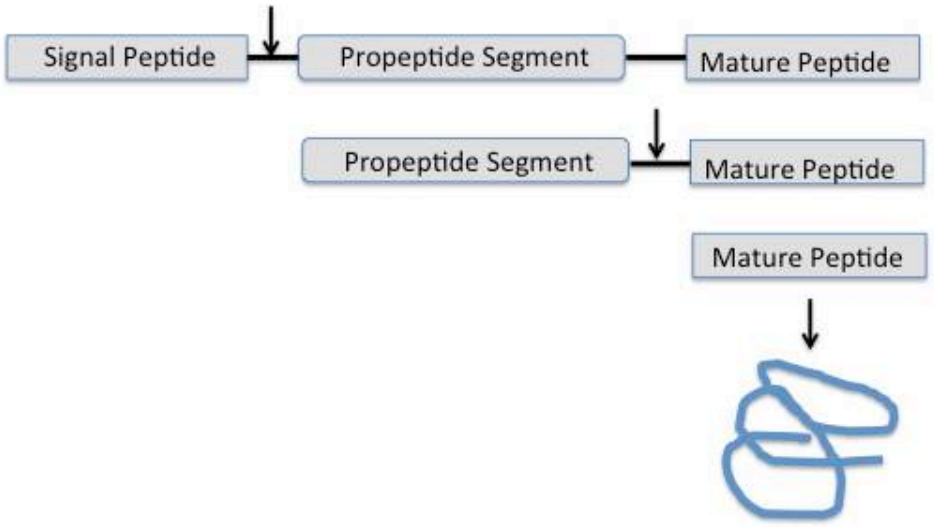

Figure 1.3. Schematic of defensing processing. Neutrophil defensins involves sequential cleavage of the preprodefensin to a prodefensin form and then eventually to a mature defensin

of α-defensins. The structure of the β-defensin precursor consists of signal sequence, a short propiece, and the mature defensin peptide at the C-terminus [72]

Defensin Activity

These small peptides are important effectors of innate immunity; possessing antimicrobial properties that are active against gram positive and negative bacteria, fungi, and many viruses. Despite a growing volume of literature on their role in the innate immune response, details of the mechanism of defensin mediated microbial killing is somewhat unclear. However, studies suggest that the cationic characteristics of the defensins allow them to interact with microbial membranes, forming pores which results in bacterial cell killing [72]; [73]. Studies with *E. coli* revelaed that HNP1-3 permeabilized inner and outer membranes of bacteria. This permeabilization coincided with termination of DNA, RNA, protein synthesis, and the loss of colony forming ability [74]. Recent evidence shows that α-defensin HNP-1 binds to lipid II, a cell wall precursor in the bacterial membrane suggesting that defensins inhibit cell wall synthesis. Furthermore, a decrease in lipid II resulted in decreased bacterial killing by HNP-1 [75]. The non-specific antimicrobial mechanisms employed by defensins may make it difficult for bacteria to develop resistance, making them of great interest in the clinical arena.

While defensins are known antimicrobial agents, it has more recently come to light that these peptides exhibit biological activities beyond the inhibition of microbial cells. Defensins have been shown to contribute to adaptive immune response by exhibiting chemotactic activity on dendritic cells [76] T cells, monocytes, and macrophages [77]. Recent evidence also suggests that β-defensins can cause the recruitment of keratinocytes [78]. Both α- and β-defensins were shown to exert chemotactic activity for dendritic cells both *in vitro* and *in vivo* [76]. β-defensins cross talk with the adaptive immune system by interacting with chemokine and Toll-like receptors on immune cells. Human beta defensin-2 has been shown to interact with the CCR6 receptor in immature dendritic cells and T cells; recruiting these cells to sites of interest [79]. Additionally, human β-defensin-3 demonstrates high affinity for CCR2 on myeloid cells resulting in chemoattraction in the absence of the natural ligand [80].

While θ-defensins have comparable antimicrobial properties to α-defensins, their antiviral properties are far superior. It has been reported that θ-defensins can protect cells from infection by HIV-1 *in vitro* [81] and herpes simplex virus type 1 and 2 [82]. θ-defensins were shown to inhibit the formation of the HIV-1 proviral DNA, indicating that they most likely inhibited viral entry [83]. Recent studies have also indicated that θ-defensins show antiviral activity against Influenza A via impairment of the viral hemagglutinin [84].

Defensins in Disease

As described, defensins are advantageous in many situations, but there are instances when defensin expression may be potentially detrimental. Defensins

are an imperative part of the host immune system, it is not surprising that they have been implicated in several conditions or diseases. There is new evidence suggesting some of these molecules may promote neoplasia. Overexpression of human beta defensin-3 in solid tumors promotes selective chemoattraction of myeloid cells to the site and stimulates the secretion of pro-inflammatory cytokines that contribute to tumor growth [85]. Furthermore, increased expression of human beta defensins-2 and -3 were associated with oral cancer lesions [80].

In Crohn's disease, an inflammatory condition of the intestinal tract, it has been shown that defensin levels are indeed altered. This disturbance in defensin levels may cause commensal bacteria to become pathogenic [86]. Skin diseases, such as psoriasis, show increased levels of human β-defensin- 2 and β-defensin-3 and as a result these lesions are rarely infected. Indeed, psoriasis skin was the organ used to identify human production of β-defensin-2 and -3 [87]. Conversely, atopic dermatitis shows decreased levels of β-defensin-2 and β-defensin-3 resulting in a skin condition that is commonly accompanied by fungal, viral, and bacterial infections [88]. Symptoms resulting from Cystic Fibrosis, such as recurring infections and inflammation, may also be the result, at least in part, of disturbed defensin levels [89]. It has been documented that defensin activity is inhibited in high salt environments [72]. Cystic Fibrosis lung fluid has been reported to be extremely high in salt and it is this environment that may be responsible for the inhibition of defensin activity.

Defensins in Wound Healing

Due to their antimicrobial and chemotactic effects, it is logical that defensins likely play an important role in wound healing. Evidence shows that defensins are stimulatory for epithelial cells and fibroblasts [90], two cell types that contribute greatly to the normal wound healing process. Niyonsaba et al. has demonstrated that β-defensins increased keratinocyte proliferation and migration [78]. Additionally, human β-defensin-2 was shown to stimulate chemotaxis and mobility of human umbilical vascular endothelial cells *in vitro* as well as stimulating the formation of capillary networks in matrigel [91]. Human β-defensins can also up-regulate the transcription of MMPs and decrease that of TIMPs suggesting a role in tissue remodeling responses [92]. Hirsch et al. showed that human β-defensin-3 treatment of *S. aureus* infected wounds both decreased bacterial and increased wound closure, suggesting a potential therapeutic for diabetic wounds [93]. Furthermore, *in vitro* experimentation with airway epithelial cells show that α-defensins 1-3 caused a dose and time-dependent increase of wound closure as well as increased cell migration that required activation of PI3-K and ERK1/2 pathways [94].

AKT1

Akt structure

The Akt family of serine threonine kinases are known downstream effectors of phosphoinositol-3-kinase (PI3K). PI3K can be activated by numerous cellular stimuli, such as growth factors, G-protein coupled receptor activation, or integrin activation. This kinase is responsible for the conversion of phophoinositol 4,5 phosphate (PIP2) to phosphoinositol 3,4,5 phosphate (PIP3). PIP3 formation at

the membrane is required for the recruitment of Akt to the membrane to allow phosohorylation of the Thr 308 site by phospho- inositide- dependent kinase-1 (PDK1) [95-97]. The second phosphorylation site, Ser473, is apparently controlled in an mTOR dependent nature (mTOR2/Rictor). As shown in **Figure 1.4**, the Akt subfamily is comprised of three isoforms (Akt1, Akt2, and Akt3). The three mammalian isoforms, which are products of distinct genes, share a conserved structure that includes an N-terminal pleckstrin homology (PH) domain, a central kinase domain, and a C-terminal regulatory domain[98]. The three specific isoforms share approximately 80% homology [96, 99]. The PH domain binds phosphoinositides with high affinity, specifically phosphatidylinositol(3,4,5)trisphosphate (PIP3) or phosphatidylinositol (3,4)-bisphosphate (PIP2) [98]. The kinase domain which is located in the center, is structurally similar to other kinases such as PKC and PKA [100]. Akt1 is activated by phosphorylation of both Thr308, which is located in the activation loop of the kinase domain, and Ser473 located within the hydrophobic motif (HM) [96].

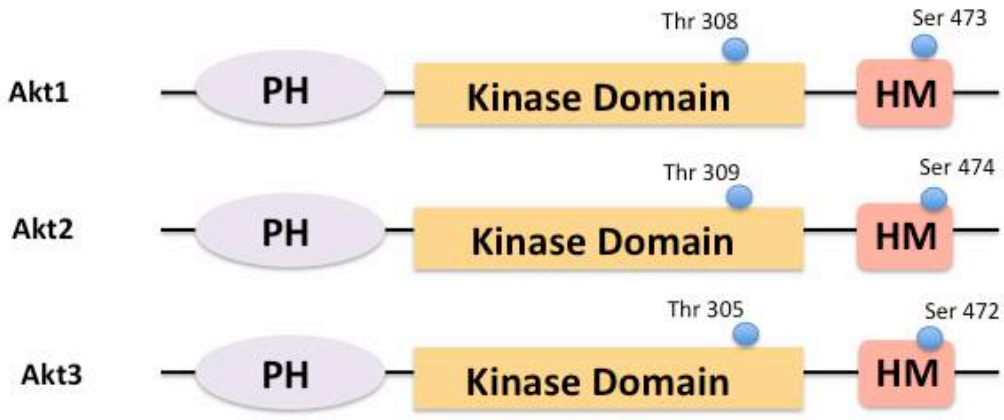

Figure 1.4. Akt Isoforms. Image illustrates the similarities and differences between the three isoforms of Akt. Image adapted and partially recreated from "Protein Kinase B At a Glance" Journal of Cell Science. [96]

Akt1 signalling

Akt, also known as protein kinase B (PKB), is a serine threonine protein kinase that has known roles in cell survival, migration, metabolism, and proliferation. Akt was originally identified as the oncogene in the transforming retrovirus Akt8 [101]. The Akt family of serine threonine kinases are known downstream effectors of PI3K signaling. Activation of Akt requires recruitment to the plasma membrane and subsequent phosphorylation at the threonine and serine residues. PI3-Kinase is activated and PIP2 (ILK) [102, 103] and the mammalian target of rapamyacin complex mTOR2 [104] are PDK2 molecules, although other molecules may also serve this role. PI3K activation can be regulated by the tumor suppressor PTEN by the dephosphorylation of PIP3 → PIP2 therefore decreasing the activity of Akt1[95]. While Akt1 signaling is complex, **Figure 1.5** illustrates Akt1 as a central regulator of many cellular functions depicts common targets for Akt.

Akt function

Akt is most well known for cell survival regulation and antiapoptotic, cancer promoting activity. BAD, a member of the Bcl-2 family of proteins that binds to promote apoptsis, but when phosphorylated by Akt1 pro-apoptotic activity is lost [105]. Akt has also been reported to phosphorylate Caspase-9, an initiator of apoptosis, resulting in ablation of its activity [106]. Furthermore, data shows that Akt can also regulate cell survival through modulation of transcription

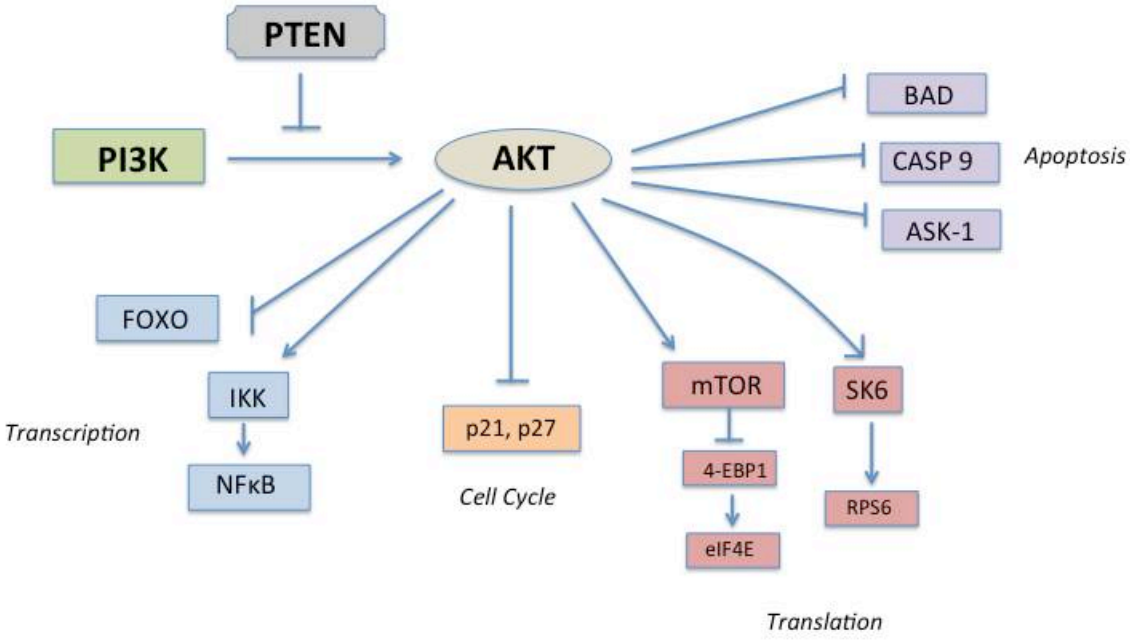

Figure 1.5. Akt signaling. Above diagram depicts a simplified version of AKT signaling. AKT plays a central role in many cellular functions including transcription, cell cycle control, translation initiation, and apoptosis.

factor activity. The Forkhead family of transcription factors may be directly phosphorylated by Akt, resulting in inhibition of forkhead transcription factors and subsequent apoptosis [107]. Akt also inhibits IκB via the regulation of IKK activity, which leads to the nuclear translocation and activation of the transcription factor NFκB, resulting in transcription of pro-survival genes [108].

While the anti-apoptotic actions of Akt are heavily studied, Akt also regulates other cellular functions such as migration, protein synthesis, and glucose metabolism [109]. Several developmental studies have shown that activated PI3K/Akt contributes to EMT driven mesoderm formation [110]. Furthermore, PI3K is required for TGFβ-mediated cell migration in mammary epithelial cells [111]. Interestingly, evidence shows that there may be isoform specific roles in cell migration. Additionally, Akt has been shown to be important for vascular homeostasis and angiogenesis. Vascular Endothelial Growth Factor (VEGF) dependent effects on cell survival and migration have been shown to be regulated bu the Akt pathway [112] .

Animal Models

Akt1, Akt2, and Akt3 knockout animals exhibit mild phenotypes which suggests functional redundancy, but these animals are on a mixed background which may mask specific phenotypes. While this redundancy does exist, there is evidence

that supports each family member having distinct roles. Akt1 is thought to act on cell size with Akt1 deficient animal exhibiting growth retardation and increased apoptosis [113] as well as neonatal mortality [114]. Akt2 is important for insulin induced glucose uptake [115]. Mice deficient for Akt2 display insulin resistance and a type 2 diabetic-like phenotype [116]. Recently, our lab has shown that Akt3 is involved in the regulation of mitochondrial biogenesis in endothelial cells [117].

To better to understand the *in vivo* roles of the PKB isoforms, animal models lacking various combinations of isoforms have been generated. Mice lacking both Akt1 and Akt2 exhibit severe growth deficiency, impaired skin and bone formation, and do not survive long after birth [118]. Mice deficient of both Akt1 and Akt3 show numerous developmental abnormalities that prove lethal around embryonic day 11 [119]. The severe phenotypes and lethality associated with these double knockout animals reiterates functional redundancy *in vivo.* Conversely, Akt2/Akt3 knockout animals display growth deficiency, impaired glucose homeostasis, and decreased brain size, but survive postnatally [120].

Akt1 in Wound Healing

The PI3K→ Akt pathway has been shown to be a regulator of VEGF stimulated endothelial cell survival [112] and has been known to play a key role in the formation of new vessels, an essential component of healing. VEGF enhancement of endothelial cell motility and tubule formation is Akt dependent [121]. It has previously been shown that Akt mutations result in abnormal

tracheal formation in Drosophila, a model system for tubulogenesis [122]. In addition to its known role in angiogenesis, Akt1 has also been implicated as a regulator of tissue growth, which is evident in mice lacking Akt1 that exhibit growth retardation [113].

An interesting study by Zhao *et al.*, based on the premise that disruption of the epithelial layer generates endogenous electric fields that are important for wound, shows that the PI3K pathway is essential to these cues. These electric fields are decreased upon ablation of PI3K, abolishes directed cell movement and migration during the healing process [123]. Recent work to further elucidate the PI3K→Akt→ mTOR pathway in wound healing shows that mTOR activation can enhance epithelial cell proliferation, migration, and wound healing, while pharmacological inhibition of mTOR delays wound closure [104]. Interestingly, several molecular pathways involved in cancer cell progression have recently been shown to also promote tissue regeneration [124]. As the PI3K → Akt1 pathway is frequently dysregulated in cancer, it is likely that Akt1 plays an important role in wound healing and tissue regeneration as well.

Poly-N-acetyl glucosamine nanofibers (pGlcNAc), a wound healing facilitator

Since the 1970s, increased effort has been directed at searching the ocean and its organisms for novel biomolecules.and marine natural products. Marine organisms have been a rich source of compounds and several marine products are currently in clinical trials for use in treating cancer and infections. Marine natural products exhibit high physiological activity in humans with the most

commonly seen activities being their uses as antibiotics, anti-inflammatory, antivirals, anticoagulants, analgesics, and antitumorogenic. These properties give marine natural products great potential in the clinical arena for treatment of infections, pain, immune diseases, and cancer [125]. Here, I will discuss the characteristics of a Poly-N-Acetyl glucosamine nanofiber derived form a marine diatom. This nanofiber has proved to be an effective hemostatic agent, but currently shows promise as a cutaneous wound healing agent.

Isolation, Purification, and Characterization

The pGlcNAc material is a unique polymer structure that is isolated and purified from large scale cultures of microalga. The strap like fibers grow from the pores of the diatom and are composed of highly crystalline β1→4 poly-N-acetyl glucosamine nanofibers. Studies focused on characterization of pGlcNAc fibers used for hemostasis show that the fibers are approximately 100μm in length and 0.5 μm in width and consist entirely of N-acetyl glucosamine sugar residues [126]. Elemental analysis of pGLcNAc confirms the material is composed of 47.3% Carbon, 6.4% Hydrogen, and 6.9% Nitrogen which is consistent with its chemical structure. Viscosity studies indicate that the average molecular weight of the fully acetylated polymer is approximately 2.8×10^6 Da and consists of approximately 50 polysaccharide molecules in which each sugar is N-acetylated [126].

Structural comparison of pGlcNAc and chitosan indicate that pGLcNAc has a unique three-dimensional structure that is highly ordered and repetitive compared

to the randomly structured chitosan [126]. Structural analysis also shows that pGLcNAc fibers are oriented in a parallel fashion and are held together in a unique three-dimensional beta crystalline conformation while other polymers such as chitin and chitosan are known to exist as random coil polymers [127]. To examine the efficacy of pGlcNAc fibers in wound healing, gamma radiation of the original pGLcNAG fibers (NAG) was used to shorten the fibers (sNAG) to an average length of 4-7 μm and a thickness of 40 – 60nm. After treatment, the polymers maintain their unique three-dimensional structure [128].

pGlcNAc, a hemostatic agent

Concentrated efforts have been made in the development of hemostatic agents to be used to control bleeding in wounds and during surgical procedures. The development of therapeutic compounds that consist of polymers containing N-acetyl glucosamine derived from natural sources such as chitins and chitosans has increased dramatically in the recent years; however, use of these materials is limited by their chemical variability and limited efficacy [127, 129-131]. A newly defined polymer, poly-N-acetyl glucosamine (pGlcNAc) was found to be an effective hemostatic agent during trauma and surgical procedures [132, 133]. When compared to Chitosan based hemostatic products, pGLcNAc nanofibers are able to significantly reduce the *in vitro* fibrin clot formation time of plasma samples and has the abiity to cause red blood cell aggregation *in vitro* [127]. The mechanism of action is not fully understood but treated platelets are fully and irreversibly activated resulting in the fibrin network formation [134]. Platelet

activation by these nanofibers is mediated by the association of pGlcNAc with integrin β3 and activation of integrin mediated signaling [135].

pGlcNAc in Wound Healing

Recent studies suggests that pure isolations of highly homogenous poly-N-acetyl glucosamine nanofibers (pGlcNAc) from a marine diatom may be an excellent therapeutic for the treatment of wounds. Treatment of cutaneous wounds with pGlcNAc nanofiber-derived membranes results in marked increases in the kinetics of wound healing. In a diabetic mouse model where wound closure is greatly delayed, pGlcNAc treatment results in a 90% closure, 9 days faster than the untreated control [136]. Studies using the shortened, more biodegradable, nanofibers showed that sNAG treatment accelerated wound closure *in vivo* and stimulated cell metabolism and migration of endothelial cells and fibroblasts *in vitro* [128]. Treatment with pGlcNAc also induces angiogenesis, apparently due to a direct effect on endothelial cells [137]. pGlcNAc treated wounds also exhibited increased vascularity, proliferation, and granulation tissue volume during healing. mRNA levels of MMP3 and MMP9, which are related to extracellular matrix remodeling in wounded tissue, are significantly increased when diabetic mouse wounds are treated with pGlcNAc [128]. Additionally, treatment of cultured primary endothelial cells derived from human umbilical vein (EC) in the absence of growth factors or serum, results in increased cell motility that is integrin mediated and dependent on the Ets1 transcription factor [137].

30,000x

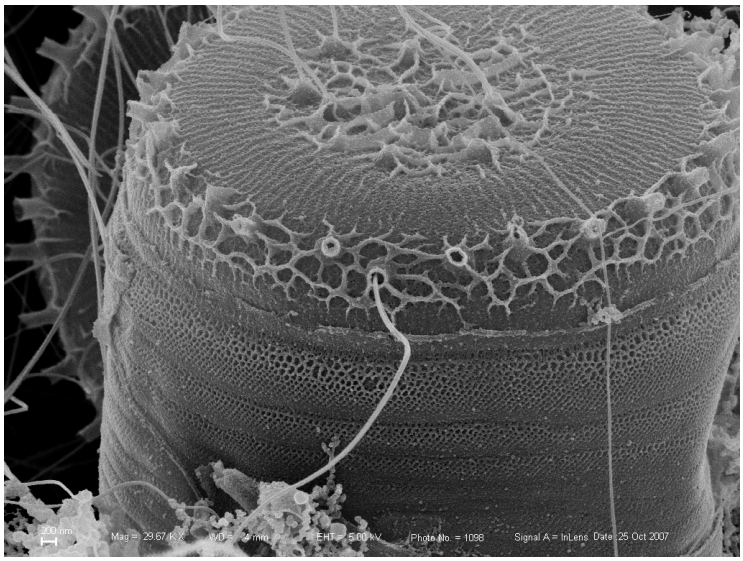

70,000x

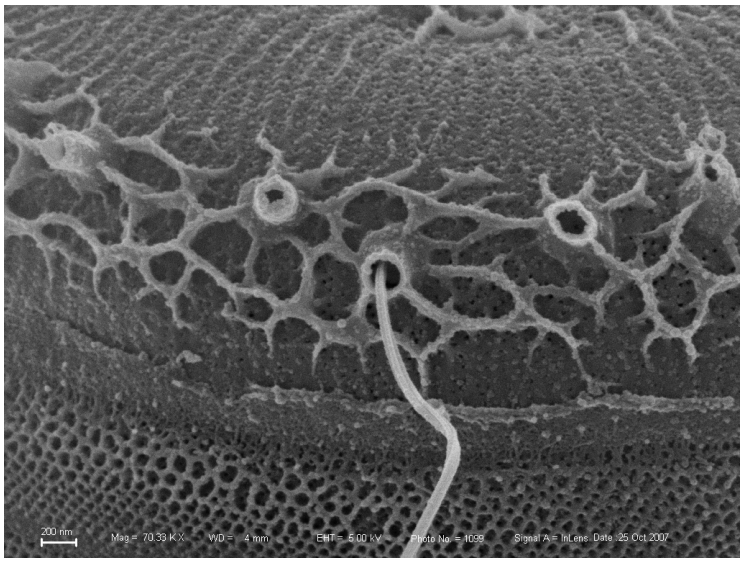

Figure 1.6 Poly-N-Acetyl Glucosamine Nanofibers. SEM images of marine diatom and high molecular weight polysaccharide nanofibers bring extruded from pores located at the ends of the cylindrical body.

Image Credit: Dr. Tom Fischer, Francis Owens Blood Lab. University of North Carolina @ Chapel Hill

CHAPTER 2

Tissue Culture, Pharmacological Inhibition

Human umbilical cord vein EC (Lonza) were maintained at 37˚ with 5% CO_2 in endothelial basal medium 2 (Lonza). Endothelial basal medium 2 (EBM2) was supplemented with EC growth medium 2 SingleQuots as described by Lonza procedures and 1% penicillin/streptomycin (Invitrogen). Serum starvation was performed at 80-90% confluency in EBM2 supplemented with 0.1% fetal calf serum (Valley Biomedical) for 24 hours followed by stimulation with highly purified pGlcNAc (50µg/ml) nanofibers (sNAG) in sterile water (provided by Marine Polymer Technologies, Inc., Danvers, Mass., USA). The pGlcNAc diatom-derived nanofibers used in this study are short biodegradable fibers derived from a native, longer form (NAG), and have an average length of 4-7µm and a polymer molecular weight of approximately 60,000Da. For inhibition using PD098059 (50µM) or wortmannin (100nM), cells were pre-treated for 45 minutes prior to 3 hour stimulation with sNAG (50µg/ml).

Lentiviral Infection

Mission shRNA lentiviral constructs directed against Akt1 were purchased from Sigma/Aldrich. A scrambled pLKO.1 shRNA vector was purchased from Addgene. Lentiviruses were propagated in 293T cells, maintained in DMEM supplemented as above. Lentiviral production was performed using psPAX2 and pMD2.G packaging vectors purchased from Addgene using the protocol for producing lentiviral particles from Addgene. For infection of target cells, 7.5 X 10^5 cells were plated on 100 mm^2 plates and allowed to incubate overnight. The next day, cells were transduced using a final concentration of 1 μg/ml polybrene and either scrambled control or Akt1 shRNA lentiviruses. After transduction, endothelial cells were serum starved overnight and stimulated with sNAG (50g/ml) for 3 hours. All infections were monitored for appropriate knockdown by RT-PCR.

RT-PCR

For semi-quantitative RT-PCR, RNA was extracted with RNAsol (Teltest, Inc.) following manufacturer's instructions. cDNA was synthesized from 2 μg total RNA with a Superscript First Strand Synthesis Kit (Invitrogen), using Oligo(dT) following the manufacturer's instructions. PCR reactions contained equal amounts of cDNA and 1.25 μM of the appropriate primer pair (Sigma-Proligo, St. Louis, MO, USA). All primer sequences used in these analyses are as follows:

Akt1 F	5' GAGGCCGTCAGCCACAGTCTG 3'
Akt1 R	5' ATGAGCGACGTGGCTATTGTG 3'
β-Defensin3 F	5' GTGGGGTGAAGCCTAGCAG 3'
β-Defensin 3 R	5' TTTCTTTCTTCGGCAGCATT 3'
α-Defensin1 F	5' CACTCCAGGCAAGAGCTGAT 3'

α-Defensin1 R	5’ TCCCTGGTAGATGCAGGTTC 3’
S26 F	5’ CTCCGGTCCGTGCCTCCAAG 3’
S26 R	5’CAGAGAATAGCCTGTCTTCAG 3’

Cycling conditions were: 94°C for 5 min; 30-35 cycles of 94°C for 1 min, 55-65°C (based on primer T_m) for 1 min, 72°C for 1 min; 72°C for 7 min and cooled to 4°C. Cycle number was empirically determined to be within the linear range of the assay for each primer pair used. All semi-quantitative RT-PCR was performed with the ribosomal protein subunit S26 primers as internal controls. Products were visualized on a BioRad Molecular Imaging System (Hercules, CA, USA). Real time PCR was performed using a Brilliant CYBR green QPCR kit in combination with an Mx3000P Real-Time PCR system both purchased from Stratagene. Primers detecting the ribosomal subunit S26 were used as internal controls.

PCR analysis of Tissue

For semi-quantitative RT-PCR cDNA was synthesized from total RNA (2-5μg), isolated from 5 day post wound tissue (treated and untreated) using RNA-STAT 60 (Tel-Test, Inc.) in procedures described by the manufacturer, with a Superscript First Strand Synthesis Kit purchased from Gibco BRL using Oligo(dT) following the manufacturer’s instructions. PCR reactions contained equal amounts of cDNA and 1.25μM of the appropriate primer pair (IDT, Inc.). The primer sequences are as follows: Collagen I: forward 5’ ACGGCTGCACGAGTCACAC 3’, reverse 5’ GGCAGGCGGGAGGTCTT 3’,

Collagen III: forward 5' GTTCTAGAGGATGGCTGTACTAAACACA 3', reverse 5' TTGCCTTGCGTGTTTGATATTC 3' and HPRT: forward 5' AAGGACCTCTCGAAGT

GTTGGATA 3' reverse 5' CATTTAAAAGGAACTGTTGACAACG 3'. Cycling conditions were: 94°C for 5 min; 20-35 cycles of 94°C for 1min, 50-65°C (based on primer T_m) for 1min, 72°C for 1min 45sec + 2sec/cycle; 72°C for 7min and cooled to 4°C. Cycle number was empirically determined to be within the linear range of the assay for each primer pair used. All semi-quantitative RT-PCR was performed in tandem with HPRT primers as an internal control.

Excisional Wound Healing Model

Wild Type C57Bl/6 and Akt1-/- [138] were used in all experiments. The Akt1 null animals were created using an insertional mutagenesis strategy at the translational start site that blocks expression of the entire protein. All experiments performed using mice were in accordance with animal procedure protocols approved by the Medical University of South Carolina Institutional Animal Care and Use Committee. Wounding was performed on anesthetized adult male mice between 8-12 weeks old. Two full thickness cutaneous wounds were created using a 4mm biopsy punch (Miltex), to create two identical wounds on each flank. Mice were anesthetized using an O_2/Isoflurane vaporizing anesthesia machine (VetEquip, Inc.). Isoflurane was used at 4% for induction; 2% for surgery. Prior to surgery hair was removed by depilation and the area was washed and sterilized using 70% ethanol. Wounds were either treated with sNAG membrane moistened with distilled water or left untreated. On days 3 and 5 animals were

euthanized and entire wounds were harvested including the surrounding skin using an 8mm biopsy punch (Miltex). Wounds were fixed in 4% paraformaldehyde overnight at 4˚, embedded in paraffin, and sectioned for analysis.

Hematoxylin and Eosin Staining (H&E)

All H&E staining was performed in the Histology Core Facility at the Medical University of South Carolina, Department of Regenerative Medicine and Cell Biology. Briefly, sections were cleared in xylene, rehydrated through a series of graded alcohols, placed in Hematoxylin followed by acid alcohol. Samples were then placed in ammonia water, rinsed in ethanol and exposed to Eosin before dehydrating through graded alcohols and clearing in xylene. Sections were mounted using Cytoseal-XYL (Richard-Allan Scientific). H&E sections were visualized using an Olympus BX40 microscope (4x objective lens, 0.13) and captured using an Olympus Camera (Model DP25) and DP2-BSW acquisition software.

Bacterial Inoculation, Tissue Gram Staining, Colony Forming Unit Quantitation

Male mice between 8-12 weeks were wounded as described above. Single colonies of *Staphylococcus aureus* (ATCC 25923) were picked and cultured overnight at 37˚ and adjusted to an absorbance of OD_{600}= 0.53. One mL of *S. aureus* was spun at 10,000rpm, re-suspended in sterile PBS, and 15µl was used to innoculate each wound. sNAG membranes were applied to the treated group thirty minutes post inoculation. Mice were euthanized on day 3 and 5 post wounding and wounds were harvested using an 8mm biopsy punch. One wound

per animal was fixed overnight in 4% paraformaldehyde at 4˚C and the other wound was cultured and plated on LB media without antibiotic for bacterial quantitation (see below). Wounds for tissue gram staining were embedded in paraffin and sectioned. Sections were cleared in xylene and rehydrated through a series of alcohol and were stained using a tissue gram stain (Sigma-Aldrich) by procedures described by the manufacturer.

For culturing, wound sections were placed in 0.5ml bacterial media an incubated for 30 min at 37^{o}C while shaking. Colony forming units (CFU) were quantitated using a dilution series plated overnight at 37˚C. Number of colonies per plate/per dilution were counted and CFU/ml were calculated. To determine CFU/ml from sNAG treated bacterial cultures, *S. aureus* cultures in solution were treated with varying concentrations of sNAG for three hours. Cultures were then plated overnight at 37˚ and CFU/ml were determined.

β-defensin 3 Peptide Application

Three test concentrations (1.0μM, 2.5μM, 5.0μM) of biologically active human β-defensin 3 peptide (Peptide Institute, Inc.) were tested for their effect on bacterial growth in the infected wound healing model described above. Each concentration negatively affected bacterial growth so the lowest concentration was chosen for analyses. After each wound was infected with *S. aureus*, 10ul of peptide was applied. After three days, wounds were harvested, embedded for sectioning and gram staining, or cultured for CFU/ml quantitation as described above.

β-defensin 3 Antibody Blockade

Wild Type male mice were wounded and infected with 15ul of *S. aureus* as described above. After inoculation, one wound was treated with 0.2ug/mL of β-defensin 3 antibody (Santa Cruz) while the other was treated with 0.2ug/mL of normal goat IgG control antibody (Santz Cruz). sNAG membranes were applied to all mice after antibody treatment on day 0. Antibody was applied every 24 hours. Mice were euthanized on day 3 and wounds were harvested using an 8mm biopsy punch. Wounds were fixed overnight in 4% paraformaldehyde at 4˚C, embedded in paraffin, sectioned, and analyzed using tissue gram stain.

Immunofluoresence, Microscopy

Paraffin embedded tissue sections were re-hydrated through xylene and a series of graded alcohols. Sections were treated with 0.01% Triton-X100 and subjected to antigen retrieval using antigen unmasking solution (Vector Laboratories) in a pressure cooker for 5min and allowed to cool. Sections were incubated in background buster (innovex Biosciences) for 30 minutes prior to antibody testing. Skin sections were labeled with β-defensin 3 goat polyclonal antibody (Santa Cruz), involucrin rabbit polyclonal antibody (Santa Cruz), TO-PRO 3-iodide (Molecular Probes), mouse monoclonal anti-Actin α-Smooth Muscle antibody (Sigma), Vimentin mouse monoclonal antibody (Dako), Phalloidin (Molecular Probes) and DAPI (Molecular Probes). Sections were incubated in primary antibody overnight at 4˚ and appropriate secondary immunofluorescent antibodies (Invitrogen) for 1 hour at room temperature. Control sections for each antibody were stained without primary antibody. Tissue sections were visualized using an Olympus FluroView laser scanning confocal microscope (Model IX70)

and captured at ambient temperature using an Olympus camera (Model FV5-ZM) and Fluoview 5.0 acquisition software. All tissue sections were imaged using 60x oil immersion lens (Olympus Immersion Oil)

HUVECs were either serum starved or treated with sNAG for 5 hours in culture and stained with antibodies directed against α-defensin 5 (FITC), β-defensin 3 (Texas Red), or TOPRO 3 (Blue). Images were taken using immunofluorescent microscopy. Cell culture defensin expression was visualized using a Zeiss Axiovert 100M confocal microscope and was captured at ambient temperature, using water as the medium, using LSM 510 camera (Zeiss Fluor 63xW/1.2A objective).

Western Blot Analysis

Endothelial cells were serum starved prior to stimulation with sNAG (50µl/ml) for a given time course. Cells were then lysed and subjected to Western blot analysis. The antibodies used for Western blot analysis are as follows: anti-p85 subunit of PI3K and phosphospecific Akt antibody (Cell Signaling Technologies).

Scar Quantification, Tensile Strength Measurements, Elasticity Measurements

For scar measurements, wild type mice were wounded as previously described and allowed to heal for 21 days. On day 21, animals were euthanized and scars were measured using a caliper.

For tensile strength, wounded animals were sacrificed after 21 days, wounds were harvested and skin was trimmed (15mm x 7mm) to insure even tension. Wounds, both treated and untreated and unwounded control skin was subjected

to tensile strength and elasticity testing using an Instron 5942 strain gauge extensometer and Bluehill 3 Testing Software. Tensile strength of the skin was determined by measuring the relative stress the skin could bear before breaking 20% and elasticity was measured as the mm of extension.

Masson Trichrome Staining, Picro Sirius Red Staining

Masson's Trichrome stain (Sigma-Aldrich) was performed according to manufacturer's instructions for tissue sections. Briefly, sections were deparrafanized to water and incubated in Bouin's solution. Slides were subjected to a series of incubations using hematoxylin, Biebrich Scarlet-Acid Fucshin, Phosphotungstic/Phosphomolybdic acid solution, Aniline Blue solution, and Acetic Acid as described by the manufacturer tissue sections were then dehydrated, cleared in xylene, and mounted using Cytoseal-XYL (Richard-Allan Scientific). Masson's trichrome sections were visualized using an Olympus BX40 microscope and images were captured using an Olympus Camera (Model DP25) and DP2-BSW acquisition software.

For Picro Sirius Red Staining, tissue sections were fixed stained in iron hematoxylin for 10 minutes followed by a 10-minute rinse in running water. Slides were placed in PSR (Sigma, St. Louis, MO) for 1-hour, followed by three 5-minute rinses in 1% acetic acid. Tissue sections were dehydrated prior to mounting. PSR staining was viewed under polarized light to distinguish mature, thick collagen fibers (red/orange) from the immature, thin collagen fibers (green/yellow) due to their intrinsic birefringence.

Extraction and Biochemical Quantitation of Collagen

Hydroxyproline assays were performed as previously described [139]. Briefly, wound tissue was harvested from wild type mice treated or untreated at 21 days post wounding (n=4 for each). Tissue was lyophilized and weighed to ascertain dry weights and finely ground. Tissue collagen underwent complete acid hydrolysis with 6 N HCl for 18 h at 120°C, and neutralized to pH 7 with 4 N NaOH. One milliliter of chloramine T was added to 2-ml volumes of the collagen sample and incubated at room temperature for 20 min. One milliliter of Ehrlich's reagent (60% perchloric acid, 15 ml 1-propanol, and 3.75 g *p*-dimethyl-amino-benzaldehyde in 25 ml) was added, and samples were incubated at 60°C for 20 min. Absorbance at a wavelength of 558 was read on a spectrophotometer. Collagen was quantified as milligrams of hydroxyproline per gram dry weight of the wound tissue.

Elastin Staining

Tissue sections from wounded animals, as described above, were stained for elastin fibers using Van Geison staining procedures (). Briefly, sections were cleared in xylene, rehydrated through a series of graded alcohols to distilled water, stained in hematoxylin (Sigma-Aldrich), differentiated in 2% ferric chloride and washed. Tissue sections were then stained in Van Geison's counterstain prior to dehydration, clearing in xylene, and mounting with Cytoseal-XYL (Richard-Allan Scientific). Tissue sections were sections were visualized using an Olympus BX40 microscope and captured using an Olympus Camera (Model DP25) and DP2-BSW acquisition software.

Tissue Culture, Fibrin Gel Assay

C3H10 Fibroblasts were maintained at 37°C with 5% CO2 in minimal essential medium with Earle's balanced salt solution (MEM/EBSS, Thermo) supplemented with 1% penicillin/streptomycin (Invitrogen). Normal human fibroblasts (ATCC) were maintained in MEM supplemented with 20% FCS. Serum starvation was performed at 80–90% confluency in MEM/EBSS supplemented with 0.1% fetal calf serum (Valley Biomedical) for 24 hours followed by stimulation with highly purified pGlcNAc (50 µg/ml) nanofiber slurry (sNAG) in sterile water (provided by Marine Polymer Technologies, Inc.).

Fibrin Gel Assays were performed in 24 well tissue culture plates (Becton Dickinson). Plates were prepared for procedure by addition of 300 ml Sylgard 184 elastomer (Dow Corning) to the bottom of the well, which was allowed to set overnight at 37°C with 5% CO2. Two 0.1 mm minutien pins (Fine Science Tools) were inserted into the Sylgard along the (16mm) diameter of the well bottom, 3mm away from each edge. Wells were blocked with 3% BSA in PBS for 30 minutes. Cells were counted and resuspended in a fibrinogen solution composed of 5% human fibrinogen (Sigma) dissolved in cold MEM/EBSS media with the addition of 10µl/ml ascorbate and plated at a concentration of 250,000 cells per well. Thrombin (100units/mL) from human plasma (Sigma) was added to 5mg/mL fibrinogen and cell solution. The gels were incubated for 30 minutes at 37° with 5% CO2 prior to the addition of 1 ml of MEM/EBSS supplemented with 5% fetal calf serum. A small pipette tip was used to gently detach gels from the well walls. Gels were then monitored for contraction over time. When

contraction was sufficient, the media was removed, and the gels were washed 3 times with PBS for 5 minutes each and fixed with 4% paraformaldehyde for 30 minutes prior to either embedding in paraffin for tissue analysis or for phalloidin staining. For phalloidin staining: fibrin gels were treated with 0.3% Triton-X100 and incubated in phalloidin for 1 hour at room temperature, and counter-stained with DAPI for 10 minutes. Sections were mounted using fluorogel. For tissue analysis, fixed fibrin gel sections were subjected to H&E staining as described above.

Chapter 3

Introduction

Wound infection is a major complication especially in patients with chronic disease such as diabetes or during immunosuppression. Such patients have disruptions in appropriate inflammatory responses, including the migration and recruitment of neutrophils and macrophage, which predisposes them to increased infection [2]. In addition, bacterial infection can lead to impairment of wound healing and sepsis. Given the ineffectiveness of many current antibiotic treatments and the increased prevalence of antibiotic resistant bacteria such as MRSA (Methycillin-resistant *S. aureus*), new clinical treatments are in high demand.

Our published data shows that treatment of primary endothelial cells with sNAG results in an increased cell migration, which is due to an integrin-dependent up-regulation of the Ets1 transcription factor. Ets1 regulates numerous processes such as immune function and embryonic development by the transcriptional regulation of genes involved in cell migration, proliferation and survival. Indeed, sNAG stimulation of endothelial cells results in the increased expression of

several cytokines and growth factors such as IL-1 and VEGF that are imperative for proper wound healing [137].

Given that sNAG stimulation results in increased secretion of cytokines important for immune function [137]; we sought to determine if sNAG treatment would result in increased expression of defensins and would therefore have antibacterial activity in addition to its wound healing activities. In this chapter, both use both *in vitro* and *in vivo* models to determine the effect of sNAG treatment on defensing expression.

Keratinocytes and endothelial cells express and secrete defensins when stimulated with sNAG

To investigate the affect of sNAG treatment on defensin expression *in vitro*, primary human umbilical vein endothelial cells in culture were used. As shown in **Figure 3.1 A** endothelial cells treated with sNAG show an up-regulation of β-defensin 3 and α-defensin 1 mRNA expression within 1 hour of stimulation. Similar upregualtion of α-defensin 4 and 5 by sNAG treatment was also observed (data not shown). Custom gene arrays containing over 25 different defensin genes were used to confirm the expression of the α-type defensins in primary

endothelial cells and the β-type defensins in keratinocytes. sNAG stimulation of endothelial cells was shown to increase the expression specifically of α-defensins 1, 4 and 5 and β-defensin 3. Additionally, sNAG stimulation of human keratinocytes increased expression of β-defensin like genes, several of which are listed in **Table 3.1**. These findings suggest that at least three α-defensin genes and β-defensin 3 are expressed in primary endothelial cells and multiple β-defensin genes are expressed in primary keratinocytes in response to sNAG stimulation.

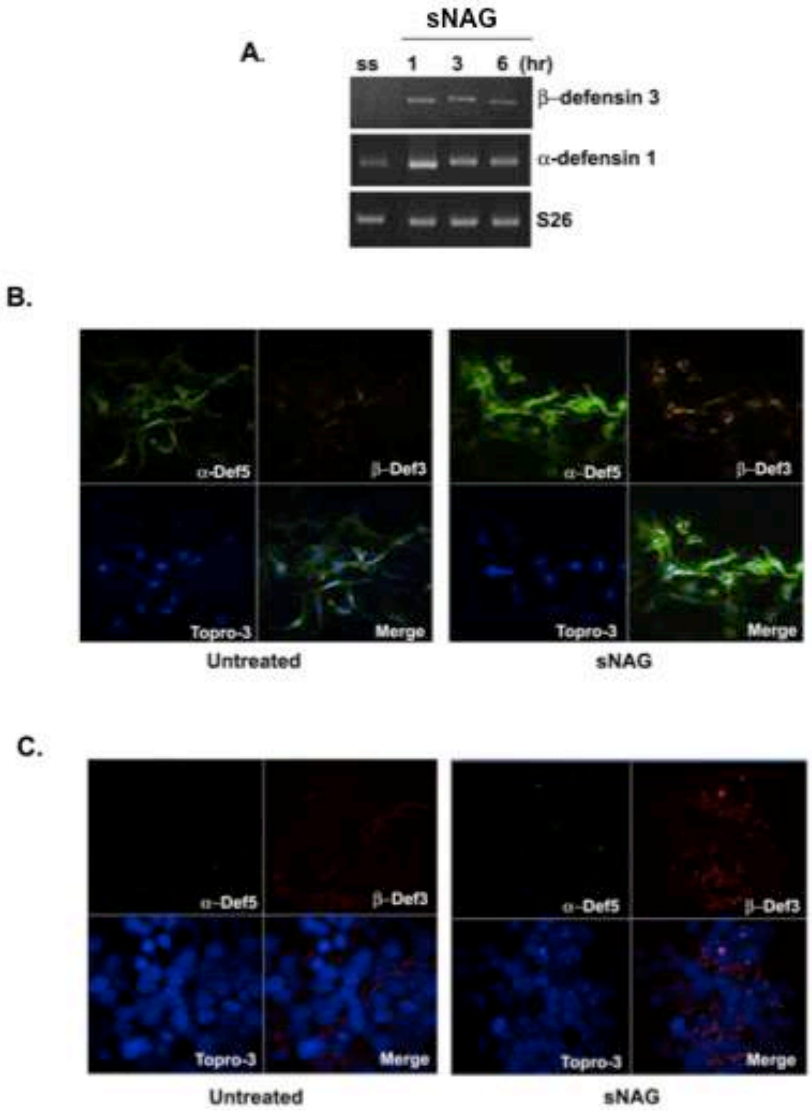

Figure 3.1 sNAG treatment results in expression and secretion of defensins *in vitro*.

Figure 3.1 sNAG treatment results in expression and secretion of defensins *in vitro*. (A) RTPCR analysis of serum starved (SS) primary endothelial cells treated with sNAG (50µg/ml) for the times indicated and assessed for expression of β-defensin 3 and α-defensin 1. **(B)** Immunofluorescent labeling of endothelial cells either serum starved (untreated) or treated with sNAG nanofibers (10µg/ml for 5hrs). Antibodies are directed against α-defensin 5 (Green, FITC), β-defensin 3 (Red, Texas Red). Nuclei are stained with TOPRO-3 (Blue). Lower right hand corner represents triple overlay. **(C)** Immunofluorescent labeling of keratinocytes (HaCat) that are either serum starved (untreated) or treated with sNAG nanofibers (10µg/ml for 5 hours). Antibodies are directed against α-defensin 5 (Green, FITC), β-defensin 3 (Red). Nuclei are stained with TOPRO-3 (Blue).

HUVEC	Gene Name	Fold Change	Keratinocyte	Gene Name	Fold Change
	α-defensin 1	+ 1.36		β-defensin 1	+ 1.4
	α-defensin 4	+ 2.74		β-defensin 126	+ 1.73
	α-defensin 5	+ 2.46		β-defensin 105B	+ 2.55
	β-defensin 1	+ 2.19		β-defensin 123	+ 1.65
	β-defensin 4	+ 3.06		β-defensin 129	+ 1.46

Table 3.1 Table demonstrating the fold change detected in expression of specific defensins in both HUVEC and keratinocyte cell ines.

To test whether the sNAG-dependent defensin expression also occurred on the protein level, sNAG stimulated endothelial cells were subjected to immunofluorescence using antibodies directed against both α and β defensins. As shown in **Figure 3.1B**, both β-defensin 3 and α-defensin 5 are up-regulated upon sNAG stimulation in this cell type. However, stimulation of primary human keratinocytes (HaCat) with sNAG did not cause increased expression of α-defensin but does cause an increase in the expression of β-defensin 3 (**Fig 3.1C**). Taken together, these experiments suggest that sNAG stimulation results in an up-regulation of defensin peptides in both primary keratinocytes and primary endothelial cells.

sNAG-dependent defensin expression requires Akt1

Previously published data show that sNAG stimulation of primary endothelial cells results in increased integrin activation, Ets1 expression and MAP kinase activation [137]. Findings from our laboratory position Akt1 upstream of Ets1 in endothelial cells and in *Drosophila* [122]. To begin to determine the signaling pathway responsible for the expression of defensins, endothelial cells were serum starved and pre-treated with pharmacological inhibitors directed against PI3K (wortmannin) or MAP kinase (PD098059) prior to sNAG stimulation. Quantitative real time PCR analysis shows that α-defensin 1 mRNA levels are greatly diminished after inhibition of either the PI3K/Akt pathway or the MAP kinase pathway (**Fig 3.2A**). RT-PCR analysis of β-defensin 3 also shows that levels are decreased by the inhibition of these pathways as well (**Fig 3.2B**). sNAG treatment of endothelial cells for a short time course leads to phosphorylation of

Akt1, a standard indicator of its activation (**Fig 3.2C**). To confirm that Akt1 is indeed required for defensin expression, lentiviral delivery of shRNA directed against Akt1 was used. Quantitative RT-PCR of serum starved endothelial cells infected with scrambled (SCR) control or Akt1 shRNA followed with sNAG treatment confirms that Akt1 expression is required for sNAG-dependent α-defensin expression (**Fig 3.2D**). Since β-defensins are known to be expressed in epithelial cells, lentiviral delivery of shRNA directed against Akt1 was used in human keratinocytes (HaCat). sNAG treatment of serum starved keratinocytes infected with scrambled (SCR) control leads to a significant increase in β-defensin 3 expression that is abrogated by Akt1 knockdown **(Fig 3.2E)**. These results illustrate that sNAG treatment activates Akt1 in endothelial cells and strongly suggest that sNAG-dependent defensin expression requires Akt1 in both endothelial cells and keratinocytes.

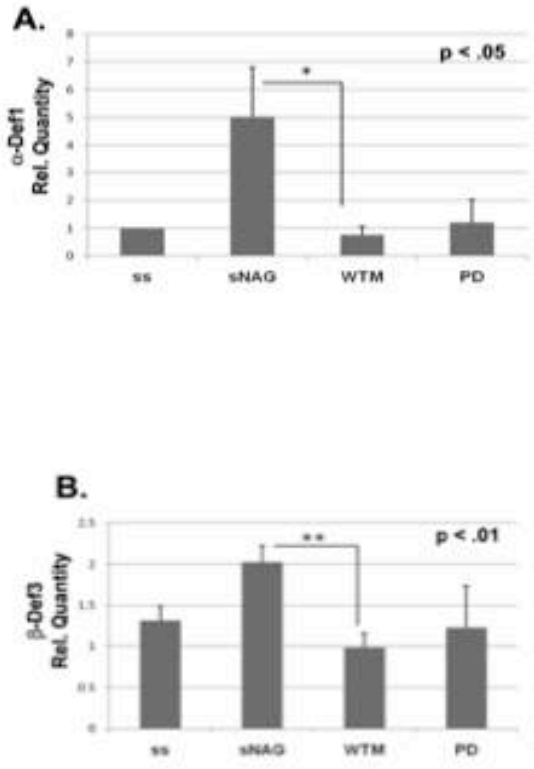

Figure 3.2 (A-B). sNAG induced defensin expression is dependent on Akt1. **(A)** Quantitative RT-PCR analyses using primers directed against α-defensin 1 from total RNA isolated from serum starved endothelial cells treated with or without sNAG for 3 hours, with or without pretreatment with PD098059 (50μM), wortmannin (100nm). Quantitation is relative to the S26 rprotein subunit. **(B)** Quantitation of β-defensin 3 expression from total RNA isolated from serum starved endothelial cells treated with or without sNAG for 3 hours, with or without PD98059 (50μm), wortmannin (100nm) and shown as relative to S26.

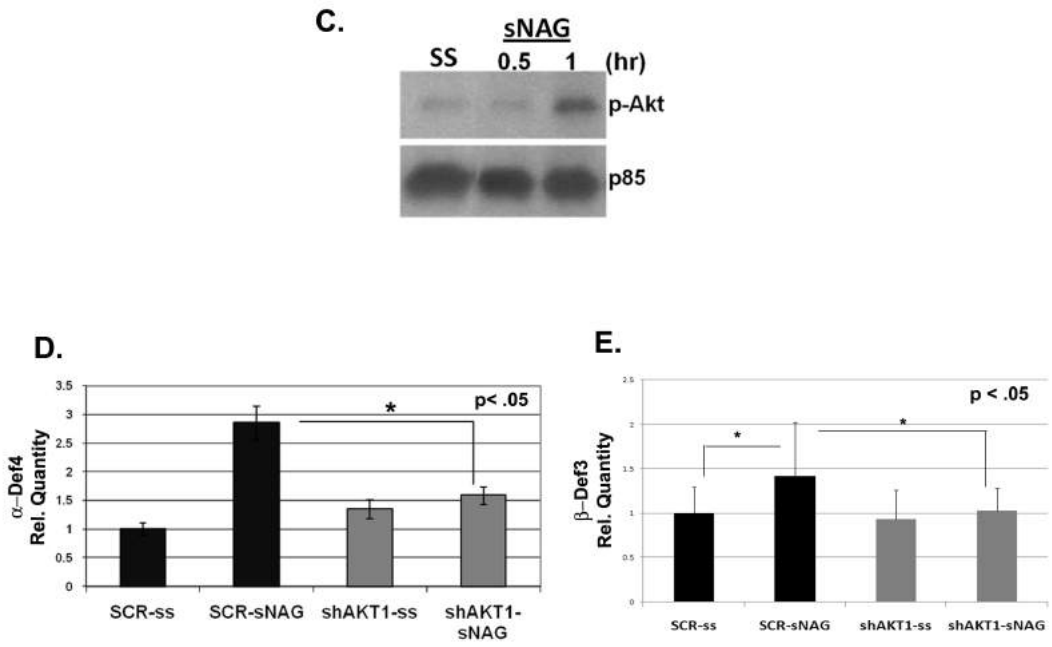

Figure 3.2 (C-E) sNAG induced defensin expression is dependent on Akt1.

(C) Western Blot analysis of phospho-Akt in serum starved endothelial cells (SS) stimulated with sNAG for the times indicated. Line indicates where lanes have been removed **(D)** Quantitative RT-PCR analyses of serum starved endothelial cells infected with a scrambled control (SCR) or Akt1 shRNA lentiviruses, treated with or without sNAG and assessed for α-defensin 4 expression. Quantitation is shown relative to S26. **(E)** Quantitation of β-defensin 3 expression from total RNA isolated from serum starved endothelial cells infected with a scrambled control (SCR) or Akt1 shRNA lentiviruses, treated with or without sNAG. Quantitation is shown relative to S26. All experiments were done in at least triplicate and repeated at least three independent times and p values are shown.

sNAG treatment of cutaneous wounds increase defensin expression *in vivo*

To confirm the dependence of Akt1 for the expression of defensins *in vivo*, wild type and Akt1 null animals were used in an excisional wound healing model. Although most mammalian leukocytes express α-defensins (human, rabbit, rat, and hamster), mouse leukocytes do not express α-defensins. We therefore focused on β-defensin expression in these mouse models. Treatment of cutaneous wounds with a dried form of sNAG, a thin biodegradable membrane, for three days results in a statistically significant increase in β-defensin 3 expression in keratinocytes of wild type animals (**Fig 3.3A**). Involucrin [140] staining (red) was used to mark the keratinocyte cell layers and show that the expression of β-defensin 3 is confined to the epidermal layer. To assess if sNAG-dependent defensin expression is dependent on Akt1, a similar assay was performed using an Akt1 null animal model. Wounds from Akt1 null mice treated with sNAG membranes show a markedly reduced induction of β-defensin 3 expression (**Fig 3.3A**). To better visualize the epidermal layers that are expressing β-defensin 3, **Figure 3.3B** shows a representative image of a sNAG treated wild type wound harvested on day 3. sNAG treatment of cutaneous wounds induced β-defensin 3 expression mainly in the suprabasal layers of skin (**Fig 3.3B).** Quantitative analyses shown in **Figure 3.3C** shows an approximate 5-fold increase in β-defensin 3 expression in sNAG treated wild type animals and that Akt1 is required for this increase.

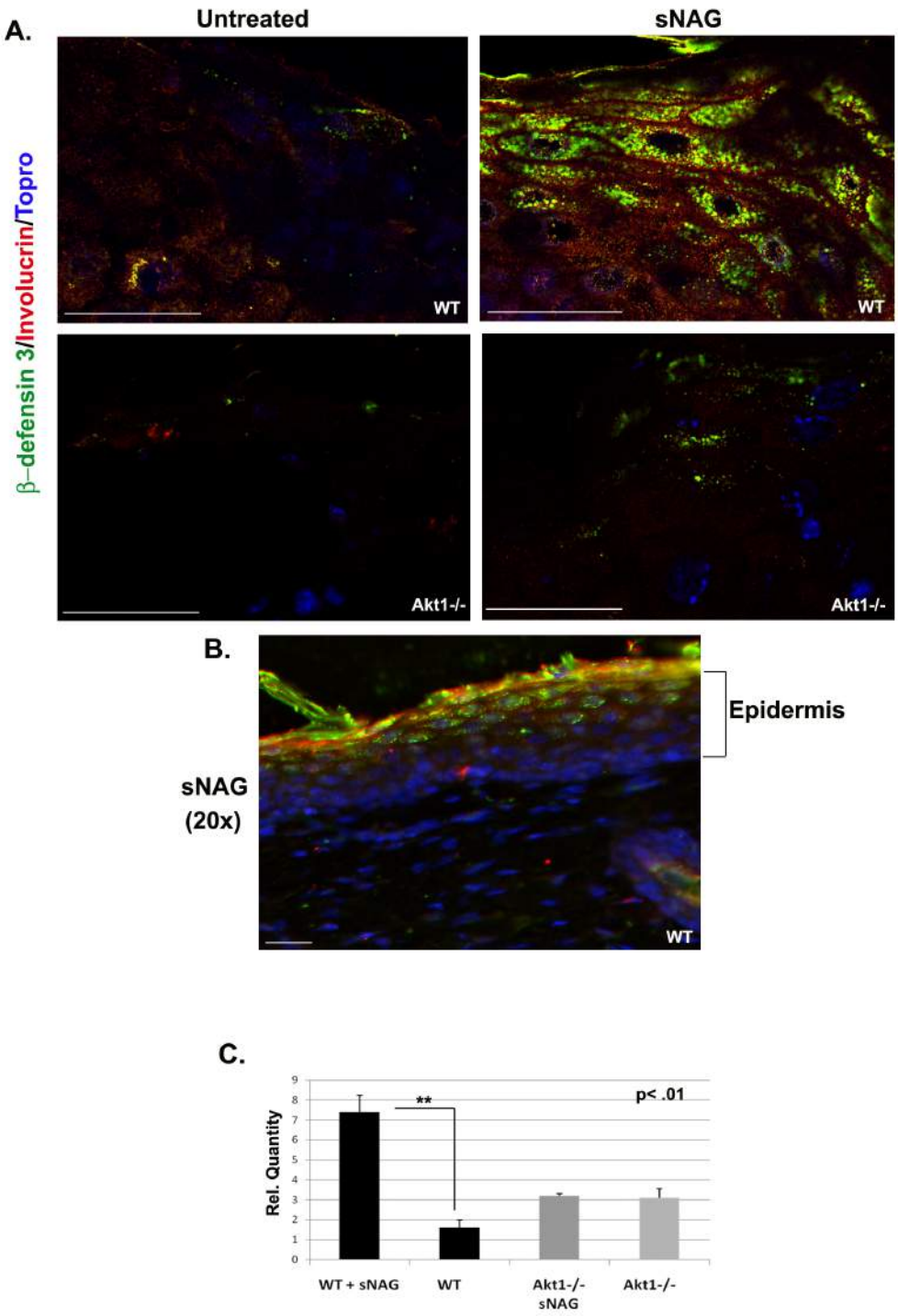
A.
Untreated
sNAG
β–defensin 3/Involucrin/Topro
WT
WT
Akt1-/-
Akt1-/-
B.
Epidermis
sNAG
(20x)
WT
C.
Rel. Quantity
**
p< .01
WT + sNAG
WT
Akt1-/-
sNAG
Akt1-/-

Figure 3.3.

Figure 3.3 sNAG induced defensin expression *in vivo* requires Akt1. (A) Paraffin embedded sections of cutaneous wounds harvested on day 3 post wounding from both WT (n=3) and Akt1 mice. Wounds were either untreated or treated with sNAG membrane. Immunofluorescence was performed using antibodies directed against β-defensin 3 (green), Involucrin (Red), and Topro (Blue). **(B)** Paraffin embedded section from WT treated with sNAG harvested on day 3. Immunofluorescence was performed using antibodies directed against β-defensin 3 (green), Involucrin (Red), and Topro (Blue). This lower magnification (20x) is included to better illustrate the epidermal layers expressing β-defensin 3. Scale bars = 50 μm. **(C)** Quantitation of β-defensin 3 expression from paraffin embedded sections was performed using NIH ImageJ software. Experiments were repeated three independent times and p values are shown.

sNAG treatment increases the kinetics of wound closure in WT animals.

Previous results have shown an increased kinetics of wound closure in diabetic mouse models in response to sNAG treatment. We tested whether sNAG had a similar affect in wild type animals. Excisional wounds were created in wild type animals which were either treated with the membrane form of sNAG or left untreated. Tissue sections were taken at 1, 3 and 5 days post wounding and subjected to H&E staining. As shown in **Figure 3.4**, sNAG treatment of wild type wounds results in complete closure, as visualized by the solid line, at day 3 post wounding. This occurs two days earlier than in the control wounds. Akt1 null animals display a delay in wound closure; these animals do not fully close the wound until 7 days post wounding. The delay in wound closure in the Akt1 null animals is not rescued by sNAG treatment**.** These findings suggest that sNAG not only induces defensin expression but also increases wound healing kinetics in wild type mice and may be a novel and effective therapeutic.

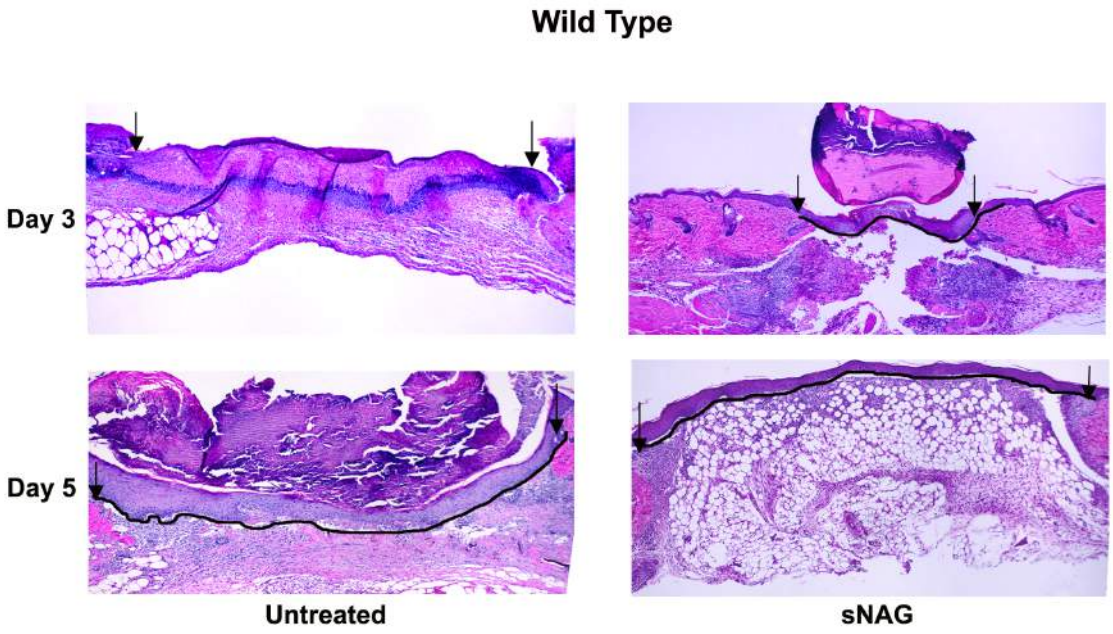

Figure 3.4 sNAG treatment increases wound closure in wild type mice (A) H&E staining of wound tissue sections derived from C57Bl6 wild type animals either untreated or treated with sNAG membrane. The day post-wound is indicated to the left of each panel. The solid black line follows the keratinocyte cell layer indicating wound closure. Black arrows indicate the margin of the wound bed

sNAG is an effective antimicrobial against *S. aureus*

It is well known that defensins are members of a large family of antimicrobial peptides. Since the treatment of endothelial cells with sNAG increases defensin expression (both α- and β-type) and that treatment of cutaneous wounds with sNAG dramatically increases β-defensin 3 expression *in vivo,* we next assessed the antimicrobial efficacy of sNAG treatment in bacterially infected wounds. Wild type and Akt1 null animals were subjected to cutaneous wounding, followed by infection with *Staphylococcus aureus*. Infected wounds were either treated with sNAG or left untreated for 3 and 5 days post infection. As shown by the tissue gram staining in **Figure 3.5A**, wild type animals treated with sNAG show a significant reduction in gram positive staining by day 5 post wounding as compared with untreated wounds. In contrast, gram stained tissue derived from untreated wounds in Akt1 null animals at 5 days post wounding show an accumulation of neutrophils which stain gram positive, indicating a potential lack of bacterial clearance in these animals that is not rescued by sNAG treatment. These findings suggest that Akt1 null animals have a defect in immune clearance mechanisms which is not rescued by sNAG treatment.

To quantitate sNAG-specific bacterial changes in colony forming units (CFU), infected wounds from both wild type and Akt1 null mice either sNAG treated or untreated were harvested and cultured. As shown in **Figure 3.5B**, at 5 days post wounding bacterial number is markedly reduced (10-fold) in wild type animals treated with sNAG. However, although the number of bacteria detected in the Akt1 null animals is reduced in comparison to wild type, sNAG treatment had a

little effect on absolute bacterial number in the Akt1 null animals. At 3 days post-infection (**Fig. 3.5C**), there is a similar 10-fold decrease in CFU in sNAG treated wild type mice as compared to untreated controls. The sNAG treated Akt1 null animals show a 2-fold decrease in CFU as compared to untreated Akt1 null animals. In general, the Akt1 null animals have a lower bacterial load per wound which may be reflective of an Akt1-dependent effect on other processes in addition to defensin expression. These findings suggest that sNAG treatment results in a marked reduction in bacterial load in infected cutaneous wounds in wild type mice but not in Akt1 null mice, suggesting the possibility that defensins are mediating the anti-bacterial response. To show that the antibacterial effect of sNAG treatment is not due to a direct effect of the nanofibers on bacterial growth or on their survival, *S. aureus* bacterial cultures were treated in solution with different amounts of sNAG, for 3 hours and colony forming units were determined. As shown in **Figure 3.5D**, sNAG treatment had no direct effect on the growth of *S. aureus*, indicating that sNAG is not directly inhibiting bacterial growth and may then be working via the up-regulation of defensins.

Application of defensin peptide mimics the sNAG antibacterial effect

To determine whether addition of defensin peptide can block bacterial infection similarly to that shown for sNAG treatment, wild type mice were wounded and inoculated with *S. aureus* as described above and then treated with biologically active human β-defensin 3 peptide (1.0μm) for three days. Tissue biopsies were stained using a tissue gram stain and CFU was quantitated. **Figure 3. 5E-5F** shows the results of these experiments. Infected mice treated with β-defensin 3

peptide have a decreased bacterial load, an approximate 7.5 fold decrease in viable bacteria **(Fig. 3.5F)**, similar to that shown in wild type mice treated with sNAG.

One of the mechanisms by which defensin expression is induced is through stimulation by bacterial LPS, possibly through the activation of Toll like receptors [88]. To test whether bacterial infection alone is able to induce β-defensin expression within the time periods tested, expression of β-defensin was assessed in infected wounds from wild type animals after three days post wounding. As shown in **Figure 3.6A**, bacterial infection alone does not induce the expression of β-defensin within 3 days of infection, as is shown with sNAG treatment. However, in wild type animals, sNAG treatment of infected wounds causes approximate 3- to 5-fold increase in the expression of β-defensin within a similar time period (**Fig. 3.6B**). These findings suggest that sNAG treatment rapidly induces the expression of defensin expression resulting in marked bacterial clearance in *S. aureus* infected wounds.

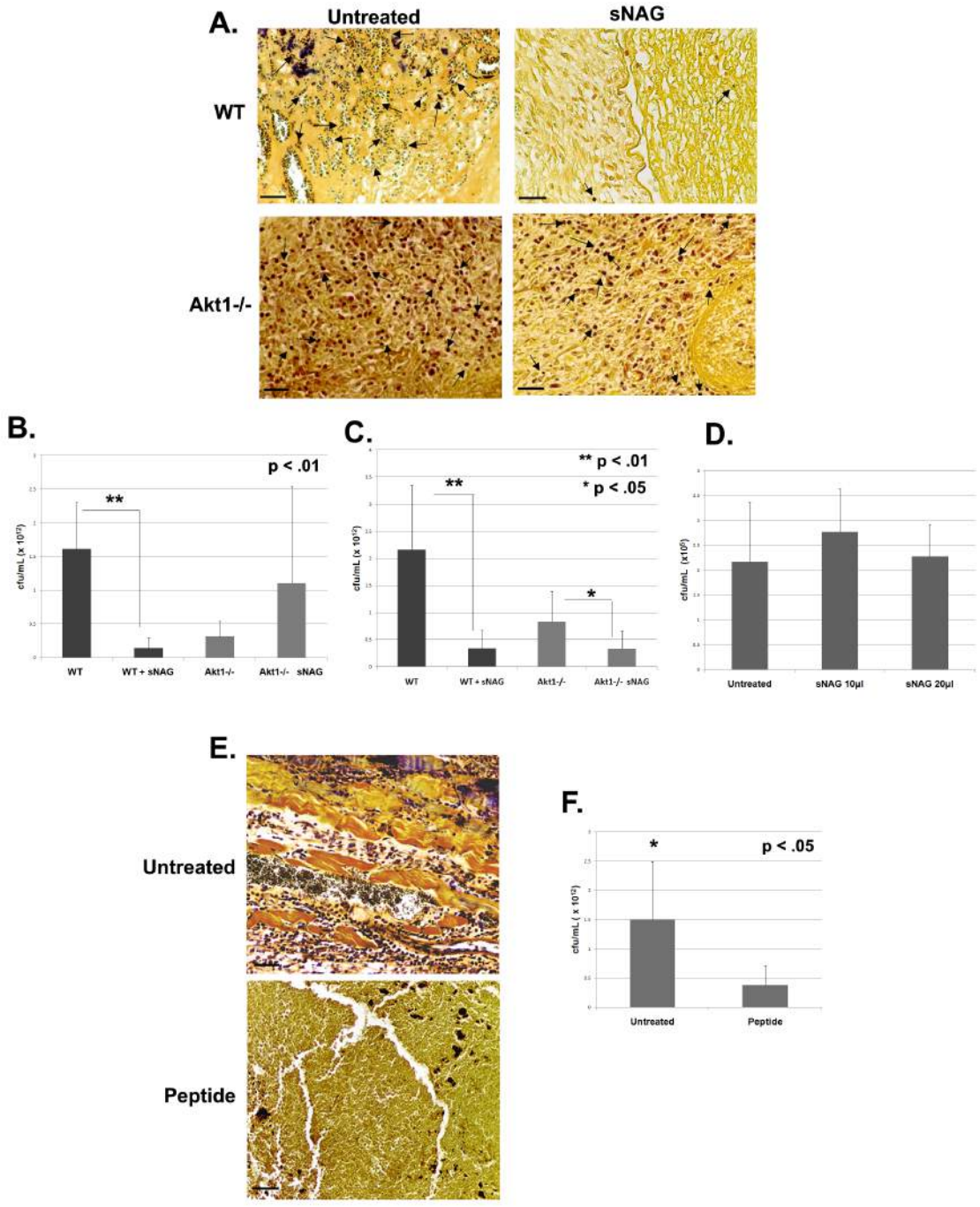
A.
Untreated
sNAG
WT
Akt1-/-
B.
p < .01
**
cfu/mL (x 10^7)
WT
WT + sNAG
Akt1-/-
Akt1-/- sNAG
C.
** p < .01
* p < .05
**
*
cfu/mL (x 10^7)
WT
WT + sNAG
Akt1-/-
Akt1-/- sNAG
D.
cfu/mL (x10^5)
Untreated
sNAG 10µl
sNAG 20µl
E.
Untreated
Peptide
F.
*
p < .05
cfu/mL (x 10^7)
Untreated
Peptide

Figure 3.5. sNAG treatment reduces bacterial infection in an Akt1 dependent manner. (A) Tissue gram staining of paraffin embedded *S. aureus* infected wounds from WT and Akt1null mice **(n=3)**. Infected wounds were either untreated or treated with sNAG membrane and wound beds were harvested on day 3 and day 5 for analysis. Dark purple staining indicates the presence of gram positive bacteria in the wound bed. Black arrows indicate examples of gram positive staining. Note the accumulation of positive staining in untreated WT that is lacking in WT animals treated with sNAG. Scale bars = 50μm. **(B)** CFUs derived from day 5 post wounding were quantitated from *S. aureus* infected wounds using both treated and untreated WT **(n= 3)** and Akt1 mice **(n=3)**. Wild type mice that were sNAG treated show a significant ($p<.01$) decrease in bacteria load in the wound beds as compared to Akt1 null animals. All experiments were repeated three independent times and the p values are shown. **(C)** CFU quantitated from infected wounds at day 3 post wounding in a similar fashion described in (B). sNAG treatment of infected wounds shows a significant decrease in CFU of both WT and Akt1 null animals on day 3, but the WT animals show an approximate 10 fold difference compared to a 2 fold difference in Akt1 animals. **(D)** Quantitation of CFUs in *S. aureus* cultures that were either untreated or treated with various amounts of sNAG nanofibers. Each experiment was performed three independent times and p values are shown. **(E)** Tissue gram staining of *S. aureus* infected wounds harvested on day 3 post wound from WT mice **(n=3)** that were treated with or without β-defensin 3 peptide. Note the decrease in gram positive staining in infected wounds that were treated

with β-defensin 3 peptide. **(F)** Quantitation of CFUs from *S. aureus* infected WT mice **(n=3)** treated with or without β-defensin 3 peptide. Infected wounds that were treated with peptide show a significant decrease ($p < .05$) in CFU. Scale bars = 50μm. Each experiment was performed three independent times and p values are shown

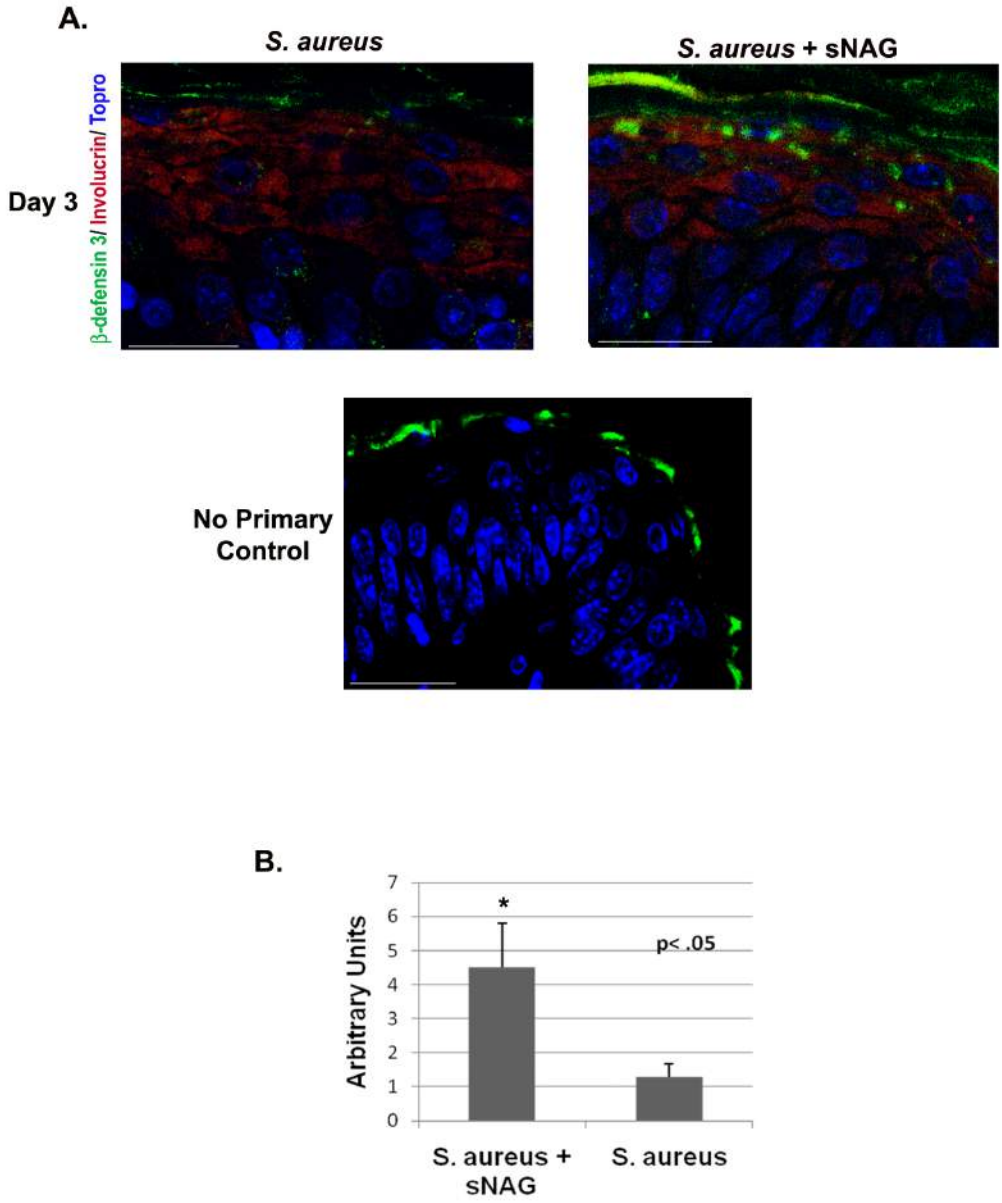
A.
S. aureus
S. aureus + sNAG
Day 3
β-defensin 3/ Involucrin/ Topro
No Primary Control
B.
Arbitrary Units
7
6
5
4
3
2
1
0
*
p< .05
S. aureus + sNAG
S. aureus

Figure 3.6

Figure 3.6. Rapid induction of defensin expression by sNAG treatment of *S. aureus* infected wounds. **(A)** Paraffin embedded tissue sections from *S. aureus* infected wounds, harvested on day 3, were subjected to immunofluorescence using antibodies directed against β-defensin 3 (green), Involucrin (red) to mark the keratinocyte layer, and Topro (blue) from both sNAG treated WT **(n=3)** and untreated WT mice **(n=3).** Non specific staining of keratin is indicated by the no primary control which was stained with secondary antibody only. Scale bar = 50μm. **(B)** Quantitation of β-defensin 3 expression from paraffin embedded sections using NIH ImageJ software. S. aureus infected wounds that were treated with sNAG show a significant increase ($p<.05$) in β-defensin 3 staining. Experiments were repeated three independent times and p values are shown.

Antibodies directed against β-defensin 3 block the antibacterial effect of sNAG

Since defensins are secreted proteins, we reasoned that antibodies directed against β-defensin 3 may be able to block the antibacterial activities. To test this hypothesis, wounds were created, infected with *S. aureus* and treated with sNAG as described above. The wounds were either treated with a β-defensin 3 antibody or an isotype control; one application each day for three days. Wound sections were obtained and stained for gram positive bacteria. As shown in **Figure 3.7A**, sections derived from wounds treated with β-defensin antibody have more gram positive bacteria than those treated with isotype control antibodies. Each section shown was derived from the wound area directly under the scab. Quantitation of CFU in these wounds shows that neutralization of β-defensin 3 prior to sNAG treatment in *S. aureus* infected wounds results in a significant increase in bacteria. Animals that were treated with an IgG isotype control show an approximate 5-fold reduction in viable bacteria **(Fig 3.7B).** Taken together, our results suggest that sNAG treatment not only results in the increased kinetics of wound healing but also promotes an endogenous anti-bacterial response and supports the use of this nanofiber as novel therapy to enhance wound healing while concurrently decreasing wound infection.

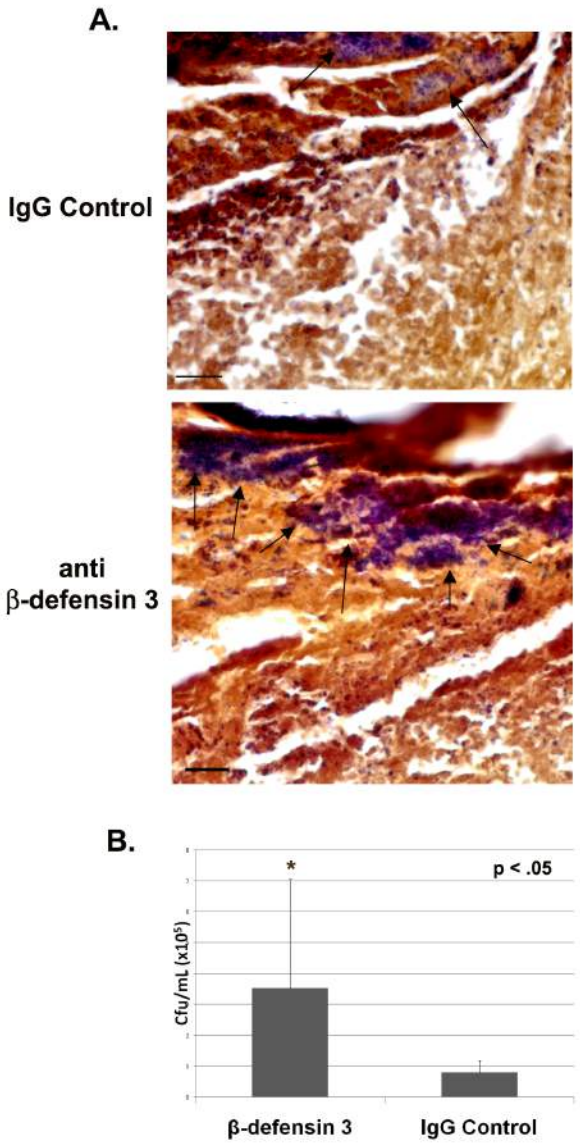

Figure 3.7 Antibodies against β-defensin 3 impedes antibacterial effects of sNAG treatment. (A) Tissue gram staining of paraffin embedded *S. aureus* infected wounds treated with sNAG from WT mice **(n=3)** that were harvested on Day 3. sNAG treated wounds were treated with either β-defensin 3 antibody or isotype control goat IgG antibody prior to sNAG treatment. Representative images show increased accumulation gram positive staining (black arrows) in the

wound beds of mice treated with an antibody directed against β-defensin 3. Scale bar = 20μm**. (B)** Quantitation of CFUs from *S. aureus* infected WT mice treated either β-defensin 3 antibody **(n=3)** or control IgG antibody **(n=3)** prior to sNAG treatment. β-defensin 3 application significantly increasedd ($p < .05$) CFU.

Discussion

The findings presented here suggest the use of a marine diatom derived nanofiber, sNAG as a novel and effective method to enhance wound healing while concurrently decreasing wound infection. We show that this FDA approved material presently used for hemostasis, stimulates the expression of both α-type and β-type defensins in primary endothelial cells and an up-regulation of the β-type in primary keratinocytes. We also show both *in vitro* and *in vivo* that Akt1 is required for defensin expression. sNAG treatment decreases *Staph aureus* infection of cutaneous wounds in wild type control animals but not in similarly treated Akt1 null animals. It is also important to note that sNAG stimulation of wild type cutaneous wounds results in an increased kinetics of wound closure. Antibody blockade of β-defensin results in a reduction in the sNAG-antibacterial activity. Taken together our findings suggest a central role for Akt1 in the regulation of defensin expression that is responsible for the clearance of bacterial infection and that sNAG treatment activates these pathways in wild type animals.

We present data that suggests that sNAG treatment of infected wounds could drastically decrease bacterial load in patients, at least in part, by the induction of

defensin expression. Control experiments indicate that the antibacterial effect of sNAG is not due to a direct interaction of the material with the bacteria but is due to downstream affects such as the regulation of defensins by Akt1 activation. It is widely accepted that defensins are important players in innate immunity and function in antimicrobial activities. Most of the evidence for their function is the direct killing of bacteria by *in vitro* mixing experiments with purified defensin peptides [88] or in similar experiments as shown in Figure 3.5 with direct application of the purified active peptide. Here we show that an induction of defensin expression in wild type animals using a topical application of sNAG results in an antibacterial response. It has recently been shown that transgenic mouse models expressing the human defensin 5 gene are resistant to *S. typhimurium,* an infection that results in death of wild-type animals [141] again suggesting the importance of defensins in the regulation of the antimicrobial response.

It has been accepted that the α-subtype of defensins are expressed in neutrophils and paneth cells, whereas the β-type defensins are epithelial in origin. We also see β-type defensin expression induced in response to sNAG in human keratinocytes both in culture and in the cutaneous wound healing model. Our *in vivo* data illustrates that β-defensin 3 is mainly expressed in the suprabasal layers after treatment with sNAG. This is consistent with previous data which localized human β-defensin 2 to the spinous and granular layers of the skin [142]. The skin is in constant contact with injury and infection and functions not only as a mechanical barrier but also maintains the ability to mount an active defense

against infection. The expression of β-defensin in the outer layers of skin supports their role in cutaneous innate immunity. However, we also show that sNAG specifically stimulates the expression of three different α-defensins (1, 4 and 5) in endothelial cells. We show this by RT-PCR, gene array analysis, immunofluorescence and ELISA (data not shown). The interaction between endothelial cells and leukocytes in tissue repair is one of the initial and most important steps in wound healing. The process of extravasation of leukocytes from the vasculature is initiated by chemotactic factors, therefore; it is interesting that α-defensins are induced by sNAG and may contribute to the necessary neutrophil/endothelial cellular interactions. More recently it has come to light that defensins exhibit biological activities beyond the inhibition of microbial cells, including their contribution to the adaptive immune response by exhibiting chemotactic activity on dendritic [76] and T cells, monocytes, and macrophages [77] and keratinocytes [143]. Previous work shows that human beta defensins 1 and 2 have the ability to chemoattract immature dendritic cells and T cells through the CC-chemokine receptor 6 (CCR6) [79], and that human beta defensin 2 can chemoattract TNFα treated neutrophils via the CCR6 receptor [78]. Human β-defensin 2 and 3 have also been shown to induce chemotaxis by interacting with CCR2, a receptor expressed on macrophages, monocytes, and neutrophils [144]. Interestingly, we show that sNAG treatment induces both α and β-defensin expression in endothelial cells. Taken together, the recent data suggest that defensins may mediate wound healing not only by their antimicrobial properties, but also by being chemotactic for other cell types necessary for

proper healing. However, application of β-defensin 3 alone did not result in an increase in wound closure (data not shown) implying that topical application of a single defensin does not sustain the cellular interactions required for increased chemo attraction, cellular recruitment and wound closure.

It is interesting to note that gram stains from Akt1 null infected mice show accumulated immune cells, likely neutrophils, which are staining positive for bacteria. This may suggest that in addition to their delay in wound healing Akt1 null mice may have immune trafficking and clearance issues. In a different Akt1 null animal using an incisional wound assay, others have shown that the primary phenotype was a lack of vascular maturation (reduced smooth muscle actin expression), but no changes in wound closure [145]. However, there are some differences between these studies and ours. First, we use a full thickness “punch” wound. Secondly, the Akt1 null animal used here was constructed using an insertional mutagenesis at the translational start site. In addition, our model is on a pure C57/Bl6 background rather than on a C57Bl6/129 background. It is well established that a genetically mixed background (especially a 129/C57Bl6 mixed background) increases hybrid vigor which can compensate for the loss of a single gene, such as Akt1, thus suppressing phenotypes in knockout animals [146, 147]. A full analysis of Akt1 dependent function during cutaneous wound healing is presently underway in the laboratory.

Our *in vivo* data using both wild type and Akt1 knockout animals confirms the requirement for Akt1 in sNAG-induced β-defensin 3 expression. Since mouse leukocytes do not express α-defensins like most other mammalian leukocytes

[148] *in vivo* α-defensin staining of infiltrating immune cells was not possible. Treatment of airway epithelial cells *in vitro* with alpha defensins 1-3 causes a dose and time-dependent increased cell migration that requires activation of PI3K and MAPK pathways [94]. We have previously shown that sNAG stimulation of endothelial cells results in the activation of MAPK [137] and in data presented here, pharmacological inhibition of MEK also inhibits the expression of the defensins *in vitro*. These findings suggest that both pathways impinge on the regulation of defensin expression by sNAG, however, Akt1 ablation results in a marked reduction of its expression both *in vitro* and *in vivo*. In myeloid cells, β-defensin 1 expression is controlled at the level of transcription, in part, by the Ets-family member PU.1 [149, 150]. PU.1 is a downstream target of Akt1 in the B-cell lineage [151]. We have shown, in primary endothelial cells that Akt1 is upstream of Ets1 both *in vitro* and *in vivo* during *Drosophila* tracheal development [122]. sNAG stimulation of endothelial cells results in increased expression of Ets1 (probably through Akt1) which is required for the migration of endothelial cells [137]. A delineation of the transcriptional regulatory mechanisms responsible for the regulation of the defensins by sNAG are currently underway in the laboratory.

Thus far, sNAG treatment has resulted in a series of downstream activities; hemostasis, cell migration, cell proliferation, increased wound closure, and as described here, stimulation of the innate immune response resulting in anti-bacterial functions. Using a custom gene chip we have also shown that a number of Toll-like receptors are up-regulated by sNAG treatment of human endothelial cells (data not shown). Toll-like receptors (TLRs) are highly conserved receptors

that recognize specific molecular patterns of bacterial components leading to activation of innate immunity. Interestingly, *Drosophila* lack an adaptive immune system but are still resistant to microbial infections [152]. This host defense is the result of an innate immune system that provides protection by synthesizing the antimicrobial peptides dToll and 18-wheeler which are induced by TLRs [153, 154]. Recent work has also linked human defensin expression to TLR activation. Human β-defensin 2 was shown to be induced in airway epithelial cells in a TLR-2 dependent manner [155]. Toll-like receptor 4 has been shown to mediate human β-defensin 2 inductions in response to *Chlamydia pneumonia* in monocytes [156]. Importantly, the PI3K/Akt pathway is a key component in TLR signal transduction, controlling cellular responses to pathogens [157]. Since it is known that stimulation of TLRs can lead to increased defensin synthesis, this work suggests the potential for sNAG as a stimulator of innate immunity and bacterial clearance via the activation of Akt1.

Given the dramatic increase of diabetic patients within the population who present with chronic wounds and complications due to wound infection, new clinical treatments are in high demand. Here, we describe marine derived pGlcNAc nanofibers that not only increase the kinetics of wound healing but act to stimulate innate immunity thus providing anti-bacterial activity. The obvious importance of these observations is the application to nosocomial infections. Of the nosocomial infections, surgical wound infections predominate; with statistics showing up to 8% of all surgical patients. The direct cost of these types of infections is approximately 4.5 billion dollars per year. Given that defensins are

part of the innate immune system, activation of these pathways will preclude the generation of resistant organisms as well as allow for the antibiotic-independent clearance of bacterial infection. Use of sNAG in a hospital setting would defray much of the cost and markedly reduce the production of antibiotic resistant species. Taken together, these findings suggest that these marine derived pGlcNAc nanofibers will be highly beneficial in the clinical arena.

Chapter 4

The inevitable result of adult wound healing is scar formation, which follows both surgical and trauma wounds. Scar formation following cutaneous wounding is due to an unorganized deposition of excess collagen and fibrous tissue that replaces normal dermal tissue. Scarring is a major medical complication that often results in restricted tissue movement, loss of function, poor aesthetics, and potential psychological distress [158]. The ability of mammals to heal without a scarring response (tissue regeneration), is restricted to a certain stage of development, after which wound healing proceeds with scarring. One major difference between tissue regeneration and scar formation is the organization and deposition of collagen. Comparisons of fetal regenerated tissue and adult scars show that each contains strikingly similar components, suggesting differences in regulation of tissue architecture and not in an abnormal molecular composition of the scar. Therefore tissue regeneration and scar-forming tissue repair share common mechanisms that may be controlled differently [159]. Fetal wound healing exhibit differences in the inflammatory response, TGFβ signaling, and hyaluronan synthesis. Fetal wounds are rich in hyaluronic acid which serves to facilitate an environment for cell migration and tissue regeneration. In adult

wounds hyaluronic acid rapidly decreases while in fetal wounds it persists after persists for several weeks [160]. In addition, scarless wounds are characterized by a reduction in overall inflammatory responses that may be partly attributed to decreased platelet degranulation [161]. Decreased platelet activity results in reduced levels of TGFβ-1 and TGFβ-2 [161], which have established roles in the regulation of scarring. Reductions in these cytokines in fetal wounds correlate to reductions in scarring and addition of the cytokine to scarless wounds results in scar formation [162]. Interestingly, addition of TGFβ-3 to adult wounds leads to a decrease in scar formation suggesting the ratio of the differing isoforms is critical to tissue regeneration and scar formation [163]. Given the impact of scar formation and the limited effectiveness of current treatments such as silicone dressings and hydrocortisone injections, the development and characterization of new treatments are needed [164].

Treatment of cutaneous wounds with pGlcNAc nanofibers (sNAG) an FDA approved material (TalyMed™) promotes accelerated wound healing in both wild type animals and in those with delayed wound healing phenotypes in murine, pig, and human models [165-169]. Increased wound repair mediated by nanofiber treatment is characterized by increased hemostasis [170, 171]. Using the db/db mouse system, thin pGlcNAc nanofiber containing membranes placed directly into the wound bed profoundly accelerated wound closure mainly by re-

epithelialization and increased keratinocyte migration, granulation tissue formation, cell proliferation, and vascularization compared with control wound treatments. These findings indicate that pGlcNAc nanofibers may provide a combinatorial therapy using a single FDA approved agent.

Here we show that pGlcNAc nanofiber treatment results in reduced scarring where reduced scar size correlates with an increased tensile strength and elasticity of the healed wound. pGlcNAc treated wounds have a decreased collagen content, decreased myofibroblasts and increased collagen organization. We show that the serine threonine kinase Akt1 is required *in vivo* for the pGlcNAc-induced increases in tensile strength and elasticity. Using a fibrin gel assay to assess fibroblast alignment within a lattice that provides tension points, we show that nanofiber stimulation results in increased fibroblast alignment by a process also requiring Akt1. Our findings suggest that pGlcNAc nanofibers stimulate an Akt1 dependent pathway that results in the proper alignment of fibroblasts, decreased scarring, and increased tensile strength during cutaneous wound healing.

Increasing numbers of patients develop scars due to a rise in both elective operations and operations following traumatic injury [172]. While there are many current therapies on the market to reduce scar formation including flavonoid creams, silicone gel sheets, pressure therapy, corticosteroid injections, and cryotherapy, many of these therapies have resulted in controversial data and limited scientific studies [172]. Here, we evaluate a novel pGlcNAc nanofiber treatment that has been shown to increase wound healing while reducing

bacterial infection. Our studies suggest that pGlcNAC treatment of cutaneous wounds results in decreased scar formation and improved tissue quality as measured by increased tensile strengths.

sNAG treatment results in decreased scar size and increased collagen alignment

Our previous findings show that pGlcNAc nanofiber treatment of cutaneous wounds results in increased wound closure in a diabetic mouse model [128] and in wild type mice [165] that is due, at least in part, to increased angiogenesis, keratinocyte proliferation and migration, and expression of several cytokines, growth factors [137] and innate immune activation [165]. We have noticed that at long time points post wounding it is very difficult to define the scar area. We therefore sought to analyze the effect of sNAG on scar formation. Excisional wounds were created in wild type animals which were either treated with a membrane form of sNAG or left untreated. At 21 days post-wounding, animals were sacrificed and scar sizes were measured. As shown by the quantitation in **Figure 4.1A**, sNAG treated wounds show an approximately 2-fold reduction in scar size as compared to untreated wounds. To examine the amount and quality of collagen in treated and untreated wounds, Masson's trichrome staining was performed on tissue sections from 10 days post wounding. As seen in **Figure 4.1B**, sNAG treatment of cutaneous wounds results in decreased collagen content as indicated by less blue staining and more organized collagen alignment, especially as visualized at the wound borders, where new collagen in appropriately aligned with existing collagen. Hydroxyproline assays were performed to quantitatively analyze the amount of collagen deposition in treated

and untreated wounds. As shown in **Figure 1C**, sNAG treated wounds have an approximately 3-fold decrease in overall collagen content.

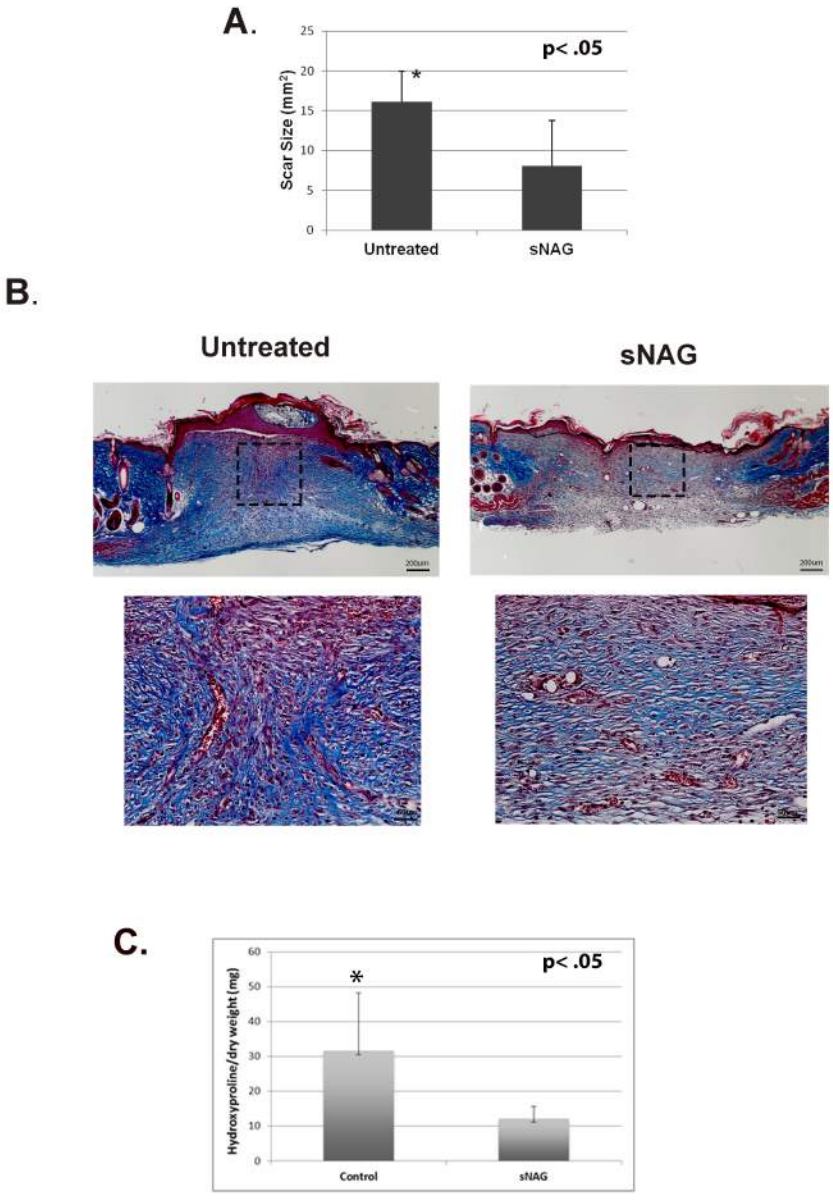
A.
p< .05
Scar Size (mm²)
25
20
15
10
5
0
*
Untreated
sNAG
B.
Untreated
sNAG
C.
p< .05
Hydroxyproline/dry weight (mg)
60
50
40
30
20
10
0
*
Control
sNAG

Figure 4.1

Figure 4.1. **sNAG treatment results in decreased scar size and more organized collagen alignment.** (**A**) Quantification of scar size from excisional wounds of Wild Type male mice (n=3) that were either treated with sNAG membrane or left untreated. Scars were measured after 21 days of healing. (**B**) Masson Trichrome staining of paraffin embedded sections of cutaneous wounds harvested on day 10 post wounding from both WT untreated and sNAG treated mice. The 4x magnification illustrates the entire skin section while the 20x magnification is focused on the regenerating tissue directly under the wounded area. Boxes are included to show the regions of magnification. (**C**) Quantitative analysis of collagen content in sNAG treated wounds compared to untreated wounds of WT mice using a hydroxyproline assay ($p<0.05$).

Myofibroblasts are an important cell type in tissue repair and have been implicated in the generation of scarring via collagen production [173, 174]. Myofibroblast populations are reduced during fetal wound healing where scarring is absent [175]. To visualize the distribution of myofibroblast populations, wound sections were labeled with an antibody directed against alpha smooth muscle actin (αSMA). As shown in **Figure 4.2A** and quantitated in **Figure 4.2B**, treated wounds show at least a 2-fold reduction in the expression of αSMA, suggesting that the reduction in collagen content are due to reduced numbers of myofibroblast cell number.

sNAG treatment causes increases in tensile strength and elasticity of wounded skin

Given that collagen imparts strength and mechanical properties [176] and that collagen deposition and scar formation differs between treated and untreated cutaneous wounds, we sought to measure whether sNAG treatment resulted in increased tensile strength and elasticity. To measure tensile strength and elasticity, cutaneous wounds generated in wild type animals, both untreated and treated, were harvested after 21 days and subjected to mechanical testing using a strain gauge extensometer. Normal unwounded skin from wild type mice was used as a control. Analysis of mechanical testing shows that sNAG treated cutaneous wounds of WT animals display an approximate 40% increase in tensile strength compared to untreated wounds (**Fig 3A**). Additionally, sNAG treated wounds exhibited tensile strength recovery at levels similar to unwounded control skin (**Fig 3A**). During tensile strength measurements, it was noted that

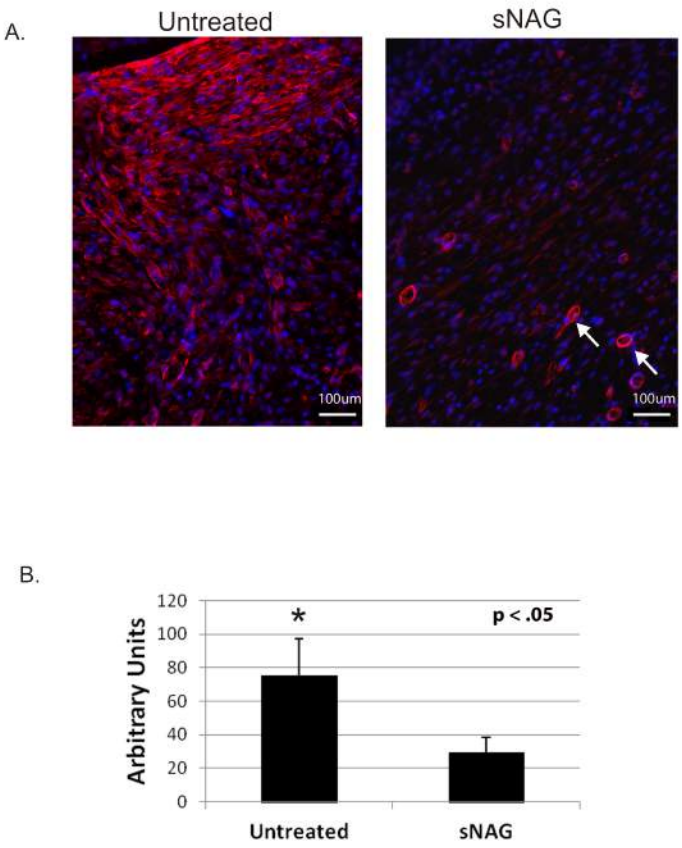

Figure 4.2. sNAG treatment results in decreased alpha smooth muscle expression. (**A**) Paraffin embedded sections of cutaneous wounds harvested on day 10 post wounding from both sNAG treated and untreated WT mice. Immunofluorescence (20X) was performed using antibodies directed against α-SMA (red), and TOPRO (Blue). White arrows indicate vasculature that is also positively stained with α-SMA antibodies. (**B**) Quantitation of α-SMA expression from paraffin embedded sections was performed using NIH ImageJ software. (*p<.05)

sNAG treated cutaneous wounds from WT animals were more elastic than control or untreated counterparts. **Figure 4.3B** illustrates that sNAG treatment results in significantly increased elasticity of the healed tissue as compared to both untreated cutaneous wounds and unwounded control skin. To assess if sNAG treatment of cutaneous wounds results in increased elastin production, Van Gieson staining was analyzed. In **Figure 3C**, wounds derived from treated animals show elastin production (as visualized by the thin black structures) in the newly healed wound whereas untreated wounds do not. These findings suggest that sNAG treatment results in increased tensile strength as well as increased elasticity and supports the hypothesis that nanofiber treatment of cutaneous wounds decreases scarring while concurrently increasing mechanical properties of healing skin.

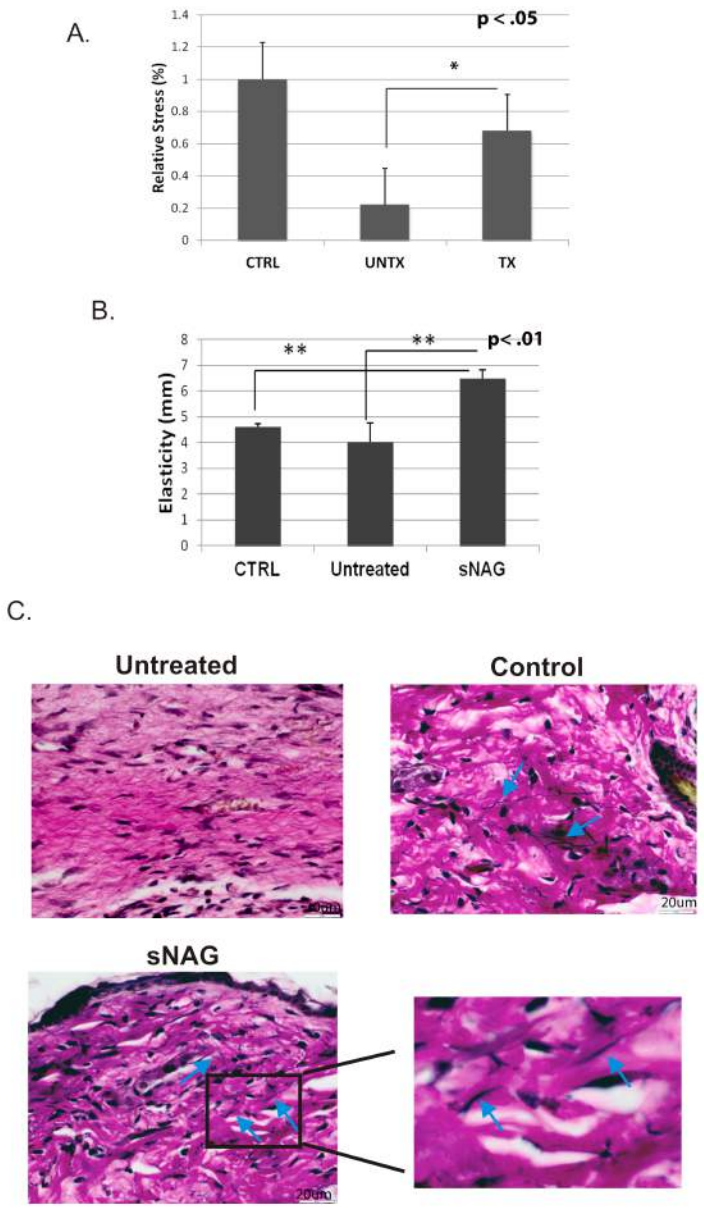
A.
p < .05
*
Relative Stress (%)
1.4
1.2
1
0.8
0.6
0.4
0.2
0
CTRL
UNTX
TX
B.
**
**
p< .01
Elasticity (mm)
8
7
6
5
4
3
2
1
0
CTRL
Untreated
sNAG
C.
Untreated
Control
20um
sNAG
20um

Figure 4.3

Figure 4.3. sNAG treatment causes increased tensile strength and elasticity of wounded skin. (**A**) Quantitation of the relative stress wounded skin could withstand from sNAG treated and untreated WT mice. Tissue was harvested 21 days post wounded and subjected to mechanical testing. Measurements are relative to control (CTRL) skin which was derived from unwounded tissue of WT animals. (**B**) Quantitation of skin elasticity from sNAG treated and untreated wounds harvested 21 days post wounding from WT animals. Control skin was derived from unwounded tissue of WT animals. (**C**) Van Gieson staining of paraffin embedded tissue sections derived from unwounded skin (control), sNAG treated, and untreated wounds of WT animals 10 days post wounding. Blue arrows indicate darkly stained elastin fibers. (*p<.05, **p<.01)

sNAG treatment results in increased fibroblast alignment and contraction of fibrin gels

Since alignment and organization of collagen fibers is likely related to appropriate alignment of fibroblasts [177], we utilized a fibrin gel assay to assess if sNAG treatment results in alignment of fibroblasts *in vitro* [178]. To test this hypothesis, fibroblasts were treated with sNAG or left untreated prior to being embedded in fibrin gels. Fibrin gels were allowed to contract overnight and were then analyzed for contraction and sectioned for analysis of cell alignment. A representative photograph of sNAG treated and untreated fibrin gels is shown in Figure 4A. To visualize cell alignment, the gels were sectioned and stained with either phalloidin or H&E. Representative images of H&E stained gel sections show that sNAG treatment results in aligned fibroblasts (**Fig. 4.4B**). Black circles indicate where pins were placed to allow tension points along which the gels could contract. sNAG-treated fibroblasts radiate from the pins in a linear, organized manner as compared to the scattered and unorganized arrangement of untreated cells. sNAG dependent fibroblast alignment was confirmed in human dermal fibroblasts (data not shown). In addition, sNAG-treated fibroblasts correlated with increased gel contraction as compared to untreated controls (see below). Taken together, these data suggest that sNAG treatment of fibroblasts results in organized cell alignment. This alignment of fibroblasts likely results in the more aligned collagen fibers and increased tensile strength shown in sNAG treated cutaneous wounds, as seen in Figures 1-3.

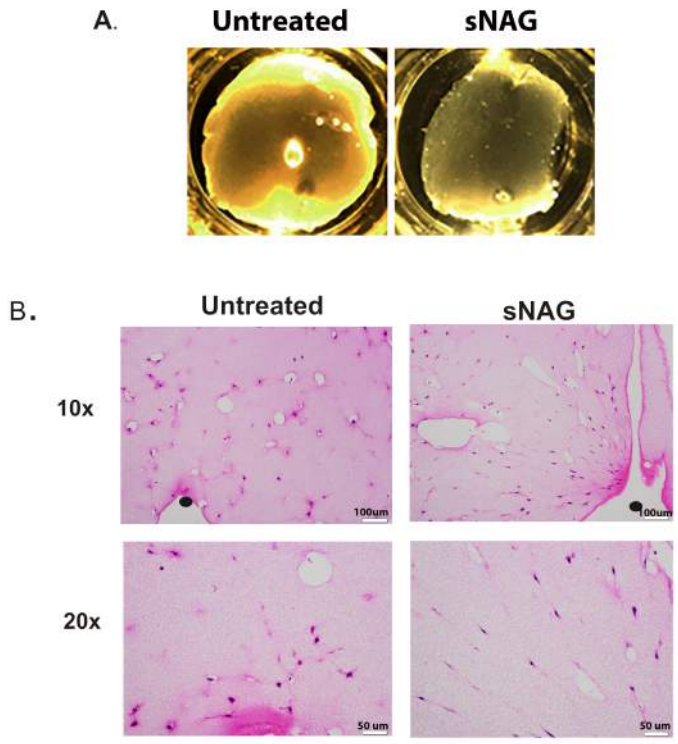

Figure 4.4 sNAG treatment results in increased fibroblast alignment. (**A**) Representative images of gel contractions. (**B**) Representative images of Hematoxylin and Eosin stained sections of paraffin embedded fibrin gels. Fibroblasts were serum starved and either left untreated or stimulated with sNAG (50µg/mL) overnight prior to embedding in fibrin gels. Black circles indicate where minutien pins are located in the fibrin gels to serve as tension points along which the gel contracts.

sNAG dependent fibroblasts alignment requires Akt1

Findings from our laboratory show that sNAG treatment results in increased cell motility and angiogenesis as a result of Akt1 activation [137]. Additionally, we have also shown that sNAG-dependent induction of innate immunity requires Akt1 [165] and that Akt1 null animals do not respond to sNAG treatment. To determine if Akt1 is also required for the sNAG-dependent increase in fibroblast alignment, fibroblasts were transduced with a shRNA expressing lentivirus directed against Akt1 prior to embedding in the fibrin gels. As shown in **Figure 4.5A**, sNAG-treated fibroblasts contracted the gels approximately 40% compared to gels containing untreated fibroblasts. Gels containing sNAG-treated shAkt1 expressing fibroblasts contracted significantly less than sNAG-treated controls. Analysis of H&E stained sections from the fibrin gels show that alignment is inhibited when Akt1 expression is blocked (**Fig 5B**). As shown in **Figure 5C**, sNAG-treated fibroblasts have an increased phosphorylation of Akt as compared to untreated controls, suggesting activation of the Akt pathway. Since the knockdown of Akt1 resulted in decreased fibroblasts alignment *in vitro*, we sought to determine if tensile strength of cutaneous wounds derived from Akt1 null animals would be affected by treatment with sNAG. Cutaneous wounds that had been treated with sNAG or left untreated were subjected to tensile strength testing using a strain gauge extensometer as described above. As shown in **Figure 4.5D**, there was no significant difference between sNAG treated and untreated wounds. Taken together, our findings suggest that Akt1 is required for the sNAG-dependent alignment of fibroblasts as well as sNAG-dependent increase in tensile strength *in vivo*.

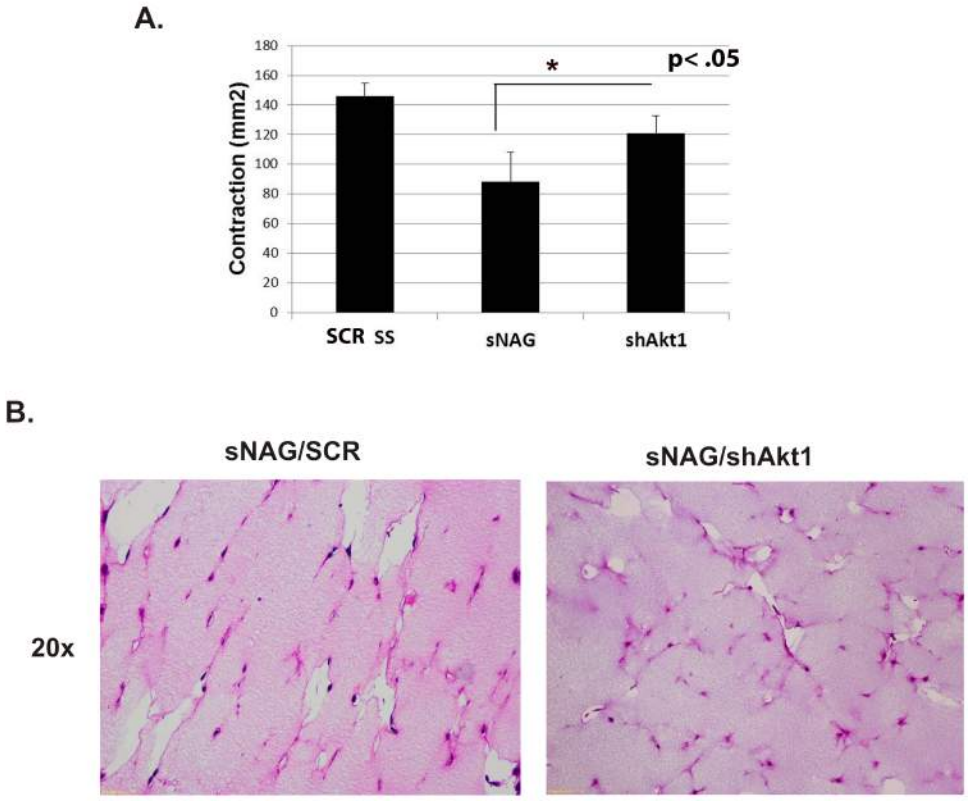

Figure 4.5 (A-B) The sNAG dependent alignment of fibroblasts requires Akt1. (**A**) Quantification of contraction of fibrin gels that were embedded with serum starved fibroblasts that were transduced with a SCR control lentivirus, sNAG treated fibroblasts, or fibroblasts that were transduced with a lentivirus directed against Akt1 prior to sNAG stimulation (50µg/mL). (**B**) Representative images from Hematoxylin and Eosin stained sections of paraffin embedded fibrin gels. Fibroblasts were serum starved and transduced with either Scrambled control or Akt1 lentivirus prior to sNAG stimulation (50µg/mL).

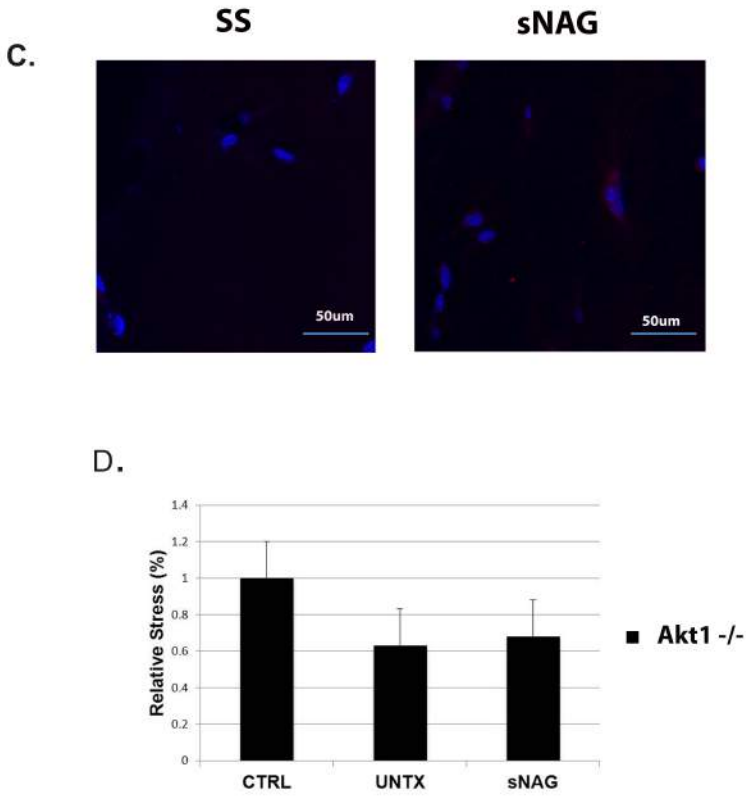

Figure 4.5 (C-D) The sNAG dependent alignment of fibroblasts requires Akt1. (**C**) Immunofluorescence of both serum starved (untreated) or sNAG treated fibrin embedded fibroblasts using an antibody directed against phospho-Akt (red) and DAPI. (**D**) Quantitation of the relative stress from sNAG treated and untreated Akt1 null animals. Tissue was harvested 21 days post wounded and subjected to mechanical testing. Measurements are relative to control (CTRL) skin which was derived from unwounded tissue of Akt1-/- animals. (*p<.05)

Discussion

Our findings show that highly purified pGlcNAc nanofiber (sNAG) treatment of cutaneous wounds results in reductions in scar formation, increased collagen organization in the absence of increased collagen, increased tensile strength and elasticity. These activities are blocked by Akt1 ablation both *in vitro* and *in vivo*. As tensile strength is determined by collagen remodeling during the maturation phase of wound healing we suggest that pGlcNAC nanofibers stimulate an Akt1 dependent pathway that leads to remodeling of collagen. Collagen remodeling is a complex process that involves both collagen synthesis and degradation by MMPs and other collagen binding proteins such as SPARC, followed by collagen crosslinking between the lysine and hydroxylysine of the peptides which is controlled by lysyl oxidase and lysyl hydroxylase which create stable bonds [179]. Akt1 is known to play a role in collagen synthesis through the control of the Ets family of transcription factors [180]. Ets family members are known regulators of MMP expression; e.g. MMP1 and 9. Taken together these findings suggest a central role for Akt1 in the regulation of scar formation. [181].

pGlcNAC nanofiber treatment leads to a more seamless collagen fiber organization, suggesting that sNAG treatment increases the kinetics of wound resolution and remodeling and decreases in α-smooth muscle actin (αSMA), suggesting a decreased number of myofibroblasts in the wound. These atypical, activated fibroblasts are the major producers of collagen in cutaneous wound healing, are active during contraction, and are cleared from the wound by apoptosis [174]. Our findings suggest that sNAG treatment effects the

differentiation of myofibroblasts, their epithelial trans-differentiation, or their recruitment from the stroma or from the circulation. Since our model is a total Akt1 null animal, it is of interest to determine which cell type is responsible for the effects on myofibroblast recruitment or differentiation. Akt1 is known to stimulate cytokine secretion in both the endothelium [137] and in macrophage/monocyte lineages [182]. Myofibroblasts are thought to be recruited as circulating fibrocytes precursors. We therefore suggest that Akt1 may be controlling their recruitment.

To understand the role of sNAG in collagen alignment, we used a fibrin gel assay that provides tension lines on which cells can align and provides fibroblasts with a lattice similar to that which occurs during normal wound healing. Making the assumption that in order for collagen to be properly deposited, the fibroblasts themselves must be aligned. Cellular alignment is crucial for the formation of proper tissue architecture and provides appropriate mechanical function. Use of a three dimensional environment that more closely mimics an *in vivo* situation, provides an *in vitro* system in which to study these cellular responses. We show that pretreatment of fibroblasts with sNAG under serum starved conditions results in a marked alignment of cells toward the tension poles and that aligned cells physically contract the fibrin clot. Both the contraction and alignment is ablated under conditions of Akt1 knockdown. Interestingly, we see a slight but reproducible increased Akt phosphorylation in aligned cells. These findings show that Akt1 is required for sNAG-induced cellular alignment *in vitro*. Akt1 null animals validate these findings since the tensile strength of wounded skin is not affected by sNAG treatment in this model.

Exactly how sNAG activation of Akt1 results in fibroblast alignment remains to be determined. Akt signals to the cytoskeleton via the Rho-family of GTPases and PAC1, among others, controlling cytoskeletal remodeling [183]. Akt can directly phosphorylate vimentin, an intermediate filament protein involved in cell shape and motility changes [184]. In motile cells, phospho-Akt is localized to the leading edge whereas in apical/basal polarized cells, phospho-Akt tends to be localized to the cell periphery. These findings suggest that Akt plays a role in cell polarity, cytoskeletal organization and directed cell movement. The general consensus in fibroblasts, as determined by both knockdown and over expression analyses, is that Akt1 positively directs migration while Akt2 blocks migration [185]. The inverse is true in epithelial cells. In the fibrin gel assay presented here, Akt1 is required for the sNAG-induced alignment of cells between two tension points. Akt1 must then be required for cytoskeletal rearrangement and cellular positioning, possibly affecting front to back cell polarity. The exact mechanisms as to how Akt1 specifically affects this cell polarity in response to tension is currently under investigation. It is interesting to note that Akt1 null and wild type animals have similar tensile strengths of unwounded skin (data not shown). This suggests that the cellular programs controlling skin development are intact in the absence of Akt1. The double Akt1/Akt2 null animal, in addition to dwarfism and early neonatal lethality, presents with a thin skin phenotype, characterized by a marked reduction in the number of cells within each skin layer. This phenotype is due to a lack of proliferation that cannot be compensated by Akt3 alone [138]. Interestingly, the presence of either Akt2 or Akt3 does not affect sNAG stimulated

wound repair and tensile strength as discussed here, or the clearance of infection and wound closure as previously reported [165]. This demonstrates that these two kinases are not functionally redundant for sNAG induced tissue repair or antimicrobial effects.

We also show that sNAG stimulation results in an increased elasticity as compared to both unwounded and wounded skin. Elasticity is conferred by elastin fibers formed during development. Elastin synthesis is absent in the adult but can be induced following injury through the up regulation of certain cytokines and growth factors, e.g. insulin-like growth factor-1 (IGFI) and interleukin 1 (IL-1), but is aberrantly deposited and is not detected until months after healing. Aberrant deposition of elastin leads to decreased elasticity and flexibility of the scar [186, 187] and is characterized by short, thin, immature fibers. sNAG treatment causes increased in elastin fiber staining that is visually similar to unwounded skin and correlates to increased trophoelastin protein expression and skin elasticity. Elastin expression is controlled, at least in part by IL-1 and IGF-1 and we show, at least *in vitro*, sNAG stimulation results in an increased expression of IL-1, suggesting a connection between this Akt1 and elastin fiber staining [137]. It is well established that Akt1 is a major kinase functioning downstream of both IL-1 and IGF-1.

In general, Akt1 has been linked to extracellular matrix assembly and fibronectin organization via the activation of β1 integrins [188]. Our previously published findings show that sNAG specifically activates integrin-dependent signaling and that this leads to Akt1 activation [189]. Therefore, it is possible that elastin

deposition in the sNAG stimulated wounds is due to an integrin/Akt1 dependent pathway. Given that elastin fiber deposition does not generally occur in the adult, it will be important to understand the mechanisms by which sNAG stimulates elastogenesis for future application to skin repair and tissue bioengineering.

Our findings suggest a model (**Fig. 4.6**) by which sNAG nanofibers stimulate outside-in integrin signaling that results in an activation of Akt1 which controls cellular alignment under tension, and reductions in collagen I deposition and scar formation. Given that scarring is a major medical complication that causes decreased tissue function and aesthetics and the limitation of current treatment options, treatment of cutaneous wounds with this FDA approved material can be used to provide hemostasis, increased wound healing kinetics, increased innate anti-microbial responses and decreased scarring and increased function, thus providing combinatorial therapy using a single FDA approved agent.

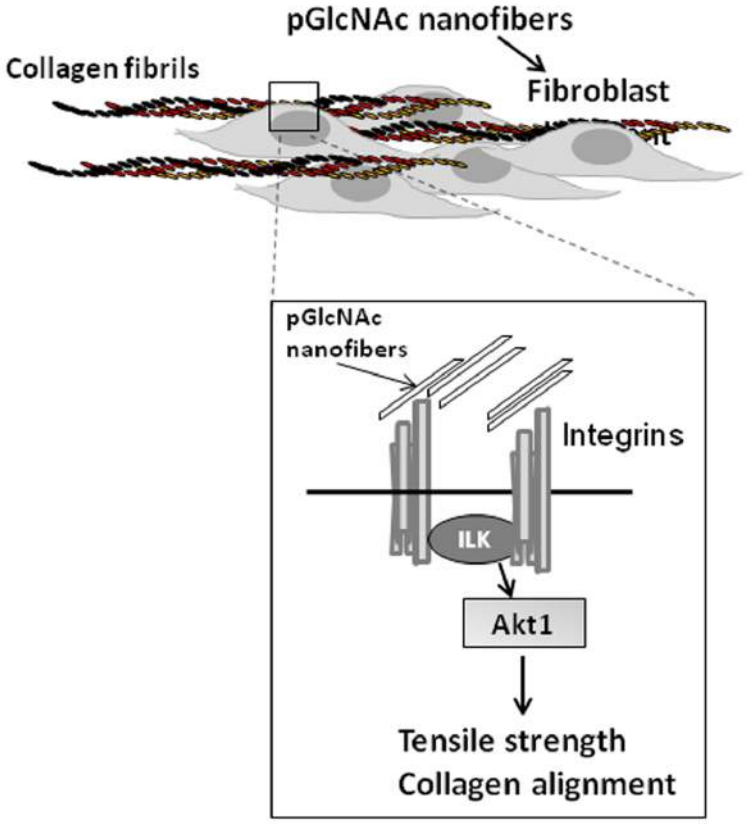

Figure 4.6. Model of sNAG-dependent regulation of collagen alignment and tensile strength. An illustration showing the interaction between pGlcNAC nanofibers and integrins, upstream of Akt1, that leads to increased collagen alignment and tensile strength in cutaneous wound healing.

Chapter 5

We have shown that pGLcNAc treatment of full thickness cutaneous wounds results in more rapid healing, increased expressions of antimicrobial peptides, and decreased scarring. Our data suggests all of these pGlcNac dependant effects are regulated through Akt1. Our *in vivo* studies also show that mice deficient in Akt1 show a delayed healing response that is not rescued or improved by treatment with pGlcNAc nanofibers. Additionally, AKT1-/- mice treated with the nanofiber do not show increased tensile strength or appropriate collagen alignment as compared to Wild Type treated animals. These data suggest AKt1 may play a critical role in tissue regeneration and remodeling.

Myofibroblasts are well established as critical cells in tissue remodeling, contraction, and scar formation. Force generation by these cells depends on the contraction of stress fibers and is mediated through Rho/Rho-kinase (ROCK) and its inhibition of myosin phosphatase [190]. Activated ROCK promotes the contraction of isolated stress fibers and could result in a long-lasting tensile activity [191]. Studies to determine the role of Rho- kinase in stress fiber organization show that treatment of cultured fibroblast with rho-kinase inhibitors results in stress fiber disassembly [191]. Investigation of collagen matric contraction after treatment with either AKt1 or Rho-kinase inhibitors further

elucidate the signaling involved. Interestingly, pharmacologic inhibition of both Akt1 and Rho-kinase resulted in complete inhibition of the matrix contraction [192]. These data raise the possibility that Rho signaling may play an important role in myofibroblasts activation and scar formation in our model. While the signaling is complex and a significant amount of cross talk exists, some evidence indicates that Rho GTPases may suppress or inactivate AKT [193]. Therefore, a lack of active Akt may lead to increased Rho resulting in increased stress fiber formation in myofibroblasts and contraction of tissue. This also raises the interesting possibility that treatment with pGlcNAC nanofibers inhibits expression of Rho GTPases through the activation of Akt1 resulting in decreased scar formation. While speculative, it would be interesting to determine the expression of Rho GTPases in our wound healing model and to determine the effect, if any, of pGlcNAc nanofiber treatment.

Transcriptional Regulation of Defensins

Previously published data from our lab positioned Akt1 upstream of Ets1 transcription factor in human primary EC [122]. ETS transcription factors have been linked to diverse biological roles. Several ETS domain proteins have been shown to play a role in angiogenesis and vasculogenesis [194] while others, PU.1 specifically, plays a role in the differentiation of lymphoid and myeloid lineages [195]. We have shown here, for the first time using *in vitro* experimentation, that primary EC express defensins (α1,α4,α5, and β3) when stimulated with sNAG nanofibers and that this expression is Akt1 dependent. Others have shown that β-defensin expression is controlled on the level of

transcription [150] but little is known about the regulation of α-defensins. β-defensins are known to be regulated by NFkB and the Ets family, both of which are downstream of Akt1 [196]. Since ETS1 as well as other Ets family members are positioned downstream of Akt1 in primary endothelial cells and since inhibition of Akt1 leads to decreased defensin expression, it is likely that nanofiber activation of defensins is dependent on the Akt1→ETS pathway. Using Genomatix software, we have mapped Akt1 dependent transcription factor binding sites in the promoter regions of α- defensins 1, 4, and 5. Interestingly, all three α-defensins have an evolutionarily conserved ETS binding site directly upstream of the mRNA transcription start site.

Our data has shown that defensin expression is regulated at the level of transcription and that transcriptional activity is induced by treatment with the nanofiber. Message stability was measured by assessment of heteronuclear RNA. Endothelial cells that were serum starved prior to nanofiber stimulation were assessed for defensin expression using intron spanning primers. To examine the role of the Akt→ Ets family in the transcriptional regulation of defensin expression, we cloned a 500 base pair region upstream of the transcription start site of alpha defensins 1 and performed site directed mutagenesis to achieve a point mutation in the ETS site. Wild Type and mutated plasmids were transformed and luciferase assays were performed to examine promoter activity. We show that nanofiber treatment results in increased transcriptional activity but we have not yet been able to show that the mutant ETS has an effect. We will continue to determine if Ets is implicated in the

transcriptional regulation of defensin expression. If Ets-binding sites are implicated in transcriptional regulation, each site can be assessed by CHIP (Chromatin immunoprecipitation) analysis to determine specifically which Ets family members are binding to the promoter.

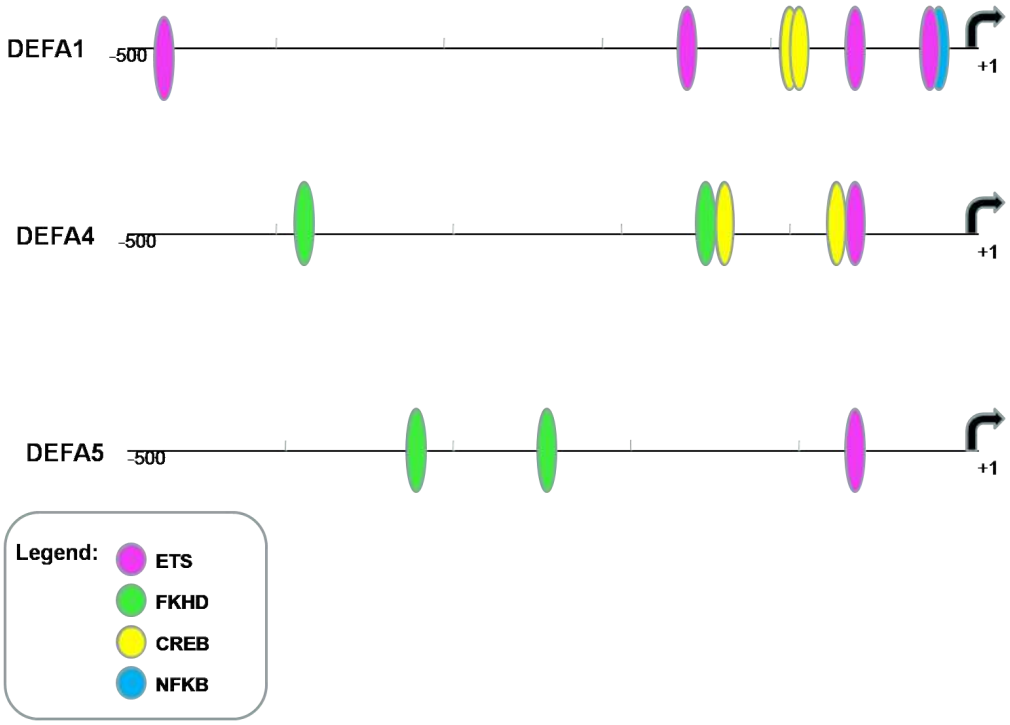

Figure 5.1 Schematic of Akt1 dependent transcription factor binding sites. Using Genomatix software, 500 bp upstream of the transcription start site was analyzed for *conserved Akt1-dependent transcription factor binding sites on the* mRNA of α-def 1, 4, and 5.

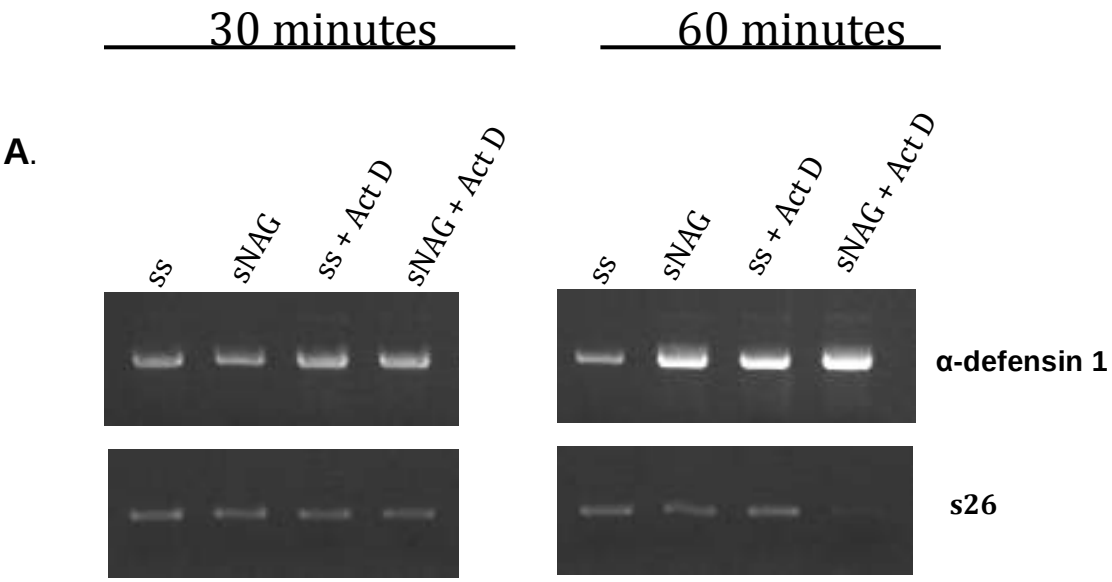
30 minutes
60 minutes
A.
ss
sNAG
ss + Act D
sNAG + Act D
ss
sNAG
ss + Act D
sNAG + Act D
α-defensin 1
s26

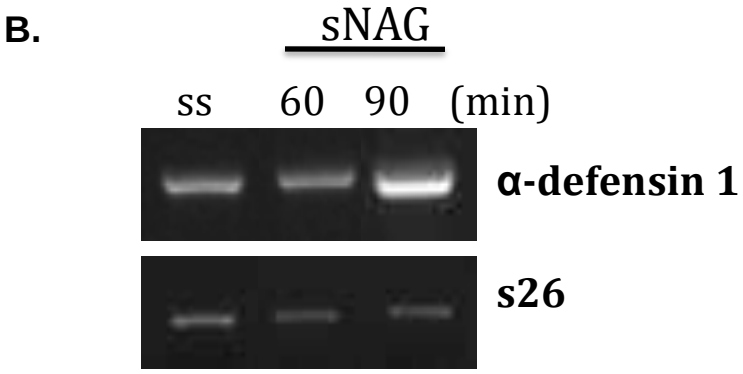
B.
sNAG
ss
60
90
(min)
α-defensin 1
s26

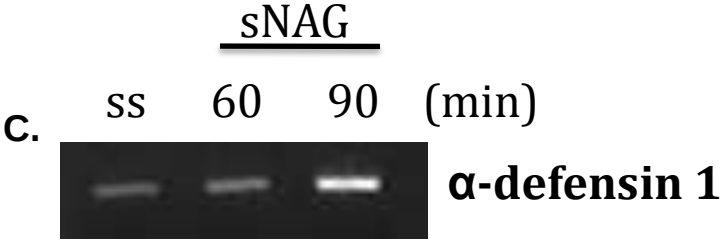
sNAG
C.
ss
60
90
(min)
α-defensin 1

D.

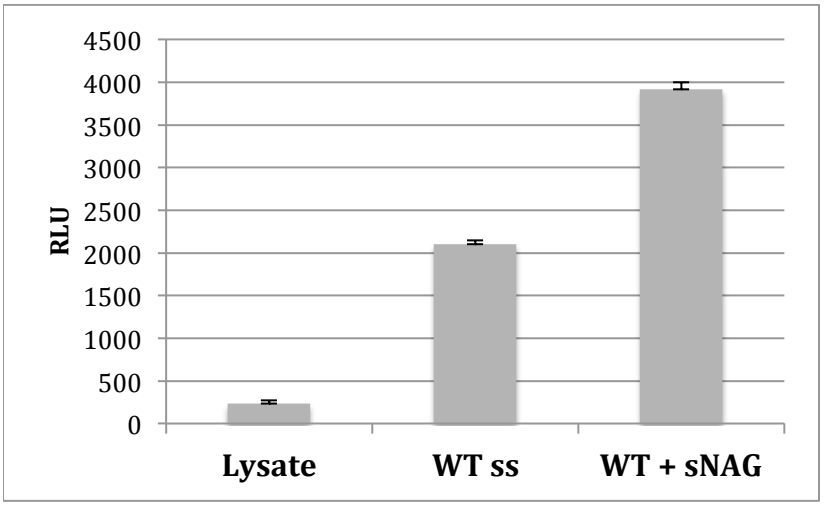

Figure 5.2 (A-D). A)Endothelial cells were serum starved and pre-treated with Actinomycin D prior to sNAG stimulation and assessed for expression of α-defensin 1. B) Endothelial cells were serum starved prior to stimulation with sNAG and assess for expression of of α-defensin1. C) Endothelial cells that were serum starved prior to nanofiber stimulation were assessed for defensin expression using intron spanning primers to determine heteronuclear RNA at the noted time points. D) A 500 base pair region upstream of the transcription start site of alpha defensins was cloned and site directed mutagenesis to achieve a point mutation in the ETS site was completed. Wild Type and mutated plasmids were transformed and luciferase assays were performed to examine promoter activity.

The Role of EPSTI1 in Cutaneous Wound Healing

Here, we have shown that pGlcNAc treatment of cutaneous wounds results in a smaller scar that has increased tensile strength and elasticity. Additionally, pGlcNAc treated wounds exhibit decreased collagen content, increased collagen organization and decreased myofibroblast content. Our data presented here provides evidence that Akt1 is central to pGlcNAc dependent activities. While we were able to show that Akt1 plays a role in fibroblast alignment with in a fibrin gel model, the exact mechanism and signaling remain unclear. Transcriptome analysis of nanofiber treated cells shows induction of many interferon-responsive genes such as Epithelial Stromal Interaction Protein 1 (EPSTI1), a novel protein involved in epithelial/stromal interactions **Table 5.1** String analysis, a program that analyzes protein interactions, indicates that this novel protein may interact with alpha defensins as well. (**Figure 5.3)** Additionally, we now have new and exciting data that EPSTI1 is up-regulated in nanofiber treated wounds of WT but not in similarly treated Akt1-/- animals **(Figure 5.4)** .

Top 20 genes Upregulated by sNAG treatment of EC
Cytidine monophasphate kinase
Chemokine (C-X-C motif) ligand 10
Radical S-adenosyl methionine domain containing 2
2'-5'-oligoadenylate synthesase-like
Receptor (chemosensory)transporter protein 4
Interferon-induced transmembrane protein 1 (9-27)
Myxovirus (influenza virus) resistance 1, interferon-inducible protein p78
Interferon-induced protein with tetratricopeptide repeats 1
Epithelial stromal interaction 1
Myxovirus (influenza virus) resistance 2
Interferon-induced protein with tetratricopeptide repeats 3
NPC-A-7
ISG15 ubiquitin-like modifier
Interferon, alpha-inducible protein 6
Bone marrow stromal cell antigen 2
Proteosome subunit, beta type, 9
Interferon-induced protein with tetratricopeptide repeats 2
solute carrier 15
Chemokine (C-X-C motif) ligand 11

Table 5.1 illustrating the top genes up regulated by sNAG in endothelial cells treated with 10µg/ml nanofiber under serum starved conditions for 24 hours and subjected to whole transcriptome analysis

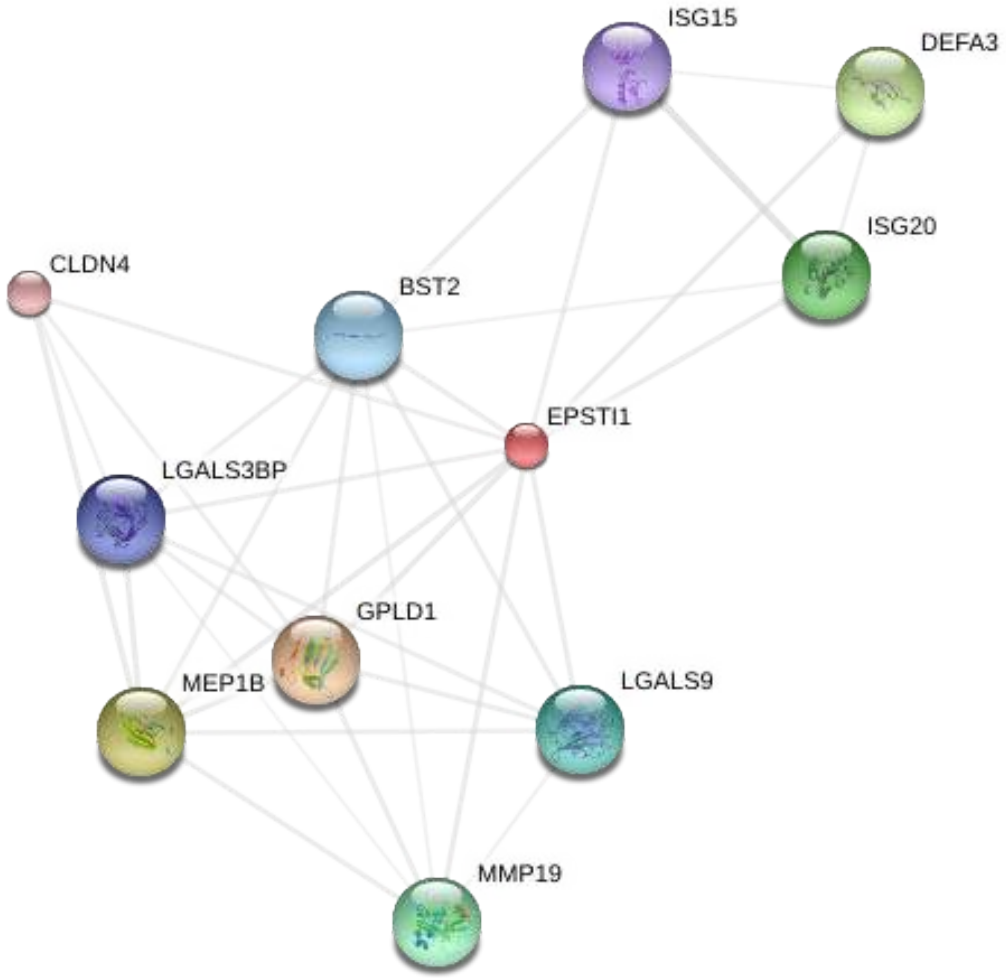

Figure 5.3 Illustration derived from String analysis, a program that analyzes protein interactions.

A.

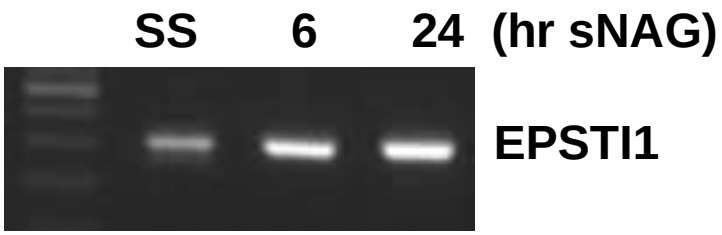

B.

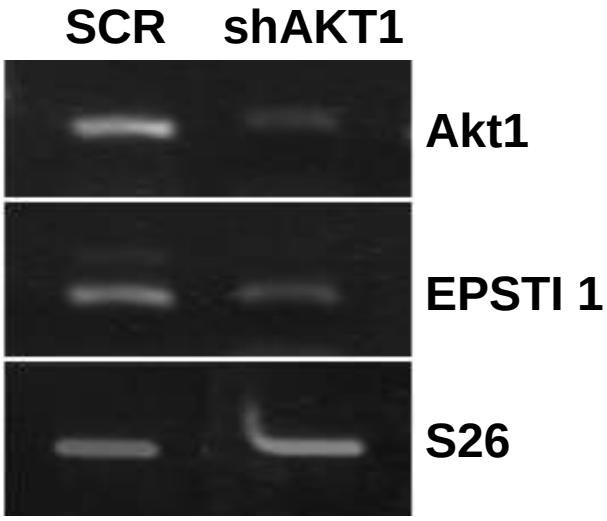

Figure 5.4 **(**A) Serum starved EC were stimulated with nanofibers for times indicated and assessed for EPSTI1 expression. (B) Analyses of sNAG stimulated EC infected with a scrambled control or Akt1 shRNA lentiviruses and assessed for expression of EPSTI1

A.

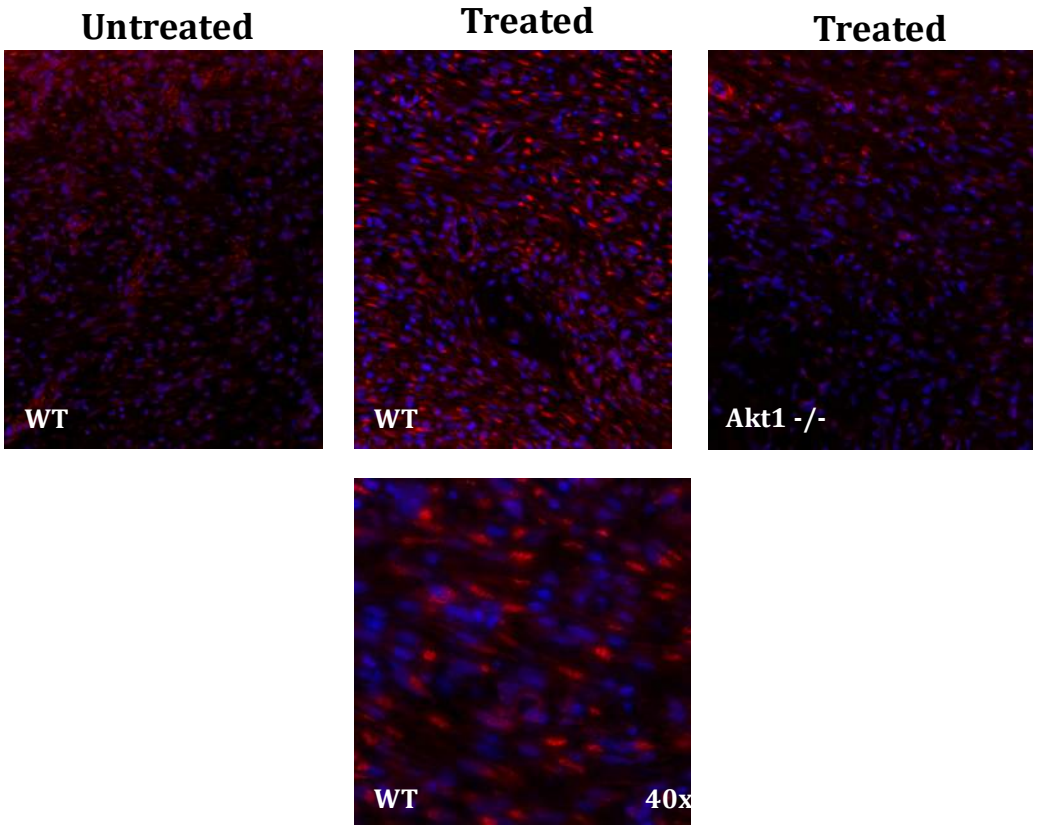
Untreated
Treated
Treated
WT
WT
Akt1 -/-
WT
40x

B.

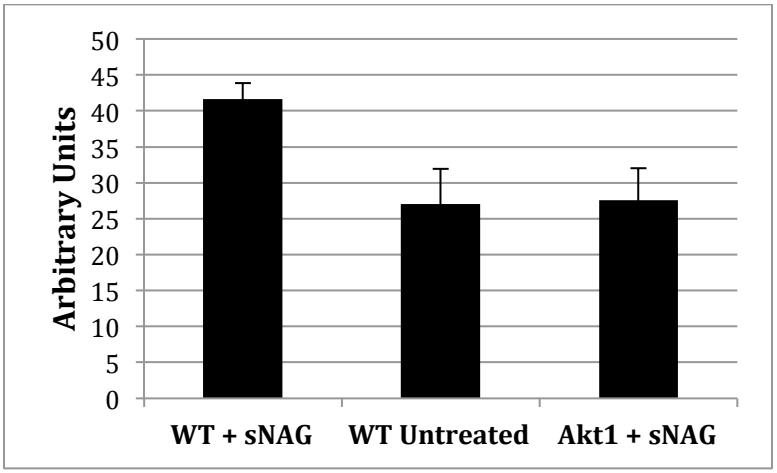
Arbitrary Units
50
45
40
35
30
25
20
15
10
5
0
WT + sNAG
WT Untreated
Akt1 + sNAG

Figure 5.5 Representative images of wound sections derived from treated and untreated WT and AKT1-/-animals labeled with antibodies directed against EPSTI1. (B) Quantification of EPSTI1 staining in wound tissue sections using NIH Image J software.

We have defined the cell type in the wound bed that express EPSTI1 as fibroblasts using a series of cell markers including hsp47 (a collagen chaperone) and vimentin. While little is known about this protein or its subcellular localization, we have shown that EPSTI1 does not co-localize with KDEL (marker for endoplasmic reticulum). While we have show that EPSTI1 functions down stream of Akt1 *in vitro,* we have been unable to define a specific and definite role for EPSTI1 in fibroblast alignment and wound healing. Previously we showed that ablation of Akt1 expression in embedded fibroblasts lead to decreased cellular organization. Unfortunately, knockdown of EPSTI1 in fibroblasts provided inconclusive results in our fibrin gel assays. Indeed, more studies are needed to clearly define the role of EPSTI1 in collagen alignment and tissue reorganization.

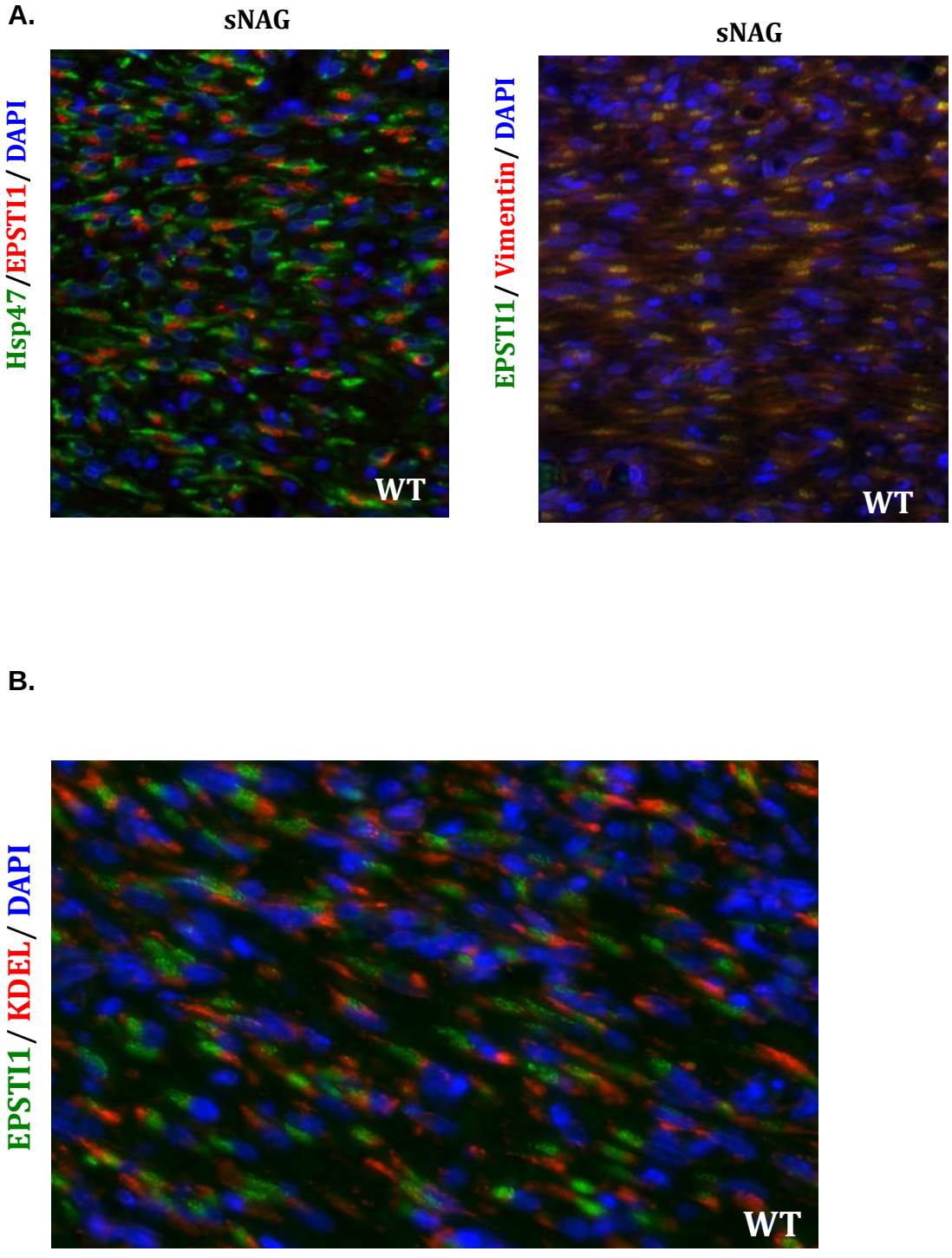
A.
sNAG
Hsp47/EPSTI1/ DAPI
WT
sNAG
EPSTI1/ Vimentin/ DAPI
WT
B.
EPSTI1/ KDEL/ DAPI
WT

Figure 5.6 (A) Tissue was harvested from WT mice 10 days post wounding and analyzed for expression of Hsp47, EPSTI1, VImentin, and DAPI. (B) Tissue was harvested from WT Mice 10 days post wounding and analyzed for expression of EPSTI1, KDEL (Endoplasmic reticulum marker), and DAPI (nuclear marker)

Oral Wound Healing vs. Cutaneous Wound Healing

Due to an interest and profession concerning dentistry and the oral cavity, a comparison of cutaneous healing and oral mucosal healing seems fitting? To elucidate the similarities and differences between healing within the different environments, each stage of wound healing will be compared. While oral wound healing progresses through the same stages of healing [197] the oral mucosa heals at a much faster rate and with a lack of scarring [198]. Animal studies comparing both cutaneous and mucosal excisional wounds show that while neutrophil infiltration follows a similar time course in both models, the overall number of neutrophils were significantly reduced in oral wounds at all time points measured [198]. Previous data using a db/db cutaneous would model showed that a reduction in inflammation and inflammatory cytokines is associated with improved tissue repair [199]. Additionaly, oral mucosal wounds exhibit significantly decreased macrophage infiltration [198, 200] and expression of inflammatory cytokines IL-6 and IL-8 as compared to dermal wounds [198]. Data also suggests that macrophages may play in important role in scar formation [201]. Comparison of cutaneous and oral mucosal wounds indicate that oral wounds show a brief increase in macrophage expression, but at later time points (days 14, 28, and 60 days post wounding), skin wounds exhibit; significant increases in the number of macrophage as compared to oral wounds [200]. Mast cells, while best known for their role in allergies and allergic responses, have also been shown to play a prominent role in wound healing and scar formation [201]. As with macrophages, oral musical wounds contain significantly fewer mast cells compared to skin wounds at 60 days of healing [200].

A comparison of oral mucosa wounds and cutaneous skin wounds in the Duroc pig also elucidated differences in the cellularity and myofibroblasts response. The density of cells with normal fibroblast morphology was significantly lower in oral wounds as compared to skin wounds. Interestingly, the fibroblasts were aligned perpendicular to wound edges in the oral mucosa while skin wounds showed randomly arranged, atypically round fibroblast cells [200]. After 60 days, the orientation, density and maturity of collagen fibers were comparable to that of unwounded tissue in the oral mucosal wounds as compared to skin indicating that of mucosal wounds showed better regeneration of connective tissue organization [200]

Scar formation

As with cutaneous wound healing, the exact mechanisms governing healing and scar formation are unknown in the oral environment. Studies comparing the oral mucosa and cutaneous wounds in red Duroc pigs shows that oral wounds exhibit significantly less scarring both clinically and histologically [202]. As discussed previously, levels of TGFβ correlate to scar formation. As would be expected, oral mucosal wounds show decreased levels of TGFβ and smad3 positive cells [200]. Additionally, cutaneous scars contained a significant number of type I procollagen immunopositive cells and an increased fibronectin content, while the oral mucosal wounds demonstrated accumulation of tenascin-C, an extracellular matrix molecule that is abundantly expressed in embryonic scarless wound healing [202]. Comparison of dermal fibroblasts and oral mucosal fibroblasts show that dermal cells embedded in collagen gels possess greater contraction

potency [203]. Collagen gels embedded with fibrobalsts serve as a valuable model for studying wound closure. Wounding of the gel results in fibroblasts migration toward the defect and closure of the gel edges [204], likely simulating wound contraction and scar formation.

As with dermal wound healing, individuals with compromised health exhibit delays in oral mucosal wound healing. Delayed vascularization, decreased innate immunity, and decreased growth factor production may be involved in the delayed healing seen in the oral mucosa of diabetic patients [205]. Since diabetic patients are immunocompromised, infection is of particular concern while patients are healing. Compounding this issue, reports indicate these patients also exhibit suppression of innate immunity. Diabetes results in decreased neutrophil migration from the vasculature as well as decreased chemotactic activity of neutrophils [206]. Interestingly, several types of antimicrobial peptides are produced by the oral epithelium, and the expression levels of beta-defensins are affected by the concentration of insulin and glucose [207]. In addition to a decreased innate immune response, diabetic patients also suffer from reduced salivary flow. Saliva is a critical component in the oral cavity and functions in digestion, antimicrobial activity, and cleaning or rinsing of the oral mucosa surfaces. The reduced saliva and reduced antimicrobial peptide expression present in diabetic patients likely contributes significantly to altered wound healing of the oral mucosa.

While similar mechanisims are involved when comparing oral mucosal healing to cutaneous wound healing, oral healing presents with a more

regenerative type of healing that is comparable to fetal wound healing. With this in mind, are there any potential therapeutic uses for pGlcNAc nanofibers in the oral cavity? Very recent data indicates that oral bacteria result in keratinocyte apoptosis and delayed oral wound healing [208]. The antimicrobial properties of pGlcNAC nanofibers may be useful for oral wound healing in both the healthy and the diabetic patient. As previously discussed, patients afflicted with diabetes heal poorly and suffer from decreased innate immunity and defensin expression. In theory, pGlcNAc nanofibers could also prove useful in the treatment of oral mucositis as a result of cancer treatment. Oral mucositis is a common and debilitating complication of head and neck radiation. Currently, most treatment modalities for oral mucositis are only supportive in nature. The effect of pGlcNAC nanofibers treatment on epithelial cells raises the question of potential therapeutic value for this painful and debilitating side effect of cancer treatment. While the pGlcNAc nanofibers we have studied have not been evaluated in the oral cavity, the potential for uses in the dental field are numerous.

REFERENCES

1. **Brigham, P.A. and E. McLoughlin, *Burn incidence and medical care use in the United States: estimates, trends, and data sources.* J Burn Care Rehabil, 1996. 17(2): p. 95-107.**
2. **Singer, A.J. and R.A. Clark, *Cutaneous wound healing.* N Engl J Med, 1999. 341(10): p. 738-46.**
3. **Broughton, G., 2nd, J.E. Janis, and C.E. Attinger, *The basic science of wound healing.* Plast Reconstr Surg, 2006. 117(7 Suppl): p. 12S-34S.**
4. **Pool, J.G., *Normal hemostatic mechanisms: a review.* Am J Med Technol, 1977. 43(8): p. 776-80.**
5. **Martin, P., *Wound healing--aiming for perfect skin regeneration.* Science, 1997. 276(5309): p. 75-81.**
6. **Beck, E., F. Duckert, and M. Ernst, *The influence of fibrin stabilizing factor on the growth of fibroblasts in vitro and wound healing.* Thromb Diath Haemorrh, 1961. 6: p. 485-91.**
7. **Inbal, A., et al., *Impaired wound healing in factor XIII deficient mice.* Thromb Haemost, 2005. 94(2): p. 432-7.**
8. **Li, J., et al., *Defensins HNP1 and HBD2 stimulation of wound-associated responses in human conjunctival fibroblasts.* Invest Ophthalmol Vis Sci, 2006. 47(9): p. 3811-9.**
9. **Springer, T.A., *Traffic signals for lymphocyte recirculation and leukocyte emigration: the multistep paradigm.* Cell, 1994. 76(2): p. 301-14.**
10. **Hubner, G., et al., *Differential regulation of pro-inflammatory cytokines during wound healing in normal and glucocorticoid-treated mice.* Cytokine, 1996. 8(7): p. 548-56.**
11. **Mirza, R., L.A. DiPietro, and T.J. Koh, *Selective and specific macrophage ablation is detrimental to wound healing in mice.* Am J Pathol, 2009. 175(6): p. 2454-62.**
12. **Goren, I., et al., *A transgenic mouse model of inducible macrophage depletion: effects of diphtheria toxin-driven lysozyme M-specific cell lineage ablation on wound inflammatory, angiogenic, and contractive processes.* Am J Pathol, 2009. 175(1): p. 132-47.**
13. **Novak, M.L. and T.J. Koh, *Macrophage phenotypes during tissue repair.* J Leukoc Biol, 2013. 93(6): p. 875-81.**
14. **Lawrence, W.T. and R.F. Diegelmann, *Growth factors in wound healing.* Clin Dermatol, 1994. 12(1): p. 157-69.**
15. **Smola, H., G. Thiekotter, and N.E. Fusenig, *Mutual induction of growth factor gene expression by epidermal-dermal cell interaction.* J Cell Biol, 1993. 122(2): p. 417-29.**

16. **Brown, L.F., et al.,** ***Expression of vascular permeability factor (vascular endothelial growth factor) by epidermal keratinocytes during wound healing.*** **J Exp Med, 1992. 176(5): p. 1375-9.**
17. **Greiling, D. and R.A. Clark,** ***Fibronectin provides a conduit for fibroblast transmigration from collagenous stroma into fibrin clot provisional matrix.*** **J Cell Sci, 1997. 110 (Pt 7): p. 861-70.**
18. **Mignatti P, R.D., Welgus HG, Parks WC,** ***Proteinases and Tissue Remodeling In: The Molecular and Cellular Biology of Wound Repair*****, ed. C. RAF1996, New York: Plenum Press. 427-474.**
19. **Ehrlich, H.P. and T.M. Krummel,** ***Regulation of wound healing from a connective tissue perspective.*** **Wound Repair Regen, 1996. 4(2): p. 203-10.**
20. **Robson, M.C., et al.,** ***Wound healing trajectories as predictors of effectiveness of therapeutic agents.*** **Arch Surg, 2000. 135(7): p. 773-7.**
21. **Steed, D.L.,** ***The role of growth factors in wound healing.*** **Surg Clin North Am, 1997. 77(3): p. 575-86.**
22. **Grinnell, F.,** ***Fibroblasts, myofibroblasts, and wound contraction.*** **J Cell Biol, 1994. 124(4): p. 401-4.**
23. **Gabbiani, G., et al.,** ***Granulation tissue as a contractile organ. A study of structure and function.*** **J Exp Med, 1972. 135(4): p. 719-34.**
24. **Hinz, B., et al.,** ***The myofibroblast: one function, multiple origins.*** **Am J Pathol, 2007. 170(6): p. 1807-16.**
25. **Darby, I., O. Skalli, and G. Gabbiani,** ***Alpha-smooth muscle actin is transiently expressed by myofibroblasts during experimental wound healing.*** **Lab Invest, 1990. 63(1): p. 21-9.**
26. **Montesano, R. and L. Orci,** ***Transforming growth factor beta stimulates collagen-matrix contraction by fibroblasts: implications for wound healing.*** **Proc Natl Acad Sci U S A, 1988. 85(13): p. 4894-7.**
27. **Desmouliere, A., et al.,** ***Transforming growth factor-beta 1 induces alpha-smooth muscle actin expression in granulation tissue myofibroblasts and in quiescent and growing cultured fibroblasts.*** **J Cell Biol, 1993. 122(1): p. 103-11.**
28. **Malmstrom, J., et al.,** ***Transforming growth factor-beta 1 specifically induce proteins involved in the myofibroblast contractile apparatus.*** **Mol Cell Proteomics, 2004. 3(5): p. 466-77.**
29. **Sandbo, N. and N. Dulin,** ***Actin cytoskeleton in myofibroblast differentiation: ultrastructure defining form and driving function.*** **Transl Res, 2011. 158(4): p. 181-96.**
30. **Gabbiani, G., G.B. Ryan, and G. Majne,** ***Presence of modified fibroblasts in granulation tissue and their possible role in wound contraction.*** **Experientia, 1971. 27(5): p. 549-50.**
31. **Katoh, K., et al.,** ***Isolation and contraction of the stress fiber.*** **Mol Biol Cell, 1998. 9(7): p. 1919-38.**
32. **Cramer, L.P., M. Siebert, and T.J. Mitchison,** ***Identification of novel graded polarity actin filament bundles in locomoting heart fibroblasts:***

implications for the generation of motile force. **J Cell Biol, 1997. 136(6): p. 1287-305.**

33. **Petroll, W.M., et al., *Quantitative analysis of stress fiber orientation during corneal wound contraction.* J Cell Sci, 1993. 104 (Pt 2): p. 353-63.**
34. **Mar, P.K., et al., *Stress fiber formation is required for matrix reorganization in a corneal myofibroblast cell line.* Exp Eye Res, 2001. 72(4): p. 455-66.**
35. **Jester, J.V., et al., *Temporal, 3-dimensional, cellular anatomy of corneal wound tissue.* J Anat, 1995. 186 (Pt 2): p. 301-11.**
36. **Hinz, B., et al., *Alpha-smooth muscle actin expression upregulates fibroblast contractile activity.* Mol Biol Cell, 2001. 12(9): p. 2730-41.**
37. **Chrzanowska-Wodnicka, M. and K. Burridge, *Rho-stimulated contractility drives the formation of stress fibers and focal adhesions.* J Cell Biol, 1996. 133(6): p. 1403-15.**
38. **Edwards, C. and R. Marks, *Evaluation of biomechanical properties of human skin.* Clin Dermatol, 1995. 13(4): p. 375-80.**
39. **Doillon, C.J., et al., *Collagen fiber formation in repair tissue: development of strength and toughness.* Coll Relat Res, 1985. 5(6): p. 481-92.**
40. **Levenson, S.M., et al., *The Healing of Rat Skin Wounds.* Ann Surg, 1965. 161: p. 293-308.**
41. **Larson, B.J., M.T. Longaker, and H.P. Lorenz, *Scarless fetal wound healing: a basic science review.* Plast Reconstr Surg, 2010. 126(4): p. 1172-80.**
42. **Colwell, A.S., et al., *An in vivo mouse excisional wound model of scarless healing.* Plast Reconstr Surg, 2006. 117(7): p. 2292-6.**
43. **Frantz, F.W., et al., *Biology of fetal repair: the presence of bacteria in fetal wounds induces an adult-like healing response.* J Pediatr Surg, 1993. 28(3): p. 428-33; discussion 433-4.**
44. **Ozturk, S., et al., *Results of artificial inflammation in scarless foetal wound healing: an experimental study in foetal lambs.* Br J Plast Surg, 2001. 54(1): p. 47-52.**
45. **Longaker, M.T., et al., *Adult skin wounds in the fetal environment heal with scar formation.* Ann Surg, 1994. 219(1): p. 65-72.**
46. **Armstrong, J.R. and M.W. Ferguson, *Ontogeny of the skin and the transition from scar-free to scarring phenotype during wound healing in the pouch young of a marsupial, Monodelphis domestica.* Dev Biol, 1995. 169(1): p. 242-60.**
47. **Martin, P. and J. Lewis, *Actin cables and epidermal movement in embryonic wound healing.* Nature, 1992. 360(6400): p. 179-83.**
48. **Brock, J., et al., *Healing of incisional wounds in the embryonic chick wing bud: characterization of the actin purse-string and demonstration of a requirement for Rho activation.* J Cell Biol, 1996. 135(4): p. 1097-107.**
49. **Martin, P., et al., *Rapid induction and clearance of TGF beta 1 is an early response to wounding in the mouse embryo.* Dev Genet, 1993. 14(3): p. 225-38.**

50. **Shah, M., D.M. Foreman, and M.W. Ferguson, *Control of scarring in adult wounds by neutralising antibody to transforming growth factor beta.* Lancet, 1992. 339(8787): p. 213-4.**
51. **Kohama, K., et al., *TGF-beta-3 promotes scarless repair of cleft lip in mouse fetuses.* J Dent Res, 2002. 81(10): p. 688-94.**
52. **Beanes, S.R., et al., *Confocal microscopic analysis of scarless repair in the fetal rat: defining the transition.* Plast Reconstr Surg, 2002. 109(1): p. 160-70.**
53. **Merkel, J.R., et al., *Type I and type III collagen content of healing wounds in fetal and adult rats.* Proc Soc Exp Biol Med, 1988. 187(4): p. 493-7.**
54. **Namazi, M.R., M.K. Fallahzadeh, and R.A. Schwartz, *Strategies for prevention of scars: what can we learn from fetal skin?* Int J Dermatol, 2011. 50(1): p. 85-93.**
55. **Beanes, S.R., et al., *Down-regulation of decorin, a transforming growth factor-beta modulator, is associated with scarless fetal wound healing.* J Pediatr Surg, 2001. 36(11): p. 1666-71.**
56. **Sayani, K., et al., *Delayed appearance of decorin in healing burn scars.* Histopathology, 2000. 36(3): p. 262-72.**
57. **Kolb, M., et al., *Proteoglycans decorin and biglycan differentially modulate TGF-beta-mediated fibrotic responses in the lung.* Am J Physiol Lung Cell Mol Physiol, 2001. 280(6): p. L1327-34.**
58. **Soo, C., et al., *Differential expression of fibromodulin, a transforming growth factor-beta modulator, in fetal skin development and scarless repair.* Am J Pathol, 2000. 157(2): p. 423-33.**
59. **Estes, J.M., et al., *Phenotypic and functional features of myofibroblasts in sheep fetal wounds.* Differentiation, 1994. 56(3): p. 173-81.**
60. **Cass, D.L., et al., *Myofibroblast persistence in fetal sheep wounds is associated with scar formation.* J Pediatr Surg, 1997. 32(7): p. 1017-21; discussion 1021-2.**
61. **Rolfe, K.J. and A.O. Grobbelaar, *A review of fetal scarless healing.* ISRN Dermatol, 2012. 2012: p. 698034.**
62. **Cederlund, A., G.H. Gudmundsson, and B. Agerberth, *Antimicrobial peptides important in innate immunity.* FEBS J, 2011. 278(20): p. 3942-51.**
63. **Lehrer, R.I., *Primate defensins.* Nat Rev Microbiol, 2004. 2(9): p. 727-38.**
64. **Rice, W.G., et al., *Defensin-rich dense granules of human neutrophils.* Blood, 1987. 70(3): p. 757-65.**
65. **Ganz, T., et al., *The structure of the rabbit macrophage defensin genes and their organ-specific expression.* J Immunol, 1989. 143(4): p. 1358-65.**
66. **Sengelov, H., et al., *Mobilization of granules and secretory vesicles during in vivo exudation of human neutrophils.* J Immunol, 1995. 154(8): p. 4157-65.**
67. **Ganz, T. and R.I. Lehrer, *Defensins.* Curr Opin Immunol, 1994. 6(4): p. 584-9.**

68. **Diamond, G.e.a.P.N.A.S.U., *Tracheal antimicrobial peptide, a cysteine-rich peptide from mammalian tracheal mucosa: peptide isolation and cloning of a cDNA.* Proc. Natl Acad. Sci. USA 1991**

. 88(May): p. 3952-3956.

69. **Yount, N.Y., et al., *Rat neutrophil defensins. Precursor structures and expression during neutrophilic myelopoiesis.* J Immunol, 1995. 155(9): p. 4476-84.**
70. **Valore, E.V. and T. Ganz, *Posttranslational processing of defensins in immature human myeloid cells.* Blood, 1992. 79(6): p. 1538-44.**
71. **Wilson, C.L., et al., *Regulation of intestinal alpha-defensin activation by the metalloproteinase matrilysin in innate host defense.* Science, 1999. 286(5437): p. 113-7.**
72. **Ganz, T., *Defensins: antimicrobial peptides of innate immunity.* Nat Rev Immunol, 2003. 3(9): p. 710-20.**
73. **Wimley, W.C., M.E. Selsted, and S.H. White, *Interactions between human defensins and lipid bilayers: evidence for formation of multimeric pores.* Protein Sci, 1994. 3(9): p. 1362-73.**
74. **Lehrer, R.I., et al., *Interaction of human defensins with Escherichia coli. Mechanism of bactericidal activity.* J Clin Invest, 1989. 84(2): p. 553-61.**
75. **de Leeuw, E., et al., *Functional interaction of human neutrophil peptide-1 with the cell wall precursor lipid II.* FEBS Lett, 2010. 584(8): p. 1543-8.**
76. **Hubert, P., et al., *Defensins induce the recruitment of dendritic cells in cervical human papillomavirus-associated (pre)neoplastic lesions formed in vitro and transplanted in vivo.* FASEB J, 2007. 21(11): p. 2765-75.**
77. **Garcia, J.R., et al., *Identification of a novel, multifunctional beta-defensin (human beta-defensin 3) with specific antimicrobial activity. Its interaction with plasma membranes of Xenopus oocytes and the induction of macrophage chemoattraction.* Cell Tissue Res, 2001. 306(2): p. 257-64.**
78. **Niyonsaba, F., H. Ogawa, and I. Nagaoka, *Human beta-defensin-2 functions as a chemotactic agent for tumour necrosis factor-alpha-treated human neutrophils.* Immunology, 2004. 111(3): p. 273-81.**
79. **Yang, D., et al., *Beta-defensins: linking innate and adaptive immunity through dendritic and T cell CCR6.* Science, 1999. 286(5439): p. 525-8.**
80. **Jin, G., et al., *An antimicrobial peptide regulates tumor-associated macrophage trafficking via the chemokine receptor CCR2, a model for tumorigenesis.* PLoS One, 2010. 5(6): p. e10993.**
81. **Owen, S.M., et al., *A theta-defensin composed exclusively of D-amino acids is active against HIV-1.* J Pept Res, 2004. 63(6): p. 469-76.**
82. **Yasin, B., et al., *Theta defensins protect cells from infection by herpes simplex virus by inhibiting viral adhesion and entry.* J Virol, 2004. 78(10): p. 5147-56.**
83. **Munk, C., et al., *The theta-defensin, retrocyclin, inhibits HIV-1 entry.* AIDS Res Hum Retroviruses, 2003. 19(10): p. 875-81.**

84. **Lehrer, R.I., A.M. Cole, and M.E. Selsted, *theta-Defensins: cyclic peptides with endless potential.* J Biol Chem, 2012. 287(32): p. 27014-9.**
85. **Kawsar, H.I., et al., *Overexpression of human beta-defensin-3 in oral dysplasia: potential role in macrophage trafficking.* Oral Oncol, 2009. 45(8): p. 696-702.**
86. **Wehkamp, J., et al., *Defensin deficiency, intestinal microbes, and the clinical phenotypes of Crohn's disease.* J Leukoc Biol, 2005. 77(4): p. 460-5.**
87. **Harder, J., et al., *Mapping of the gene encoding human beta-defensin-2 (DEFB2) to chromosome region 8p22-p23.1.* Genomics, 1997. 46(3): p. 472-5.**
88. **Selsted, M.E. and A.J. Ouellette, *Mammalian defensins in the antimicrobial immune response.* Nat Immunol, 2005. 6(6): p. 551-7.**
89. **Dhople, V., A. Krukemeyer, and A. Ramamoorthy, *The human beta-defensin-3, an antibacterial peptide with multiple biological functions.* Biochim Biophys Acta, 2006. 1758(9): p. 1499-512.**
90. **Murphy, C.J., et al., *Defensins are mitogenic for epithelial cells and fibroblasts.* J Cell Physiol, 1993. 155(2): p. 408-13.**
91. **Baroni, A., et al., *Antimicrobial human beta-defensin-2 stimulates migration, proliferation and tube formation of human umbilical vein endothelial cells.* Peptides, 2009. 30(2): p. 267-72.**
92. **McFarland, K.L., et al., *Expression of genes encoding antimicrobial proteins and members of the toll-like receptor/nuclear factor-kappaB pathways in engineered human skin.* Wound Repair Regen, 2008. 16(4): p. 534-41.**
93. **Hirsch, T., et al., *Human beta-defensin-3 promotes wound healing in infected diabetic wounds.* J Gene Med, 2009. 11(3): p. 220-8.**
94. **Aarbiou, J., et al., *Neutrophil defensins enhance lung epithelial wound closure and mucin gene expression in vitro.* Am J Respir Cell Mol Biol, 2004. 30(2): p. 193-201.**
95. **Song, G., G. Ouyang, and S. Bao, *The activation of Akt/PKB signaling pathway and cell survival.* J Cell Mol Med, 2005. 9(1): p. 59-71.**
96. **Fayard, E., et al., *Protein kinase B/Akt at a glance.* J Cell Sci, 2005. 118(Pt 24): p. 5675-8.**
97. **Alessi, D.R., et al., *Characterization of a 3-phosphoinositide-dependent protein kinase which phosphorylates and activates protein kinase Balpha.* Curr Biol, 1997. 7(4): p. 261-9.**
98. **Hanada, M., Feng, J. and Hemmings, B. A. , *Structure, regulation and function of PKB/AKT–a major therapeutic target. .* Biochim. Biophys. Acta 2004: p. 3-16.**
99. **Nakatani, K., et al., *Identification of a human Akt3 (protein kinase B gamma) which contains the regulatory serine phosphorylation site.* Biochem Biophys Res Commun, 1999. 257(3): p. 906-10.**
100. **Peterson, R.T. and S.L. Schreiber, *Kinase phosphorylation: Keeping it all in the family.* Curr Biol, 1999. 9(14): p. R521-4.**

101. **Bellacosa, A., et al.,** ***A retroviral oncogene, akt, encoding a serine-threonine kinase containing an SH2-like region.*** **Science, 1991. 254(5029): p. 274-7.**
102. **Persad, S., et al.,** ***Regulation of protein kinase B/Akt-serine 473 phosphorylation by integrin-linked kinase: critical roles for kinase activity and amino acids arginine 211 and serine 343.*** **J Biol Chem, 2001. 276(29): p. 27462-9.**
103. **Delcommenne, M., et al.,** ***Phosphoinositide-3-OH kinase-dependent regulation of glycogen synthase kinase 3 and protein kinase B/AKT by the integrin-linked kinase.*** **Proc Natl Acad Sci U S A, 1998. 95(19): p. 11211-6.**
104. **Sarbassov, D.D., et al.,** ***Phosphorylation and regulation of Akt/PKB by the rictor-mTOR complex.*** **Science, 2005. 307(5712): p. 1098-101.**
105. **Datta, S.R., et al.,** ***Akt phosphorylation of BAD couples survival signals to the cell-intrinsic death machinery.*** **Cell, 1997. 91(2): p. 231-41.**
106. **Cardone, M.H., et al.,** ***Regulation of cell death protease caspase-9 by phosphorylation.*** **Science, 1998. 282(5392): p. 1318-21.**
107. **Brunet, A., et al.,** ***Akt promotes cell survival by phosphorylating and inhibiting a Forkhead transcription factor.*** **Cell, 1999. 96(6): p. 857-68.**
108. **Kane, L.P., et al.,** ***Induction of NF-kappaB by the Akt/PKB kinase.*** **Curr Biol, 1999. 9(11): p. 601-4.**
109. **Shiojima, I. and K. Walsh,** ***Role of Akt signaling in vascular homeostasis and angiogenesis.*** **Circ Res, 2002. 90(12): p. 1243-50.**
110. **Xue, G. and B.A. Hemmings,** ***PKB/Akt-dependent regulation of cell motility.*** **J Natl Cancer Inst, 2013. 105(6): p. 393-404.**
111. **Bakin, A.V., et al.,** ***Phosphatidylinositol 3-kinase function is required for transforming growth factor beta-mediated epithelial to mesenchymal transition and cell migration.*** **J Biol Chem, 2000. 275(47): p. 36803-10.**
112. **Gerber, H.P., et al.,** ***Vascular endothelial growth factor regulates endothelial cell survival through the phosphatidylinositol 3'-kinase/Akt signal transduction pathway. Requirement for Flk-1/KDR activation.*** **J Biol Chem, 1998. 273(46): p. 30336-43.**
113. **Chen, W.S., et al.,** ***Growth retardation and increased apoptosis in mice with homozygous disruption of the Akt1 gene.*** **Genes Dev, 2001. 15(17): p. 2203-8.**
114. **Yang, Z.Z., et al.,** ***Protein kinase B alpha/Akt1 regulates placental development and fetal growth.*** **J Biol Chem, 2003. 278(34): p. 32124-31.**
115. **Bae, S.S., et al.,** ***Isoform-specific regulation of insulin-dependent glucose uptake by Akt/protein kinase B.*** **J Biol Chem, 2003. 278(49): p. 49530-6.**
116. **Dummler, B. and B.A. Hemmings,** ***Physiological roles of PKB/Akt isoforms in development and disease.*** **Biochem Soc Trans, 2007. 35(Pt 2): p. 231-5.**
117. **Wright, G.L., et al.,** ***VEGF stimulation of mitochondrial biogenesis: requirement of AKT3 kinase.*** **FASEB J, 2008. 22(9): p. 3264-75.**

118. **Peng, X.D., et al., *Dwarfism, impaired skin development, skeletal muscle atrophy, delayed bone development, and impeded adipogenesis in mice lacking Akt1 and Akt2.* Genes Dev, 2003. 17(11): p. 1352-65.**
119. **Yang, Z.Z., et al., *Dosage-dependent effects of Akt1/protein kinase Balpha (PKBalpha) and Akt3/PKBgamma on thymus, skin, and cardiovascular and nervous system development in mice.* Mol Cell Biol, 2005. 25(23): p. 10407-18.**
120. **Dummler, B., et al., *Life with a single isoform of Akt: mice lacking Akt2 and Akt3 are viable but display impaired glucose homeostasis and growth deficiencies.* Mol Cell Biol, 2006. 26(21): p. 8042-51.**
121. **Morales-Ruiz, M., et al., *Vascular endothelial growth factor-stimulated actin reorganization and migration of endothelial cells is regulated via the serine/threonine kinase Akt.* Circ Res, 2000. 86(8): p. 892-6.**
122. **Lavenburg, K.R., et al., *Coordinated functions of Akt/PKB and ETS1 in tubule formation.* FASEB J, 2003. 17(15): p. 2278-80.**
123. **Zhao, M., et al., *Electrical signals control wound healing through phosphatidylinositol-3-OH kinase-gamma and PTEN.* Nature, 2006. 442(7101): p. 457-60.**
124. **Schafer, M. and S. Werner, *Cancer as an overhealing wound: an old hypothesis revisited.* Nat Rev Mol Cell Biol, 2008. 9(8): p. 628-38.**
125. ***Organic Products from the Sea: Pharmaceuticals, Nutraceuticals, Food Additives, and Cosmoceuticals.***
126. **Vournakis, J.N., et al., *Isolation, purification, and characterization of poly-N-acetyl glucosamine use as a hemostatic agent.* J Trauma, 2004. 57(1 Suppl): p. S2-6.**
127. **Fischer, T.H., et al., *Comparison of structural and hemostatic properties of the poly-N-acetyl glucosamine Syvek Patch with products containing chitosan.* Microsc Res Tech, 2004. 63(3): p. 168-74.**
128. **Scherer, S.S., et al., *Poly-N-acetyl glucosamine nanofibers: a new bioactive material to enhance diabetic wound healing by cell migration and angiogenesis.* Ann Surg, 2009. 250(2): p. 322-30.**
129. **Whistler, R.L. and M. Kosik, *Anticoagulant activity of oxidized and N- and O-sulfated chitosan.* Arch Biochem Biophys, 1971. 142(1): p. 106-10.**
130. **Youngken, H.W., Jr., *The biological potential of the oceans to provide biomedical materials.* Lloydia, 1969. 32(4): p. 407-16.**
131. **Herrmann, J.B. and S.C. Woodward, *An experimental study of wound healing accelerators.* Am Surg, 1972. 38(1): p. 26-34.**
132. **Cole, D.J., et al., *A pilot study evaluating the efficacy of a fully acetylated poly-N-acetyl glucosamine membrane formulation as a topical hemostatic agent.* Surgery, 1999. 126(3): p. 510-7.**
133. **Jewelewicz, D.D., et al., *Modified rapid deployment hemostat bandage reduces blood loss and mortality in coagulopathic pigs with severe liver injury.* J Trauma, 2003. 55(2): p. 275-80; discussion 280-1.**
134. **Thatte, H.S., et al., *Mechanisms of poly-N-acetyl glucosamine polymer-mediated hemostasis: platelet interactions.* J Trauma, 2004. 57(1 Suppl): p. S13-21.**

135. **Fischer, T.H., et al., *Synergistic platelet integrin signaling and factor XII activation in poly-N-acetyl glucosamine fiber-mediated hemostasis.* Biomaterials, 2005. 26(27): p. 5433-43.**
136. **Pietramaggiori, G., et al., *Improved cutaneous healing in diabetic mice exposed to healthy peripheral circulation.* J Invest Dermatol, 2009. 129(9): p. 2265-74.**
137. **Vournakis, J.N., et al., *Poly-N-acetyl glucosamine nanofibers regulate endothelial cell movement and angiogenesis: dependency on integrin activation of Ets1.* J Vasc Res, 2008. 45(3): p. 222-32.**
138. **Mao, C., et al., *Unequal contribution of Akt isoforms in the double-negative to double-positive thymocyte transition.* J Immunol, 2007. 178(9): p. 5443-53.**
139. **Baicu, C.F., et al., *Effects of the absence of procollagen C-endopeptidase enhancer-2 on myocardial collagen accumulation in chronic pressure overload.* Am J Physiol Heart Circ Physiol, 2012. 303(2): p. H234-40.**
140. **Watt, F.M., *Involucrin and other markers of keratinocyte terminal differentiation.* J Invest Dermatol, 1983. 81(1 Suppl): p. 100s-3s.**
141. **Salzman, N.H., et al., *Protection against enteric salmonellosis in transgenic mice expressing a human intestinal defensin.* Nature, 2003. 422(6931): p. 522-6.**
142. **Oren, A., et al., *In human epidermis, beta-defensin 2 is packaged in lamellar bodies.* Exp Mol Pathol, 2003. 74(2): p. 180-2.**
143. **Niyonsaba, F., et al., *Antimicrobial peptides human beta-defensins stimulate epidermal keratinocyte migration, proliferation and production of proinflammatory cytokines and chemokines.* J Invest Dermatol, 2007. 127(3): p. 594-604.**
144. **Rohrl, J., et al., *Human {beta}-Defensin 2 and 3 and Their Mouse Orthologs Induce Chemotaxis through Interaction with CCR2.* J Immunol, 2010.**
145. **Somanath, P.R., J. Chen, and T.V. Byzova, *Akt1 is necessary for the vascular maturation and angiogenesis during cutaneous wound healing.* Angiogenesis, 2008. 11(3): p. 277-88.**
146. **Simpson, E.M., et al., *Genetic variation among 129 substrains and its importance for targeted mutagenesis in mice.* Nat Genet, 1997. 16(1): p. 19-27.**
147. **Threadgill, D.W., et al., *Genealogy of the 129 inbred strains: 129/SvJ is a contaminated inbred strain.* Mamm Genome, 1997. 8(6): p. 390-3.**
148. **Ganz, T., *Defensins: antimicrobial peptides of vertebrates.* C R Biol, 2004. 327(6): p. 539-49.**
149. **Yaneva, M., et al., *PU.1 and a TTTAAA element in the myeloid defensin-1 promoter create an operational TATA box that can impose cell specificity onto TFIID function.* J Immunol, 2006. 176(11): p. 6906-17.**
150. **Ma, Y., Q. Su, and P. Tempst, *Differentiation-stimulated activity binds an ETS-like, essential regulatory element in the human promyelocytic defensin-1 promoter.* J Biol Chem, 1998. 273(15): p. 8727-40.**

151. **Rieske, P. and J.M. Pongubala, *AKT induces transcriptional activity of PU.1 through phosphorylation-mediated modifications within its transactivation domain.* J Biol Chem, 2001. 276(11): p. 8460-8.**
152. **Imler, J.L. and J.A. Hoffmann, *Signaling mechanisms in the antimicrobial host defense of Drosophila.* Curr Opin Microbiol, 2000. 3(1): p. 16-22.**
153. **Lemaitre, B., et al., *The dorsoventral regulatory gene cassette spatzle/Toll/cactus controls the potent antifungal response in Drosophila adults.* Cell, 1996. 86(6): p. 973-83.**
154. **Williams, M.J., et al., *The 18-wheeler mutation reveals complex antibacterial gene regulation in Drosophila host defense.* EMBO J, 1997. 16(20): p. 6120-30.**
155. **Hertz, C.J., et al., *Activation of Toll-like receptor 2 on human tracheobronchial epithelial cells induces the antimicrobial peptide human beta defensin-2.* J Immunol, 2003. 171(12): p. 6820-6.**
156. **Romano Carratelli, C., et al., *Toll-like receptor-4 (TLR4) mediates human beta-defensin-2 (HBD-2) induction in response to Chlamydia pneumoniae in mononuclear cells.* FEMS Immunol Med Microbiol, 2009. 57(2): p. 116-24.**
157. **Weichhart, T. and M.D. Saemann, *The PI3K/Akt/mTOR pathway in innate immune cells: emerging therapeutic applications.* Ann Rheum Dis, 2008. 67 Suppl 3: p. iii70-4.**
158. **Marti, G., et al., *Electroporative transfection with KGF-1 DNA improves wound healing in a diabetic mouse model.* Gene Ther, 2004. 11(24): p. 1780-5.**
159. **Occleston, N.L., et al., *Therapeutic improvement of scarring: mechanisms of scarless and scar-forming healing and approaches to the discovery of new treatments.* Dermatol Res Pract, 2010. 2010.**
160. **Longaker, M.T., et al., *Studies in fetal wound healing. V. A prolonged presence of hyaluronic acid characterizes fetal wound fluid.* Ann Surg, 1991. 213(4): p. 292-6.**
161. **Olutoye, O.O., et al., *Lower cytokine release by fetal porcine platelets: a possible explanation for reduced inflammation after fetal wounding.* J Pediatr Surg, 1996. 31(1): p. 91-5.**
162. **Krummel, T.M., et al., *Transforming growth factor beta (TGF-beta) induces fibrosis in a fetal wound model.* J Pediatr Surg, 1988. 23(7): p. 647-52.**
163. **Shah, M., D.M. Foreman, and M.W. Ferguson, *Neutralisation of TGF-beta 1 and TGF-beta 2 or exogenous addition of TGF-beta 3 to cutaneous rat wounds reduces scarring.* J Cell Sci, 1995. 108 (Pt 3): p. 985-1002.**
164. **Bayat, A., D.A. McGrouther, and M.W. Ferguson, *Skin scarring.* BMJ, 2003. 326(7380): p. 88-92.**
165. **Lindner, H.B., et al., *Anti-bacterial effects of poly-N-acetyl-glucosamine nanofibers in cutaneous wound healing: requirement for Akt1.* PLoS One, 2011. 6(4): p. e18996.**

166. **Pietramaggiori, G., et al., *Effects of poly-N-acetyl glucosamine (pGlcNAc) patch on wound healing in db/db mouse.* J Trauma, 2008. 64(3): p. 803-8.**
167. **Kelechi, T.J., et al., *A randomized, investigator-blinded, controlled pilot study to evaluate the safety and efficacy of a poly-N-acetyl glucosamine-derived membrane material in patients with venous leg ulcers.* J Am Acad Dermatol, 2012. 66(6): p. e209-15.**
168. **Maus, E.A., *Successful treatment of two refractory venous stasis ulcers treated with a novel poly-N-acetyl glucosamine-derived membrane.* BMJ Case Rep, 2012. 2012.**
169. **Hankin, C.S., et al., *Clinical and cost efficacy of advanced wound care matrices for venous ulcers.* J Manag Care Pharm, 2012. 18(5): p. 375-84.**
170. **Hirsch, J.A., et al., *Non-invasive hemostatic closure devices: "patches and pads".* Tech Vasc Interv Radiol, 2003. 6(2): p. 92-5.**
171. **Palmer, B.L., et al., *Effectiveness and safety of manual hemostasis facilitated by the SyvekPatch with one hour of bedrest after coronary angiography using six-French catheters.* Am J Cardiol, 2004. 93(1): p. 96-7.**
172. **Gauglitz, G.G., et al., *Hypertrophic scarring and keloids: pathomechanisms and current and emerging treatment strategies.* Mol Med, 2011. 17(1-2): p. 113-25.**
173. **van Amerongen, M.J., et al., *Bone marrow-derived myofibroblasts contribute functionally to scar formation after myocardial infarction.* J Pathol, 2008. 214(3): p. 377-86.**
174. **Sarrazy, V., et al., *Mechanisms of pathological scarring: role of myofibroblasts and current developments.* Wound Repair Regen, 2011. 19 Suppl 1: p. s10-5.**
175. **Adzick, N.S. and H.P. Lorenz, *Cells, matrix, growth factors, and the surgeon. The biology of scarless fetal wound repair.* Ann Surg, 1994. 220(1): p. 10-8.**
176. **Buehler, M.J., *Nature designs tough collagen: explaining the nanostructure of collagen fibrils.* Proc Natl Acad Sci U S A, 2006. 103(33): p. 12285-90.**
177. **Wang, J.H., et al., *Cell orientation determines the alignment of cell-produced collagenous matrix.* J Biomech, 2003. 36(1): p. 97-102.**
178. **Kalson, N.S., et al., *An experimental model for studying the biomechanics of embryonic tendon: Evidence that the development of mechanical properties depends on the actinomyosin machinery.* Matrix Biol, 2010. 29(8): p. 678-89.**
179. **Oxlund, H., et al., *Collagen deposition and mechanical strength of colon anastomoses and skin incisional wounds of rats.* J Surg Res, 1996. 66(1): p. 25-30.**
180. **Yordy, J.S. and R.C. Muise-Helmericks, *Signal transduction and the Ets family of transcription factors.* Oncogene, 2000. 19(55): p. 6503-13.**
181. **Clark, R.A., *Wound repair.* Curr Opin Cell Biol, 1989. 1(5): p. 1000-8.**

182. **Kelley, T.W., et al., *Macrophage colony-stimulating factor promotes cell survival through Akt/protein kinase B.* J Biol Chem, 1999. 274(37): p. 26393-8.**
183. **Zhou, G.L., et al., *Akt phosphorylation of serine 21 on Pak1 modulates Nck binding and cell migration.* Mol Cell Biol, 2003. 23(22): p. 8058-69.**
184. **Zhu, Q.S., et al., *Vimentin is a novel AKT1 target mediating motility and invasion.* Oncogene, 2011. 30(4): p. 457-70.**
185. **Fayard, E., et al., *Protein kinase B (PKB/Akt), a key mediator of the PI3K signaling pathway.* Curr Top Microbiol Immunol, 2010. 346: p. 31-56.**
186. **Pierce, R.A., C.H. Moore, and M.C. Arikan, *Positive transcriptional regulatory element located within exon 1 of elastin gene.* Am J Physiol Lung Cell Mol Physiol, 2006. 291(3): p. L391-9.**
187. **Vrhovski, B. and A.S. Weiss, *Biochemistry of tropoelastin.* Eur J Biochem, 1998. 258(1): p. 1-18.**
188. **Somanath, P.R., et al., *Akt1 signaling regulates integrin activation, matrix recognition, and fibronectin assembly.* J Biol Chem, 2007. 282(31): p. 22964-76.**
189. **Beeson, C.C., et al., *Integrin-dependent Akt1 activation regulates PGC-1 expression and fatty acid oxidation.* J Vasc Res, 2012. 49(2): p. 89-100.**
190. **Hinz, B. and G. Gabbiani, *Mechanisms of force generation and transmission by myofibroblasts.* Curr Opin Biotechnol, 2003. 14(5): p. 538-46.**
191. **Katoh, K., et al., *Rho-kinase--mediated contraction of isolated stress fibers.* J Cell Biol, 2001. 153(3): p. 569-84.**
192. **Abe, M., et al., *Evidence that PI3K, Rac, Rho, and Rho kinase are involved in basic fibroblast growth factor-stimulated fibroblast-Collagen matrix contraction.* J Cell Biochem, 2007. 102(5): p. 1290-9.**
193. **Ming, X.F., et al., *Rho GTPase/Rho kinase negatively regulates endothelial nitric oxide synthase phosphorylation through the inhibition of protein kinase B/Akt in human endothelial cells.* Mol Cell Biol, 2002. 22(24): p. 8467-77.**
194. **Lelievre, E., et al., *The Ets family contains transcriptional activators and repressors involved in angiogenesis.* Int J Biochem Cell Biol, 2001. 33(4): p. 391-407.**
195. **Scott, E.W., et al., *PU.1 functions in a cell-autonomous manner to control the differentiation of multipotential lymphoid-myeloid progenitors.* Immunity, 1997. 6(4): p. 437-47.**
196. **Lu, Q., et al., *Expression of human beta-defensin-3 in gingival epithelia.* J Periodontal Res, 2005. 40(6): p. 474-81.**
197. **Walsh, L.J., P.R. L'Estrange, and G.J. Seymour, *High magnification in situ viewing of wound healing in oral mucosa.* Aust Dent J, 1996. 41(2): p. 75-9.**
198. **Szpaderska, A.M., J.D. Zuckerman, and L.A. DiPietro, *Differential injury responses in oral mucosal and cutaneous wounds.* J Dent Res, 2003. 82(8): p. 621-6.**

199. **Wetzler, C., et al., *Large and sustained induction of chemokines during impaired wound healing in the genetically diabetic mouse: prolonged persistence of neutrophils and macrophages during the late phase of repair.* J Invest Dermatol, 2000. 115(2): p. 245-53.**
200. **Mak, K., et al., *Scarless healing of oral mucosa is characterized by faster resolution of inflammation and control of myofibroblast action compared to skin wounds in the red Duroc pig model.* J Dermatol Sci, 2009. 56(3): p. 168-80.**
201. **Wilgus, T.A., *Immune cells in the healing skin wound: influential players at each stage of repair.* Pharmacol Res, 2008. 58(2): p. 112-6.**
202. **Wong, J.W., et al., *Wound healing in oral mucosa results in reduced scar formation as compared with skin: evidence from the red Duroc pig model and humans.* Wound Repair Regen, 2009. 17(5): p. 717-29.**
203. **Lee, H.G. and H.C. Eun, *Differences between fibroblasts cultured from oral mucosa and normal skin: implication to wound healing.* J Dermatol Sci, 1999. 21(3): p. 176-82.**
204. **Genever, P.G., E.J. Wood, and W.J. Cunliffe, *The wounded dermal equivalent offers a simplified model for studying wound repair in vitro.* Exp Dermatol, 1993. 2(6): p. 266-73.**
205. **Abiko, Y. and D. Selimovic, *The mechanism of protracted wound healing on oral mucosa in diabetes. Review.* Bosn J Basic Med Sci, 2010. 10(3): p. 186-91.**
206. **Collison, K.S., et al., *RAGE-mediated neutrophil dysfunction is evoked by advanced glycation end products (AGEs).* J Leukoc Biol, 2002. 71(3): p. 433-44.**
207. **Barnea, M., Z. Madar, and O. Froy, *Glucose and insulin are needed for optimal defensin expression in human cell lines.* Biochem Biophys Res Commun, 2008. 367(2): p. 452-6.**
208. **Bhattacharya, R., et al., *Effect of bacteria on the wound healing behavior of oral epithelial cells.* PLoS One, 2014. 9(2): p. e89475.**